KTH Land and Water
Resources Engineering

DISTRIBUTION AND MOBILITY OF ARSENIC IN THE SHALLOW AQUIFERS OF NORTHEASTERN OF LA PAMPA PROVINCE, ARGENTINE

Anna Aullón Alcaine

September 2013

TRITA-LWR Degree Project 13:34
ISSN 1651-064X
LWR-EX-13-34

Master Degree Project
In association with Groundwater Arsenic Research Group
Department of Land and Water Resources Engineering
Royal Institute of Technology (KTH)
SE-100 44 STOCKHOLM, Sweden
Reference should be written as: Aullón Alcaine, A (2013) "Distribution and Mobility of Arsenic in the Shallow Aquifers of Northeastern of La Pampa Province, Argentine" TRITA LWR Degree Project 13:34

SUMMARY IN ENGLISH

High concentrations of geogenic arsenic (As) in groundwater have been reported in different parts of the Chaco-Pampean Plain, in central Argentina, where more than 2 million people may be exposed to high levels of As and F in their drinking water. Groundwater from the shallow aquifer is far exceeding the recommended WHO Standard limit of 10 μg\L for As and 1.5 mg\L for fluoride, as well as the provisional Argentinean Standard limit of 50 μg\L for As. A long-term consumption of As-contaminated groundwater may increase the risk of suffering HACRE (chronic arsenic poisoning) where skin diseases, cardiovascular effects, lung, skin, kidney and liver cancers may develop. The geogenic As results from the weathering of volcanic ash deposits (90% of rhyolitic material) and loess sediments originated by volcanic eruptions from the Andean Mountains and transported to the area by wind. Geo-availability and enrichment of As in shallow aquifers may be influenced by the semi-arid climatic conditions due to seasonal cycles with high evaporation rates and small recharge of water leading to the accumulation of salts and As in low-laying discharge areas. A total of 44 groundwater samples were collected in two rural areas in the shallow aquifers in the NE of La Pampa province, Quemú Quemú (32 wells) and Intendente Alvear (12 wells). T (ºC), pH, EC (μS cm^{-1}) and redox potential (Eh) were measured in-situ in the field. Groundwater samples were collected in replicates of filtered (0.45 μm) and filtered plus acidified with 7M HNO_3. Major anions were analyzed by ion chromatography at the laboratory of KTH and major cations and trace elements were analyzed by optical emission spectrometry (ICP-OES) at Stockholm University. Moreover, 10 soils samples were collected in the area of Quemu Quemu to determine the mineralogical composition and sequential extractions.

The analytical results showed circum-neutral to alkaline groundwater (pH 7.43-9.18), predominantly oxidizing (Eh ~0.24 V) and with widely variation of EC (456-11,400 μS/cm). The major cation dissolved in groundwater was Na+, while the major anions were HCO_3^-, Cl^- and SO_4^{2-}, respectively. Water type was mostly Na-HCO_3^- in QQ and the composition differed in IA among Na-HCO_3^- and Na-Cl-SO_4^{2-} water types. Groundwater composition showed high degree of mineralization evidenced by high EC. In discharge areas high evaporation rates result in high salinity of shallow aquifers and visible salts incrustations on the surface of the lakes. Elevated concentrations of NO_3^- and PO_4^{3-} observed in some wells indicated possible anthropogenic contamination. Total As concentration in groundwater of QQ study area varied from 5.58 to 535μg/L, where 94% of the wells exceeded the WHO standard limit in drinking water, while 54% of the wells exceeded the Argentine standard limit for As. Fluoride also showed high and heterogeneous concentrations (0.5-14.2 mg/L) with 78% of samples exceeding the WHO standard limit. Total dissolved As concentration was mainly arsenate (As^V) and showed positive correlation with dissolved F^-, HCO_3^-, B and V and negative correlation with Fe, Al and Mn ions, as they might be precipitated as secondary oxy- hydroxides.

Some of the mechanisms that can trigger to the mobilization of As are the rise of pH, changes in the redox conditions induced by water table oscillations and the presence of ions competing for sorption sides (HCO_3^-, PO_4^{3-}, Si, V oxyanions, etc.). Secondary Fe, Mn, Al oxy-hydroxide minerals play an important role in the mobility of As, as they are strong adsorbents for As at neutral to alkaline pH (up to 8.5) but weakly adsorbents at higher pH conditions. The rise of pH in groundwater may be induced by the dissolution of carbonates found in calcrete layers, known as "toscas", and by the slow dissolution of silicates. In addition, long-term consumption of drinking water from groundwater could be a considerable threat for the health of the population in rural areas of NE of La Pampa province.

SUMMARY IN SPANISH

Altas concentraciones de As fueron detectadas en las aguas subterráneas de la llanura Chaco-Pampeana en Argentina. Se estima que más de dos millones de personas están expuestas a niveles tóxicos de arsénico (>10 μg/L según la OMS) y flúor (1.5 mg/L) en agua potable (WHO. 2004). Según la comisión nacional de alimentos de la Republica Argentina el límite provisional de As es de 50 μg/L (CAA. 1994). Por lo que una ingestión prolongada de agua subterránea a estos niveles de As o superiores puede producir daños severos para la salud humana, dando lugar a largo plazo al Hidroarsenicismo Crónico Regional Endémico (HACRE). Los principales síntomas afectan la piel, pulmones, sistema nervioso, sistema cardiovascular, incluso la aparición de cáncer cutáneo y de órganos internos. El origen del As es considerado geogénico, debido a la meteorización de cenizas volcánicas que fueron transportadas por el viento desde la cordillera volcánica de los Andes, con material de tipo riolítico. Además, factores climáticos como la fuerte evaporación y presencia de aguas alcalinas puede producir una acumulación de As en las zonas bajas y de descarga. En este estudio se investigan 44 pozos de agua subterránea (molinos y bombas sumergibles) situados en dos localidades al noreste de la provincia de La Pampa, en Quemú Quemú y Intendente Alvear. La T (ºC), pH, conductividad eléctrica (CE) y potencial redox (Eh) del agua fueron analizados in-situ. Los aniones se analizaron por cromatografía iónica en el laboratorio de la KTH y los cationes y metales mediante ICP-OES en la Universidad de Estocolmo (SU). Además, 10 muestras de loess y ceniza volcánica fueron recogidos para determinar la composición mineralogía (XRD) y química del suelo, mediante extracciones secuenciales. Los resultados muestran que el agua subterránea es neutra a alcalina (pH entre 7.43 y 9.18), moderadamente oxidante (Eh ~0.24 V) y con elevada conductividad eléctrica (456-11,400 μS/cm). Los aniones y cationes mayoritarios son HCO_3^- / Cl^- y Na^+/K^+, respectivamente, y se presentan aguas del tipo Na-HCO_3 y Na-Cl-SO_4^{2-}. Las altas concentraciones de nitratos y fosfatos en aguas someras indican una posible contaminación antropogénica, por el uso fertilizantes en la agricultura. Las concentraciones de As son altas en las aguas subterráneas someras y varían desde 5.58 a 535 μg/L. El 94% de los pozos muestreados en QQ exceden el límite permitido por la OMS (10 μg/L) y el 54% el límite Argentino (50 μg/L). El ion fluoruro está también presente en altas concentraciones, mayoritariamente en los pozos con alto contenido de As. El 78% de los pozos en QQ exceden el límite de F permitido por la OMS (1.5 μg/L). El arsénico pentavalente o arseniato (As^V) se estima ser presente en el 99% de las muestras analizadas, mientras que el As trivalente (As^{III}) no se encuentra pero podría estar presente en aguas reductoras a mayor profundidad. Se observa una correlación positiva entre la concentración de As total y el F-, HCO_3, pH, B, V, U, Mo. Mientras que, por lo contrario, no existe correlación entre el As y el Fe, Al y Mn disuelto. Eso es debido a la presencia de precipitados y fases minerales de Fe, Al, Mn como óxidos e hidróxidos secundarios. Los principales procesos que controlan la movilidad del As en el agua subterránea son adsorción-desorción, precipitación-dilución y oxidación-reducción. El As(V) se adsorbe en óxidos e hidróxidos de Fe, Al y Mn, sin embargo, un aumento de pH, por encima de 8.5, podría favorecer su disolución y movilización en el agua subterránea. No obstante, hay otros factores que pueden promover la movilidad del As como las variaciones de nivel del agua, cambios de potencial redox, flujos lentos y aumento del tiempo de retención del agua en los sedimentos y la presencia de iones competidores con el As por ser adsorbidos en las superficies de los minerales de Fe. El aumento del pH puede explicarse por disolución de los minerales carbonatados (Tosca) y por la disolución de silicatos presentes en el loess. Finalmente, las aguas subterráneas someras investigadas en la zona del NE de la Pampa presentan una calidad pobre para el consumo humano y se deberían aplicar medidas de remediación para un consumo prolongado con el fin de evitar serios problemas para la salud humana.

SUMMARY IN SWEDISH

Höga halter av löst arsenik (As) i grundvatten har rapporterats från olika delar av Chaco-Pampas-slätten, där över 2 miljoner människor utsätts för höga arsenik och fluorid-koncentrationer i sitt dricksvatten. Koncentrationerna i grundvattnet överskrider WHO:s riktvärden (10 μg/L för arsenik och 1.5 μg/L för fluorid), liksom det argentinska riktvärdet på 50 μg/L för As. Långvarig konsumtion av As-förorenat vatten leder till hög risk för s.k. hydroarsenicism (HACRE), hudsjukdomar och cancer.

Arseniken kommer från vittring av vulkanisk aska (90% av ryolitiskt material) och magmatiska mineral i lössjord, som härrör från de andinska vulkanutbrotten. Ackumulation av As i grunda akvifärer kan påverkas av de torra och halvtorra klimatförhållandena på grund av hög avdunstning samt låg infiltration av vatten under torrperioden. Sammanlagt har 44 grundvattenprover tagits från de grunda akvifärerna i den nordöstra delen av La Pampa-provinsen, lokaliserade i två landsbygdsområden som täcker en yta på 600km² i Quemú Quemú och 300km² i Intendente Alvear. Temperatur (°C), pH, elektrisk konduktivitet (μS/cm) och redox potential (Eh) uppmättes i fält och flera vattenprover togs. Dessa prover var filtrerade (0.45 μm) och surgjorda med 7M HNO_3. Viktigare anjoner analyserades med jonkromatografi vid laboratoriet på KTH. Viktigare katjoner och spårämnen analyserades med plasmaemissionsspektrometri (ICP-OES) vid Stockholms universitet.

Grundvattnet var neutralt till svagt alkaliskt (pH 7.43-9.18), övervägande oxiderande (Eh~0.24 V) med ett brett intervall för den elektriska konduktiviteten (456-11400 μS/cm). De mest förekommande jonerna var HCO_3^-/Cl^-(anjoner) och Na^+/K^+(katjoner). Grundvattentypen karaktäriserades som Na-HCO_3^-. Vattenproverna visade hög grad av mineralisering vilket framgick av den höga elektriska konduktiviteten. I utströmningsområdenaresulterarade hög avdunstning i hög salthalt i grunda akvifärer och synliga saltbeläggningar på sjöytor. Förhöjda halter av nitrat och fosfat i vissa brunnar kan möjligtvis tyda på antropogenförorening.

Grundvattnets As-koncentration varierade mellan 5.58 och 535 μg/L. 94% av brunnarna i Quemú Quemú överskred WHO:s riktvärde för dricksvatten, medan 56% av brunnarna översteg det argentinska riktvärdet. Fluoriduppvisade höga men varierande koncentrationer (0.5-14.2 mg/L), och 78% av proverna översked WHO:s riktvärde. Totalkoncentrationen löst Asvar postivt korrelerad till löst F^-, HCO_3^-, B och V, och negativt korrelerad tilllöst Fe, Al och Mn, sannolikt eftersom de fälls ut som sekundära (hydr)oxider.

De processer som styr rörligheten av As kan vara adsorption/desorption, utfällning/upplösning och oxidation/reduktion. Närvaro av Fe-, Mn-, och Al-(hydr)oxider spelar en viktig roll, eftersom adsorberarAs vid lågt pH (upp till 8.5). Förändringar i redoxförhållandena på grund av variationer i grundvattennivån samt lågt flöde som ökar uppehållstiden för vatten och konkurrerande joner är mekanismer som skulle kunna frigöra As till grundvatten genomreduktiv upplösning av (hydr)oxider med adsorberad As. Det höga pH-värdet är en följd av karbonatjämvikt ilager av kalkkrusta benämnda "Tosca", som påverkats av katjonutbyte från Na-HCO_3-vatten. Långvarig konsumtion av detta grundvatten kan utgöra en stor hälsorisk för befolkningen på landsbygden i den nordöstra delen av La Pampa-provinsen.

ACKNOWLEDGEMENTS

First, I would like to acknowledge my supervisor Professor Prosun Bhattacharya, for giving me this opportunity and opening to me a wide range of new professional chances. Professors Jochen Bundschuh and Roger Thunvik thanks for funding the trip to Argentina. Thanks to both PhD students Oswaldo Ramos and Arifin Sandhi for the help and guidance as co-supervisors. I am especially grateful to Emeritus Prof. Gunnar Jacks, for providing me assistance in the lab and inspiring me with your knowledge of geochemistry. Thanks to Bertil Nilsson and Ann Fylkner for taking your time with the analyses and assistance in the lab of LWR department at KTH. My sincere appreciation to Magnus Mörth and Edyta for the ICP-OES analysis of my samples carried out at the Department of Geology and Geochemistry at Stockholm University, and also to Arto Peltola from the University of Turku in Finland for the XRD analysis. Especially thanks to Prof. Jon-Peter Gustafsson, for the instructions using Visual Minteq software and for the feedback given on the writing part.

My warm appreciation to the PhD students from the Department of LWR at KTH, very especially to my friends Lea, Sofi, Caroline, Imran, Robert, Kedar, Juan and Benoir. Thanks for the support, friendship and pleasant fika times we had together at the uni. Also a much deserved thanks to Aira Saarelainen, for your every day's happiness and your efficiency handling bureaucracy. Thanks to Joanne Fernlund for the useful teachings for formatting the thesis.

Thanks to all the Argentineans that I met in La Pampa:

First, I would like to acknowledge Dr. Carlos Schulz for the coordination and organization of the field work in La Pampa. A much deserved thank to all the collaborators and students from the National University of La Pampa (Facultad de Ciencias Exactas y Naturales) especially to Mariana, Gabriela, Marcos, Eduardo, Javier and Mariano for your warm welcome, hospitality and support during my time there. Sampling campaigns would not be possible without the support of the municipal authorities and the staff from COSYPRO and COSERIA water service cooperatives.

Much deserved thanks to the University of Barcelona (Faculty of Chemistry) for the Erasmus Placement Scholarship and also to the Swedish-Spanish Foundation in Stockholm for the initial funding.

Finally, my sincere appreciation to all my catalan friends, especially to Davinia, Jaume, Laura and Jordi and to those living in Sweden, like Ari and family, Leire, Anna, Vincent, Joseph and others. And much deserved thank to my family for the support and encouragement throughout my studies in Sweden.

ABBREVIATIONS

CAA	Argentinean Food Code
CEC	Cation Exchange Capacity
DMA	Dimethylarsinic Acid
EC	Electrical Conductivity
HACRE	Hidroarsenicismo Cronico Regional Endemico (in Spanish)
IA	Intendente Alvear
IAP	Ion Activity Product
IC	Ion Chromatography
ICP-OES	Inductively Coupled Plasma-Optical Emission Spectrometry
MMA	Monomethylarsonic Acid
PZC	Point of Zero Charge
QQ	Quemú Quemú
SI	Saturation Index
TDS	Total Dissolved Solids
TMAO	trimethylarsine oxide
WHO	World Health Organization
XRD	X-Ray Diffraction

TABLE OF CONTENTS

ABSTRACT

More than two million people in the Chaco-Pampean plain in central Argentina are affected by high As levels in groundwater. The concentrations of As are far exceeding the WHO standard limit for safe drinking water of 0.1 μg/L and the provisional Argentinean limit of 0.5 μg/L. The NE of La Pampa province is one of the areas affected with geogenic As in shallow aquifers within the Chaco-Pampean plain. These aquifers are in closed basins and they are only available water resource of the region for drinking and agriculture purposes. The Pampean aquifer is composed of a multi-layered system of Quaternary loess deposits covered by aeolian sands and also containing layers of rhyolitic volcanic ash, which is considered the primary source of As. Volcanic ash layers can be visible in the shallow sediments or intermixed in the loess. During the weathering of volcanic ash sediments As is dissolved to the aqueous phase and can be quickly adsorbed or co-precipitated on secondary Fe, Al and Mn oxy-hydroxides under favourable conditions. Also, previous more arid climatic conditions have led to the formation of carbonate "calcrete" layers in the top sequences of the loess and this has affected the geochemistry of the aquifer. Two sites were investigated in the NE of La Pampa province in order to assess (i) the quality of groundwater for drinking water use, (ii) the distribution of As and other trace elements in shallow aquifers and (iii) to understand better the factors controlling its mobility in groundwater. The results showed that groundwater was circum-neutral to alkaline and under moderate oxidizing conditions. The predominant groundwater composition was of Na-HCO_3 for fresh water and Na-Cl-SO_4^{2-} for brackish water types. High salinity levels are evidenced by the high Electrical Conductivity and might be explained by to the high evaporation rates. Groundwater sampled in both areas was enriched with As, F and other trace elements at different ranges of concentration. From the total As concentrations, arsenate As(V) predominated over arsenite As(III) species. Shallow groundwater is also enriched with fluoride exceeding the WHO standard limit of 1.5 mg/L and placed in the same As hotspots. One possible factor controlling the mobility of As is the high pH of groundwater, which is controlled by the carbonates equilibrium. Under this high pH conditions As is less strongly bind to Fe, Al and Mn oxy-hydroxides and can be easily mobilized to groundwater when other competing ions are getting adsorbed on the surface sites of binding minerals.

Key words: Arsenic, fluoride, shallow aquifer, La Pampa, loess sediments and volcanic ash

1 INTRODUCTION

Having good quality of water is vital for the healthy functioning of ecosystems and human well-being. One of the most problematic contaminants in drinking water is inorganic arsenic (As), which is largely distributed in natural environments. The contamination of As in groundwater and its toxicity in long term of exposure has emerged a major environmental crisis in many parts of the world. Arsenic is naturally present in waters at low concentrations (between 1 and 2 μg/L). However, it can be found at higher levels in surface and groundwater deriving from sulfide mineral deposits and volcanic sediments, resulting in severe human health threats (WHO. 2004). The largest mass As poisoning in the world via well water occurred in West Bengal and Bangladesh, where more than 100 million people were exposed to high As concentrations in drinking water and food (Bhattacharya et al. 2002). Other affected places worldwide have been reported in the USA, China, Bangladesh, Taiwan, Mexico, Australia, New Zealand, Vietnam, India, etc. (Bhattacharya et al. 2002; Bundschuh et al. 2004; Nicolli et al. 2012). South American countries have also been a cause of concern for high As in groundwater since many years, especially in arid and semi-arid part of Chile, Argentina, Bolivia and Peru. A clear example of an affected semi-arid region is the vast Chaco-Pampean Plain, in central and north Argentina. Here the contamination of As occurs under neutral-alkaline pH conditions and oxidizing groundwaters (Nicolli et al. 1989; Smedley et al. 2000, 2002; Bhattacharya et al. 2006). Typically, under these conditions the precipitation of

secondary oxy-hydroxide minerals is favourable and arsenate can be re-adsorbed or co-precipitated into oxy-hydroxide minerals. However, an increase of alkalinity (≥8.5-9.5) can trigger to the desorption of As and release into groundwater (O'Reilly et al. 2010).

Arsenicosis is the As poisoning disease and it was recognised for first time 100 years ago in the village of Bell Ville, in the province of Córdoba, central Argentine. It was discovered when mny people from this area showed similar symptoms of skin problems after the long-term consumption of groundwater contaminated with As. For this reason, it was known as the "Bell Ville disease" (Nicolli et al. 1989; Bundschuh et al. 2011b). The main symptoms associated to As poisoning are skin lesions, like pigmentation and keratosis of hands and feet, respiratory effects and increased risk of internal cancers. Recently, in the 21st century arsenic-related health problems have increased sharply in South America affecting the populations of 14 out of 21 countries (Bundschuh et al. 2011b).

1.1 Arsenic in the Chaco-Pampean Plain

The Chaco-Pampean Plain extends from the Paraguayan border in the north to the Patagonian region in the south and to the Andean Mountains in the west to Paraná River in the east (Nicolli et al. 2012). This region belongs to one of the largest areas of loess deposition in the world and is extended over an area of 1.2 million of km² (Smedley and Kinniburgh. 2002; Farías et al. 2004; Bhattacharya et al. 2006). The Chaco-Pampean Plain is also one of the largest areas known for the occurrence of geogenic As in groundwater, especially in the shallow aquifers in closed basins. The most affected areas reported in this region are in the Tucumán province and Santiago del Estero (A), The Chaco province (B), South of Santa Fe (C), East of Córdoba (D), Southeast of Buenos Aires (E) and the Northeast of La Pampa province, investigated in this study (F) (Fig. 1) (Smedley et al. 2002, 2005; Bundschuh et al. 2011b; Nicolli et al. 2012). Besides the high levels of As, high salinity and other toxic trace elements like F, V, Mo, U, and Se have been reported in groundwater, being sometimes groundwater quality very poor and unsuitable for human consumption.

Important health threats are manifested due the high fluoride concentrations in groundwater, where many people might show dental fluorosis symptoms and osteofluorosis after the long term consumption of drinking water.

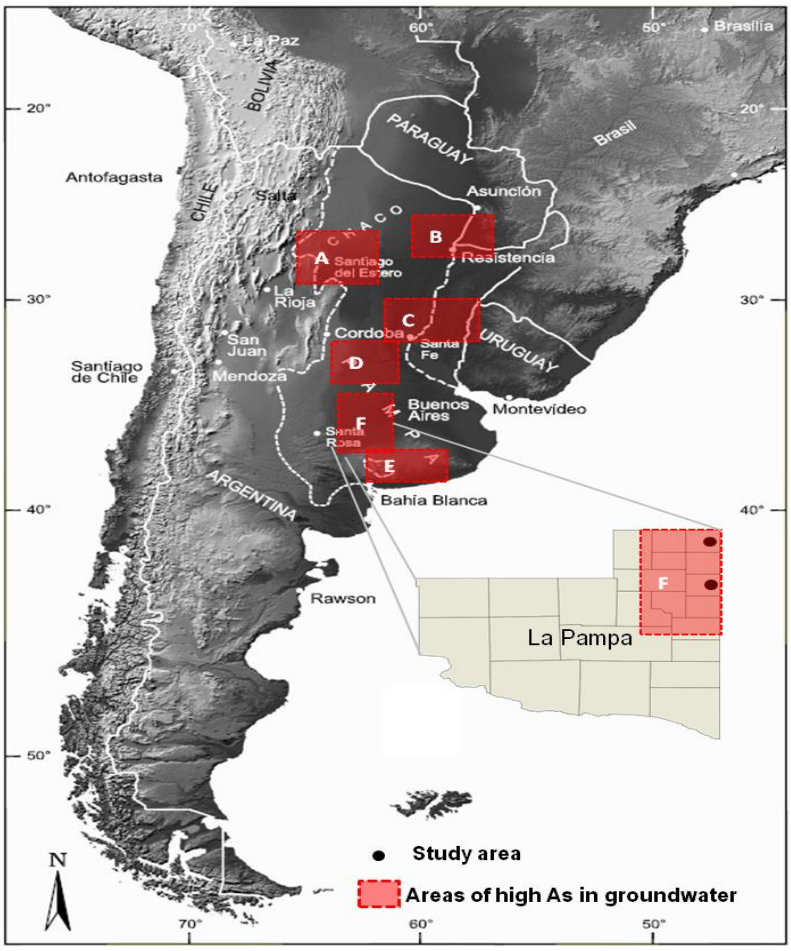

Figure 1: DEM map showing the regions of the Chaco-Pampean plain with high As-concentrations in groundwater (adapted from Bundschuh et al. 2011)

The primary source of As in shallow aquifers is considered sourced from the volcanic ash sediments ejected from the Andean volcanic eruptions and deposited in the vast area by wind (Smedley et al. 2000, 2002). Once volcanic ash has been deposited in the sediments it undergoes to irreversible geochemical reactions, like oxidation and slow dissolution of minerals, releasing potentially toxic trace metals to the aquatic system (i.e., As, Mo, U, V, F). The Pampean aquifer is composed of Quaternary loess sediments, from Pleistocene to Holocene period, covered by aeolian sands and silts of volcanic material that has been reworked (Nicolli et al. 1989; Casentini et al. 2010).

High variability of As concentrations in groundwater has been reported by Nicolli et al.(2010) in the Tucumán province in the north of the Chaco Plain, with concentrations ranging between 11.4-1660 μg/L. Smedley et al. (2002) also found in the NE of La Pampa province, As concentrations ranging over four orders of magnitude (<4-5300μg/L). Also, O'Reilly et al. (2010) found in Eduardo Castex (NE La Pampa) As ranging from 3 to 1326μg/L with higher As(III) than As(V). Bhattacharya et al. (2006) found the highest levels of As in the shallow aquifer of Santiago del Estero alluvial cone (7-14969 μg/L), where groundwater is under oxidizing and slightly reducing redox conditions. As correlated well with other trace elements such as V, U, Mo and B. Fernandez-Cirelli et al. (2004) also reported high concentrations of As in the SE of Córdoba province, at concentrations of in shallow aquifers (80-4500μg/L) and (<20-200μg/L) in the deep aquifers. These investigations reported that the source of As was geogenic from the weathering of volcanic ash deposits. Volcanic ash layers were observed in different parts of the vast area and in varying degrees of thickness. For example, from 2-3 cm in La Pampa Province and up to 30-50 cm in Santiago del Estero province (Claesson et al. 2003; Smedley et al. 2005).

Drinking water is mostly extracted from the Pampean aquifer by windmill hand-pumps or by submerged electrical pumping systems. Different urban and rural places have been already surveyed in the Chaco-Pampean plain, however due to the large extension of land these are very scattered and it is difficult to determine all the affected population in order to take mitigation measures. Furthermore, all the data obtained in further studies will be compiled in a database and used in other areas with similar climatic, geological and hydrological characteristics. The most important aspects of this environmental problem are to understand the geogenic occurrence of As in shallow aquifers and the mechanisms controlling its mobility and the behaviour under different aquatic conditions.

1.2Aim and Objectives

The aim of this study is to investigate the geochemical characteristics of the shallow aquifers in two areas of the NE La Pampa, focusing on the occurrence of As in groundwater, in order to understand the main mechanisms controlling its mobility, attenuation and accumulation in the shallow groundwater.

The specific objectives are:

- Determine the chemical composition of groundwater for an assessment of the drinking water quality according to the WHO standard limits and the Argentinean standard regulations.
- Determine the spatial distribution of As concentrations and other associated trace elements to target contaminated areas, as well as the predominant As species dissolved in groundwater.
- Quantify the amount of As released from the sediments and volcanic ash in order to determine the possible minerals binding As in the shallow aquifers.
- Understand the key factors controlling the mobilization, attenuation and accumulation of As and other associated trace elements in the shallow aquifers on NE of La Pampa.

2 STUDY AREA DESCRIPTION

The study area lies in the northeast of La Pampa province, in the southwest of the Chaco-Pampean Plain in central Argentina. Two rural areas were investigated in the NE of La Pampa province, both placed within the same hydrological basins where the only freshwater available is from groundwater (Fig. 2). The first site is situated towards north east at 80 km from the capital of the province Santa Rosa, and lies around the village of Quemú Quemú (QQ). This rural village have around 3,800 inhabitants which are mainly old people or families living from the agriculture (Rodriguez. 2011). QQ study site covers an area of around 600km^2 and is extended over the geographical coordinates 35°53' - 36°07' S latitude and 63°28' - 63°45' W

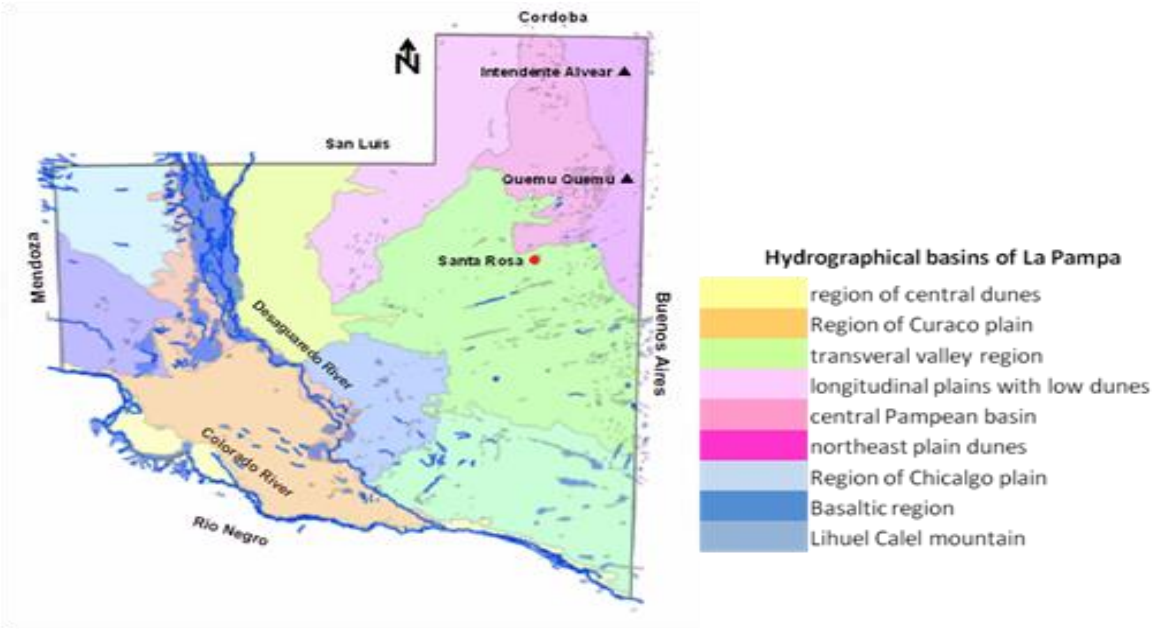

Figure 2 Hydrological basins of La Pampa province, study areas sites investigated within the same hydrological basin

longitude. The second study area is situated in the north east border of La Pampa, at 130km from Santa Rosa. The aquifer sampled called Las Mercedes is placed between the villages Intendente Alvear (IA) and Ceballos, and covers an area of around 300 km^2. The regional aquifer is extended to the Pampean and Post-Pampean formation and constitutes one of the largest sedimentary aquifers of the region with some closed basins of small aquifers and aquitards of multilayer type (Castro. 2008).

The main economic activities of the region are agriculture and cattle ranching, which have high water demand. For this reason, groundwater is one of the most important natural resources for the socio-economic development of the region and its preservation is of concern for the population and municipal authorities. However, groundwater is highly saline in some aquifers and it may also contain high concentrations of toxic trace elements like As, F, Mo, U, Se, etc affecting its quality and exposing the population to have serious severe health problems. The only drinking water available is from the shallow aquifers, which is fresher than in deep aquifer. Groundwater is pumped out from wells to elevated storage tanks and then is submitted to chlorination as a pre-treatment before it is supplied to the population (APA. 2001).

2.1Regional Settings of La Pampa

The morphology of La Pampa is characterized by an undulated system of sand dunes with flat grasslands located at an average altitude of 120m.a.s.l. The province stretches from Mendoza in the west to Buenos Aires province in the east, and from the northern border of Córdoba and San Luis to Rio Negro in the south. La Pampa province has around 300.000 inhabitants, where half are living in large cities like Santa Rosa and General Pico and the other half are spread in villages of few thousands of inhabitants and rural settlements, like the sites selected for this study. The main economy is largely based on agriculture and cattle breeding, and the production of meat, milk and grain cultivation such as cereals, oilseeds, corn, wheat, sunflower, sorghum and soybeans (Galindo et al. 2007). Natural vegetation consists of Pampean steppe in the eastern plain and *"caldén"* forests in the western upland side (Smedley et al. 2002). Groundwater divisions are not clearly defined within the closed basins of the plain which makes a difficult hydraulic organization of the territory (Castro. 2008). The principal surface water resources are two rivers situated one at the southern border of the province, The *Colorado River* placed in the border of the Río Negro province, and the other The *Desaguaradero River* just crossing the first one.

2.2 Climatic characteristics

The province of La Pampa is characterized by a sub-humid semi-arid temperate climate and flat topography. Climate variations can be distinguished between *"The humid Pampas"* in the eastern part, strongly influenced by the Atlantic sea proximity, and *"The dry Pampas"* in the western part of the region. The average annual precipitation of the province is 600 mm, ranging from 500 to 900 mm between SW and NE (Castro. 2008). High precipitations occur mainly

in summer and beginning of autumn (October to March), while low precipitations occur mainly in winter (between May and September) (APA. 2001). Big storms with electrical discharges and winds are often abundant on the plain, usually when contrasting air masses from cold polar air and warm humid air impact the region (Blouet & Blouet. 2009). Thermal amplitude occurs between day and night which may be reflected by the steppe vegetation typical of semi-arid regions. The average annual temperature of La Pampa province ranges from 7-10ºC in winter and from 25-30ºC in summer (APA. 2001). Besides the annual climatic variability, some episodes of severe floods and droughts have occurred in the plain during the last 50 years. High temperatures over 40ºC were achieved during the dry-season, while between the years 2000 and 2005, abundant precipitations caused some floods that affected the crop production and the village infrastructures (Castro. 2008). Furthermore, during the last years strong winds during the dry season with extreme high temperatures produced some fires in the region.

The average annual temperature registered in Quemú Quemú was 16ºC (for the period 1961-2006). The maximum value was 24ºC reached in February and the minimum 5°C for July (Rodriguez. 2011). For the same period, the average annual precipitation was 700 mm, increasing towards the north-northeast (Rodriguez. 2011). The area of Intendente Alvear showed similar climatic conditions than Quemú Quemú, but with higher precipitations and humidity. The average monthly precipitation for QQ was 900 mm (for the period 1961-2006) (Castro. 2008). The flooding and drought cycles involve changes in the water table, which can be shallow or very close to the surface. For this reason, one important factor to be considered when studying the mobilization of trace elements is the extreme climatic variations between dry and wet seasons which changes the water table depth and is importantly linked to geochemistry and groundwater composition (Rodriguez. 2011).

2.3 Geology and Hydrogeology

The geology of La Pampa province is characterized by a crystalline basement covered by clastic sediments (from Miocene period) of fine texture and low permeability that comprises the Pre-Pampean aquifer. Above, are found the Pampean sandy silts sediments of loess, with a thickness between 90 and 150m (from Superior Tertiary and Quaternary period), and the upper sequence is formed by Post-Pampean Aeolian fine sands, (from Holocene to the Present).The upper mantle can range from 3 m thick in the depressions until 15m in the sandy dune slopes (Nicolli et al. 1989; Smedley et al. 2000, 2005).The altitude above the sea level varies from 90 to 150m from the west to the east (Nicolli et al. 1989). The Pampean loess aquifer was formed during the first stages of the last Pleistocene glaciations with fractions of Andean igneous rocks that were reworked during dry periods and underwent pedogenesis under humid periods (Nicolli et al. 1989; Smedley et al. 2002, 2005). Volcanic ash layers can be visible near the surface or in the cutting of the roads. The thicknesses of ash layers vary depending on the degree of mineralization (Bundschuh et al. 2004; Bhattacharya et al. 2006)

Figure 3: Visible carbonate concretions petrified on the roots of the trees. Accumulation of salts incrustations on the surface of the lake due to the high evaporation rates in dry season.

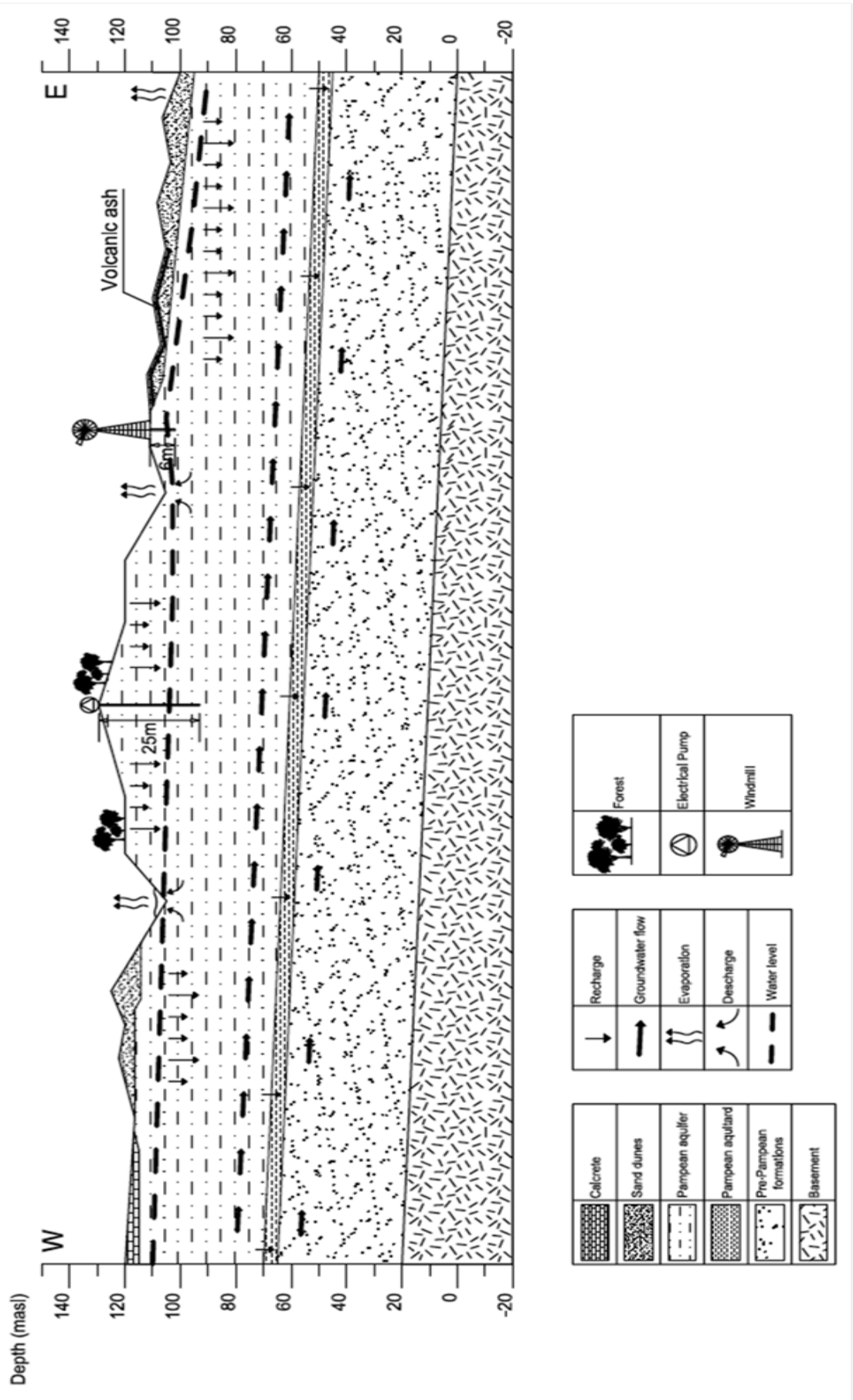

Figure 4: Sketch map of the hydrological system of the Pampean aquifer in the area of QQ (adapted from Smedley et al. 2002)

Volcanic ash has typically an important content of volcanic glass (around 90%) of rhyolitic or dacitic composition, with different content of As depending on the area and the degree of volcanic ash depletion.

The Pampean loess displays the evidence of the post-depositional alteration. This region experienced a more arid climate than the present semi-arid/sub-humid conditions, which is evidenced by the presence of secondary carbonate concretions, locally known as *"tosca"*. These are usually found in the shallow parts at 1 to 2 m underground and can reach the roots of the trees (Fig 3, left). Quaternary loess sediments are mainly composed of 90% of plagioclase, K-feldspars, quartz, micas and also volcanic glass (Nicolli et al. 2012).

The top soils have good porosity and good permeability in recharge areas and often rich in organic matter which is added from the extensive agriculture and livestock activities. However, soil degradation by wind is significant in some cultivated areas (Smedley et al. 2002).

Groundwater is hosted in a multilayered sequence of sedimentary sandy and silty aquifers and aquitards that originates a deep interconnected aquifer system. The base is comprised of thick marine sediments (green clays) where are hosted the most saline waters of Na-SO_4^2-Cl type (Nicolli et al. 2012). The main recharge of freshwater is from rainwater but also the aquifers are recharged from groundwater flowing from the neighbors Pampean aquifers and aquitards (Rodriguez. 2011). During the wet season, there is a high recharge of rainwater that is filled from the eastern sand dunes, considered the recharge zone, and it runs underground until it is discharged towards the southeast depressions, considered the discharge zone. During the dry season the surface water of the lakes quickly evaporates and results in visible salt incrustations on the margins of the lake and also salty shallow groundwater concentrations (Fig. 3, right). The general groundwater flow crosses the region from NW to SE following the topographic gradient with low flow velocities (Castro. 2008). However, there are other groundwater flows with different directions that exist locally within the basin. Groundwater from shallow aquifer has specific flow rates of 1.5 m^3/hm reaching maximum values of 6m^3/hm (Tullio and Giai. 1990). Groundwater is highly saline in some parts basically due to vertical flow transportation of solutes and the high evaporation rates. Groundwater composition is mainly of Na-bicarbonate water types with abundant Na-sulfate and Na-chlorite water types depending on the topography and the lithological composition of the soils (porosity). In recharge areas the rainwater drainage is fast because the sandy dunes have good porosity and there is a big slope gradient. Even though, in some parts of the upper western side, shallow carbonate concretions retain some water that infiltrates or overflows until it is discharged into the lakes (Castro. 2008). In the area of QQ they have monitored the variations of the water table between the periods 1986 to 2007 and the variation ranged from 1-2 m to 6-7 m depth (APA. 2001). In the area of Intendente Alvear the variation of the water table reported was similar than in QQ but with an increase of the depth to 7-8 m from 2008 to 2010. The measured water table is usually shallower in the eastern part (3-4m) than in the western side of the area (Smedley et al. 2005). Generally, vertical flows predominate (infiltration-evaporation) over horizontal flow patterns (surface runoff) (Castro. 2008). The sketch map (Fig. 4) represents the hydro-geological system of the QQ study area with the sand dunes and the different Pampean aquifers and aquitard, also the regional and some local flows are represented. The hydrological characteristics are similar in other areas within the same closed basins.

3 GEOCHEMISTRY OF ARSENIC

Arsenic is a naturally occurring element in the environment and is classified as metalloid for its metallic and non-metallic properties. On the periodic table it is placed in the group 15 (element 33) together with nitrogen (N), phosphorous (P), bismuth (Bi) and antimony (Sb) (Henke. 2009). Chemically, it is similar to phosphorous, an essential component of life processes, and for this reason As can be present in phosphate minerals as substitute for P (Fendorf et al. 2010). The only natural stable occurring isotope of As is As^{75} (Ferguson and Gavis. 1972). Arsenic is stable in four oxidation states (-3, 0, +3 and +5) under the most common redox conditions for groundwater. However, the inorganic forms arsenate As(V) and arsenite As(III) predominate in the aquatic environments. Dissolved arsenite species As(III) are stable under reducing conditions, while arsenate species As(V) are occurring under more oxidizing conditions (Smedley and Kinniburg. 2002; Lizama et al. 2011). Organic forms can occur as a result of methylation reactions which are usually catalyzed by microbial activity

(bacteria, yeasts or algae). The predominant organic species are DMA (dimethylarsinic acid), MMA (monomethylarsonic acid) and TMAO (trimethylarsine oxide), which are less abundant in aquatic systems and less toxic for humans. As metal occur very rare in the environment and arsine gas (AsH_3) is the most toxic form and only occurs under extremely anoxic conditions (Ferguson and Gavis. 1972; Frankeberg and Arshad. 2002).

3.1Sources of Arsenic

Arsenic is a natural constituent of the Earth crust and is placed the 20th element in abundance in relation to other elements. It can be found in both igneous and sedimentary rocks. The average content of As in the continental crust is reported around 2-3 mg/kg (Nicolli et al. 1989). Several As-bearing minerals can occur in the nature in more than 200 minerals and in different ranges of concentrations. The most common As minerals include: elemental As, arsenides, sulfides, oxides, silicates, carbonates, sulfates and other minerals (Boyle and Jonasson. 1973) (Table 1). The most abundant As in content is found in sulfide minerals like Arsenopyrite (FeAsS), Realgar (AsS), Orpiment (As_2S_3) and Pyrite (Smedley and Kinniburg. 2002).

The primary sources of geogenic As in Argentina is considered to be associated to volcanic origin. On the one hand, from geothermal waters occurring in the Andean hydrothermal areas and by the other hand, from volcanic ash layers transported by wind and deposited in the vast arid and semi-arid regions. These regions are composed of deep sedimentary aquifers and groundwater is found under high pH conditions.

Human activities can also contribute to increase As contamination in groundwater. One of the major anthropogenic source of As in the environment is by the exploitation of sulfide ore deposits in mining areas, by the accumulation of mine wastes in tailings. Sulfide minerals rich in As like pyrite and arsenopyrite from mine tailings can be oxidized by atmospheric O_2 and Fe^{3+} producing acid mine drainage (AMD) conditions and releasing large amounts of As and other toxic trace elements into groundwater. The oxidation of arsenopyrite produces arsenate, sulfate and acidification of waters:

$$4FeAsS + 6H_2O + 13O_2 \leftrightarrow 4Fe^{2+} + 4H_2AsO_4^- + 4SO_4^{2-} + 4H^+$$

When Fe, Mn and Al are released from primary minerals these are oxidized and can precipitate as secondary oxy-hydroxide minerals. As species can be adsorbed or co-precipitated into secondary oxy-hydroxides, being these minerals potential sources of As when their conditions are favorable for its mobilization (Sracek et al. 2004).

Other sources of As are As-based pesticides for agriculture, waste disposal activities, wood preservatives and also the combustion of coal and fossil fuels (Alarcón-Herrera et al. 2012). The high concentrations of rare elements and toxic trace elements into fertilizers are related to its content in the raw mineral used for manufacturing. Carbonatites and phosphorites may be natural source of As (Otero et al. 2005).

Table 1: Common As-bearing minerals present in the environment (Boyle. 1973; Smedley and Kinniburgh. 2002)

Mineral	As range (mg kg $^{-1}$)
Sulfide minerals	
Pyrite	100-77000
Pyrrothite	5-100
Marcasite	20-126000
Galena	5-10000
Sphalerite	5-170000
Chalcopyrite	10 - 5000
Oxide minerals	
Hematite	up to 160
Fe oxide	up to 2000
Fe(III)oxyhydroxide	up to 76000
Magnetite	2.7 - 41
Illmenite	< 1
Silicate minerals	
Quartz	0.4 - 1.3
Feldspar	<0.1 - 2.1
Biotite	1.4
Amphibole	1.1 - 2.3
Olivine	0.08 - 0.17
Pyroxene	0.05 - 0.8
Carbonate minerals	
Calcite	1 - 8
Dolomite	<3
Siderite	<3
Sulfate minerals	
Gypsum/anhydrite	<1 - 6
Barite	<1 - 12
Jarosite	34 -1000
Other minerals	
Halite	<3 - 30
Fluorite	<2
Apatite	<1 - 1000

The primary source of As in the vast Chaco-Pampean Plain is mainly considered geogenic from the weathering of volcanic ash sediments intermixed in the loess. Usually the deposits are found at shallow levels and of few cm of thickness. Volcanic glass is of rhyolitic composition and may contain between 2-12 mg/kg of As (average 6 mg/kg) (Blanco et al. 2006), and it is rapidly weathered because is thermodynamically unstable. Volcanich ash of rhyolitic composition has mainly quartz, feldspars, micas, pyroxenes, amphibole, and sulfide minerals rich in As (Gitari et al. 2010).

Additionally, it has reported that, the content of As in volcanic ash layers can be also found in the crystalline structure of minerals of loess sediments, which is made of volcanic material in 5%-10% (Welch et al. 2006). Weather if primary the source of As is geogenic or from the abuse of synthetic products in agriculture is not completely resolved and further work need to be explored in order to determine all the sources and mobility factors of As in groundwater (Blanco et al. 2006; Bhattacharya et al. 2006). By the other hand, sometimes the amount of As in sediments is considerable low (only few mg/kg), but enough to trigger thousands of μg L^{-1} in groundwater and cause serious health problems for humans.

3.2 Arsenic in aqueous solutions

The toxicity, availability and mobility of arsenic depend on its speciation (Litter et al. 2010).

Under oxidizing conditions and circum-neutral and alkaline pH (7-8.5) conditions, arsenate species predominate, such as $H_2AsO_4^-$ found at pH below 6.9 and $HAsO_4^{2-}$ at higher pH values. Under reducing conditions and over a wide range of pH, arsenic is found in its most mobile form, the uncharged arsenite species like H_3AsO_3 predominate. As(-III) occurs rarely in the aquatic systems only under very extreme

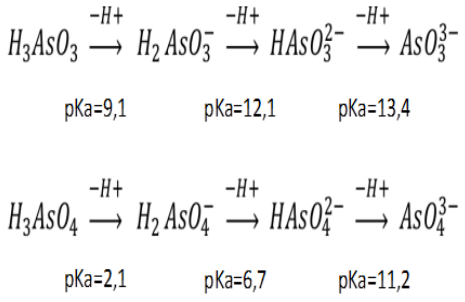

Figure 5 Inorganic aqueous As species with the corresponding dissociation products and pka values.

reducing conditions (<<Eh). The dissociation products of arsenate and arsenite with the corresponding p_{Ka} values are described in Fig. 6: (Mohan and Pittman. 2007).

The oxidation and reduction of As can be enhanced by microbial activity, iron species, nitrates, dissolved organic matter (DOM) and manganese oxides (Henke. 2009; Johnston et al. 2010). However, As(V) converts faster into As(III) in reducing environments than As(III) transforms into As(V) in oxidizing conditions (Boyle and Jonasson. 1973; Smedley and Kinniburgh. 2002). Redox reactions and adsorption processes are important key factors controlling the mobilization of As in groundwater. Under oxidizing and neutral to alkaline pH, As is strongly adsorbed on Fe, Mn and Al hydroxide minerals. The reductive dissolution of these minerals can release in groundwater As and other oxyanions like V, Mo, Se and U. However, the presence of phosphates, orto-silicic acids and bicarbonate ions can compete with As for the sorption sites on minerals surfaces. Adsorption processes are mainly pH dependent, being higher at low pH (Smedley et al. 2002).

3.3 Geochemical pathways for the mobilization of Arsenic

Key factors controlling the mobilization of arsenic in groundwater are redox potential (Eh) and pH conditions.

Arsenic is one of the most problematic contaminants for humans and the aquatic ecosystems because it can be mobilized in both oxidizing and reducing redox potential and at near-neutral pH. Arsenic is highly mobile compared to other metal-oxyanions such as, selenates, vanadates and uranyl, which are commonly mobilized only under reducing conditions (Ferguson and Gavis. 1972; Zhang and Selim. 2008).

The dissolution of As and resulting mobility can be governed by a combination of biogeochemical processes linked to hydrologic factors.

Two different environmental situations can trigger to the occurrence of As on large scale:

1. *Occurrence of As under oxidizing conditions and high pH.*

This may involve arid and semi-arid regions where groundwater is found under high pH conditions due to the weathering of silicates and carbonates minerals. The process is accompanied by ion exchange reactions between

sediments and water. Dissolved As is accumulated in shallow aquifers mainly in closed basins with lack of water flushing. Under these conditions, arsenate is usually the dominant As specie. And at high pH As is less strongly adsorbed onto the surfaces of Fe, Al oxy-hydroxide minerals. However, the desorption of As at high pH (>8.5) can also induce the release of other ions such as vanadate, uranyl, molybdate and phosphate, being also accumulated in groundwater (Smedley and Kinniburgh. 2002).

2. *Occurrence of As under reducing conditions and neutral pH.*

The second case of high As mobilization is under strong reducing conditions and circum neutral pH, where desorption of As from secondary oxide minerals occur due to reductive dissolution of Fe oxides (Smedley and Kinniburgh. 2002; Sracek et al. 2004). When the conditions are very reducing, SO_4^{2-} ions are reduced to S^{2-} and As is precipitate as secondary sulfate minerals.

Arsenic species may be exposed to different geochemical transformations: (1) methylation in contact with biological organisms, (2) oxidation and reduction, (3) adsorption and desorption, (4) precipitation or co-precipitation and (5) ion displacement (Zhang and Selim. 2008). The factors influencing the occurrence of these processes are related to hydro-chemical conditions, redox potential, pH and the kinetics of dissolution and precipitation of minerals.

Redox processes

The reduction of arsenate As(V) to arsenite As(III) is an important pathway for the release of As from the solid phase into groundwater because is weakly adsorbed on Fe and Al oxy-hydroxides minerals. However, Mn oxides can do the opposite effect oxidizing As from arsenite to arsenate (Fendorf et al. 2010).

Sorption processes

Sorption processes are very important to understand the mobilization of As from sediments to groundwater. Both arsenite (As(III)) and arsenate (As(V)) can be adsorbed on Fe, Al and Mn oxy-hydroxide minerals but with different behaviors. As(III) and As (V) are bound to Fe oxides by an inner-sphere ligand-exchange mechanism, similar to the sorption of phosphates by Fe hydroxides. Sorption processes can occur on permanent charge surfaces (ion exchange) or on variable charge surfaces due to surface complexation (Goldberg and Johnston. 2001). Arsenate is easily adsorbed on Fe-oxides at low pH 3-5, while arsenite will be adsorbed at higher pH from 7 to 8.5. PZC (Point of Zero Charge) is the pH at which the net surface charge of the mineral is zero. The PZC for the most crystalline Fe-mineral hematite is 8.5 and at this pH arsenate species will be desorbed (Smedley et al. 2005). The most common As-bearing Fe-oxide minerals are ferrihydrite (brown), goethite (yellow), hematite (red) and magnetite (Smedley et al. 2002, 2005; Bundschuh et al. 2004; Bhattacharya et al. 2006). Furthermore, the reductive dissolution of these secondary Fe, Al, Mn oxide minerals can release large amounts of As into groundwater. Not only Fe hydroxides are the most common adsorbents for As but also Al and Mn hydroxides and aluminosilicates may retain significant concentrations (Fendorf et al. 2010). Arsenate can also be adsorbed weekly on calcite, increasing with decreasing concentration of carbonates in groundwater, but is not affecting arsenite (Ugilt et al. 2006). As can also be bind to organic matter in soils and sediments, being the maximum retention of As in humic acids (Fendorf et al. 2010).

Precipitation and co-precipitation

Precipitation refers to dissolved As species reacting with other dissolved species (Ca, Mg, Al, Fe(III)) to form solid insoluble products (Henke. 2009).

Co-precipitation refers to As that adsorbs onto the fresh precipitate of other species. Generally, the chemical equilibrium of groundwater determines the chemistry of arsenic. The geochemistry of iron is linked to the geochemistry of arsenic, since iron oxy-hydroxides are important adsorbents of arsenic in natural systems.

Ion exchange

Arsenic partitioning to the aqueous phase can be induced by other competitive ions with more affinity for the sorption sites, like phosphates, dissolved silicates, natural organic matter (NOM) and carbonates (Paige et al. 1997; Fendorf et al. 2010). However, arsenate is more strongly adsorbed on iron oxides than phosphates. Arsenate ions can be replaced by bicarbonate on sorption sites at high pH values. Silicates may inhibit the adsorption of As at pH around 10, while sulfates may decrease the arsenate adsorption at pH from 4 to 7 (Carabante. 2012).

3.4 Toxicity

Arsenic is considered a potential carcinogenic, and a threat for human health and for the aquatic ecosystems. According to the WHO standard guideline established in 1993, the permissible standard limit of As in drinking water was lowered from 50 to 10 μg/L. However, in some parts of the world, especially under developed countries, this limit cannot be afforded due to the high natural concentration of As in groundwater that is poisoning millions of people, also for the scarcity of natural water resources and the lack of instruments to measure such low concentrations (WHO. 1993). In those affected areas the old limit is still prevalent. One example is in the Chaco-Pampean Plain Argentina, where in some regions have been reported high concentrations of As in groundwater, and sometimes the population is not even aware of the toxicity of As and the bad drinking water quality they are exposed. For this reason and according to the Argentinean Food Code regulations (law 12.284) the limit of As for safe drinking water in Argentina is provisionally established at 50 μg/L (Argentinean Food Code. 1994), and it will be re-assessed when the national epidemiological studies will be completed and evaluated by the experts.

The first arsenic poisoning symptoms on humans exposed to contaminated drinking water were discovered in Argentina in 1914, in the Bell Ville city in Cordoba province. This disease is currently known in Argentina as Chronic Endemic Regional Hydroarsenicism (HACRE, in Spanish) (Nicolli et al. 1989; Litter et al. 2010). The main symptoms of HACRE include: skin lesions like melanosis and hyperkeratosis of hands and feet (known as black foot disease) (Fig. 6), respiratory effects, cardiovascular diseases, neurological disorders, hepatic damage, skin cancer, diabetes and high risk of lung, liver, kidney and urinary bladder cancer. Once As is absorbed in the body, it is converted in the liver to a less toxic methylated form and later is largely excreted by the urine (Pimparkar and Bhave. 2011). Generally, urinary As is a good indicator for estimating the exposure, also hair and nail samples may reflect the exposure in the past. However, there is currently no medical treatment for As poisoning and the only way to prevent the disease is by drinking safe water free of As (Litter et al. 2010). On the other hand, it is difficult to identify whether the internal cancer was produced by As or induced by other factors. Both inorganic forms As are toxic for humans,

Figure 6 Skin pigmentation symptoms after the consumption of drinking water contaminated with As.

wherefore previously As(V) was considered less toxic than As(III), in recent studies it has been demonstrated that As(V) can be reduced into As(III) when enters the body causing the same toxicological effects (Lindback and Sjölin. 2006). The most vulnerable communities are usually poor people living in rural areas, with deficient nutritional status, with pre-existent diseases, and also pregnant women and young children.

3.5 Remediation technologies on As contaminated sites

Economic aspects are one of the most important factors for the selection of an As-removal technology, especially in rural populations with low income. The selection of a feasible method to remove As depends on the groundwater chemical composition, speciation, hardness, pH, redox potential conditions, and the volume of water to be treated (Litter et al. 2010). The first aspect to explore is the possibility of tapping an alternative water source free of As. Another option is to drill a new borehole well in a safe aquifer but the costs are high. If these options are not available, conventional or alternative water treatments would be required to ensure safe drinking water for human consumption. However, first is important to have reliable equipments to quantify arsenic concentrations in water, especially, at very low levels (Litter et al. 2010).

Conventional technologies for drinking water treatment include different processes like: oxidation, coagulation-filtration, precipitation, adsorption and ion exchange, membrane

technologies and biological methods (Mohan and Pittman. 2007). These processes can be applied alone or in combination. The techniques used to remove As are mainly based on arsenate adsorption processes, because it is negatively charged and more strongly adsorbed than arsenite that is uncharged. For this reason oxidation of arsenite is the first step previous to other processes (Mohan and Pittman. 2007).

Precipitation is performed by adding salts of iron, magnesium, manganese to arsenate solutions. Coagulation-filtration processes are commonly used in Argentina. In this process, arsenate is absorbed into coagulated flocculs and is separated by filtration. Iron chloride ($FeCl_3$) is the best coagulant because it generates larger flocculs than other coagulants (Mohan and Pittman. 2007). These technologies are simple, cost effective and can be used for large volumes of water. However, they generate large volumes of As-containing sludge which should be treated to avoid potential source of As contamination. Membrane technologies like reverse osmosis, is highly effective for As and F removal, but has high costs of performing and maintenance (membrane fouling) and also has a significant water losses (Alarcón-Herrera et al. 2012). Ion exchange resins are an effective removal for As(V) but not for As(III), but suspended solids and iron precipitates interfere in the process causing clogging (Litter et al. 2010).

Conventional and non-conventional systems are more suitable in large scale than in small villages, mainly for economic reasons. In the last few years, As remediation studies were more focused on adsorption processes using the low-cost adsorbent materials (Mohan and Pittman. 2007). However, further research is required to ensure the low-cost and efficiency of emergent technologies at domestic household levels.

Two water treatment plants were built in the 80's in La Pampa province, working to remove the salts and toxic elements from water for domestic drinking water. The treatments consisted of microfiltration to remove solid particles and reverse osmosis for removal of salts and As. The last purification process uses UV radiation and ozone (O_3) or chlorine to ensure safe distribution of drinking water (O'Reilly et al. 2010). However, these treatments are only installed in major cities, but in many small rural villages of the Chaco-Pampean Plain Argentina, tap water from the shallow aquifers is only submitted to chlorination process (APA. 2001).

4 MATERIALS AND METHODS

4.1Field work

Fieldwork consisted of groundwater and sediments sampling and measurement of the physicochemical parameters. Sampling campaigns were carried out in September 2011.

4.1.1 Groundwater sampling

A total of 44 groundwater wells were sampled in the shallow aquifers of the NE of La Pampa province. 32 groundwater samples were collected in the area of Quemú Quemú (Fig. 7) and 12 samples in the area of Intendente Alvear (Fig. 8). Groundwater was pumped out from the shallow aquifers by windmills (at 5-6 m depth) and by submerged electrical pumps (from 10-25m depth). The locations of the wells were selected according to previous hydrological studies carried out in the same area by other students from the National University of La Pampa in Santa Rosa. Field work was carried out in collaboration with the municipal authorities and the cooperatives for water service and management, COSYPRO in Quemú Quemú and COSERIA in Intendente Alvear. The private cooperatives are responsible for the monitoring, supply and control of the public water system. Sewage waters from the village are not treated and grey waters are discharged into the field in controlled lagoons. Groundwater from municipal wells of QQ could not be sampled because of non-functioning of the pumps during field work. Information of water usage and well depth was asked directly to the owner. Each well was geo-referenced using a GPS Garmin Etrex model Legend. Before measurement and sampling groundwater was purged for 5-10 minutes to collect a representative water sample from the shallow aquifer.

The following physico-chemical parameters were recorded in the field prior to filtration and acidification of the water sample:

Temperature, electrical conductivity and TDS were measured using an electrical conductivity meter HANNA HI9635 with operating range 0-220 mS/cm; pH and redox potential (Eh) were measured using a portable pH-meter Orion-250A. Eh values were normalized to the Standard Hydrogen Electrode by adding +244.3mV according to the standard protocols (Appelo and Parkhust. 2005).

Groundwater for major anion, cation and trace elements analysis was filtered using a sterile single use cellulose filter of 0.45μm. Samples for major cations and trace elements analysis were

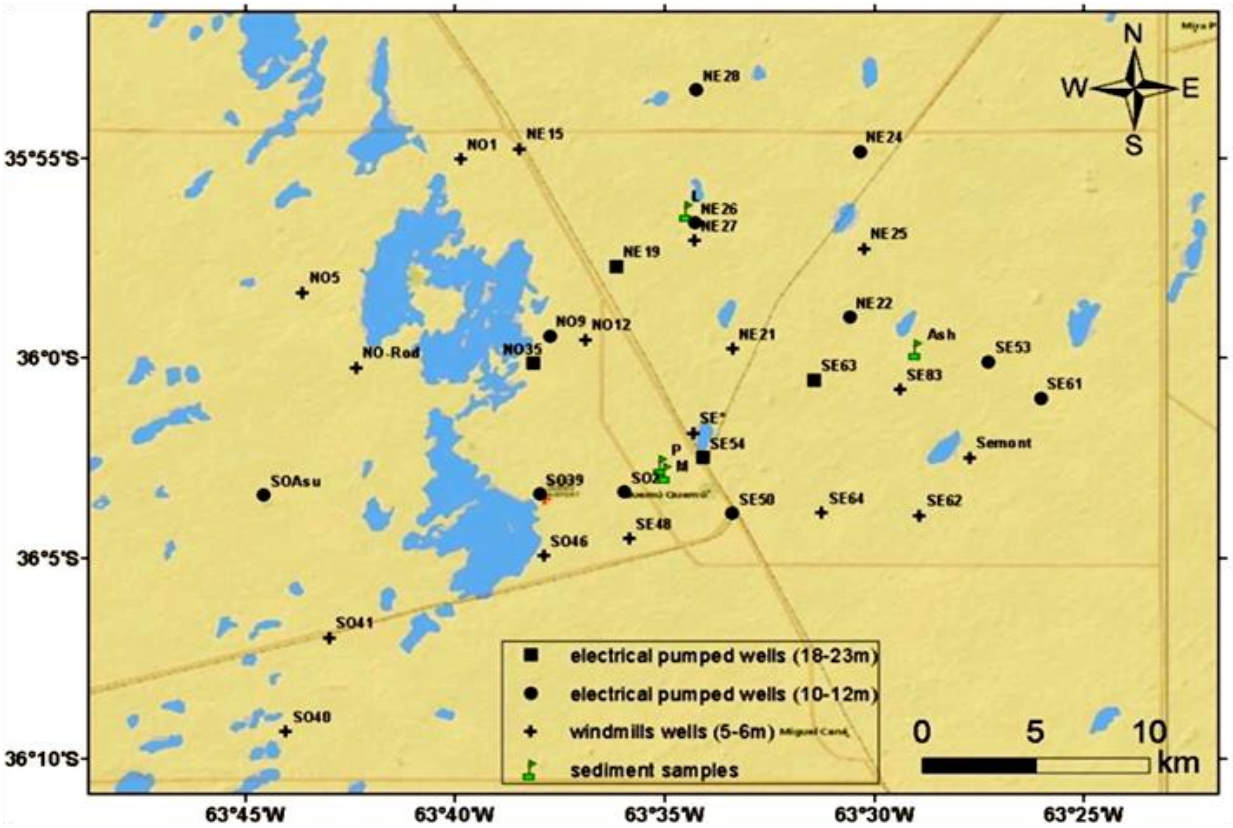

Figure 7 Map of the groundwater and sediments samples collected in Quemú Quemú study area.

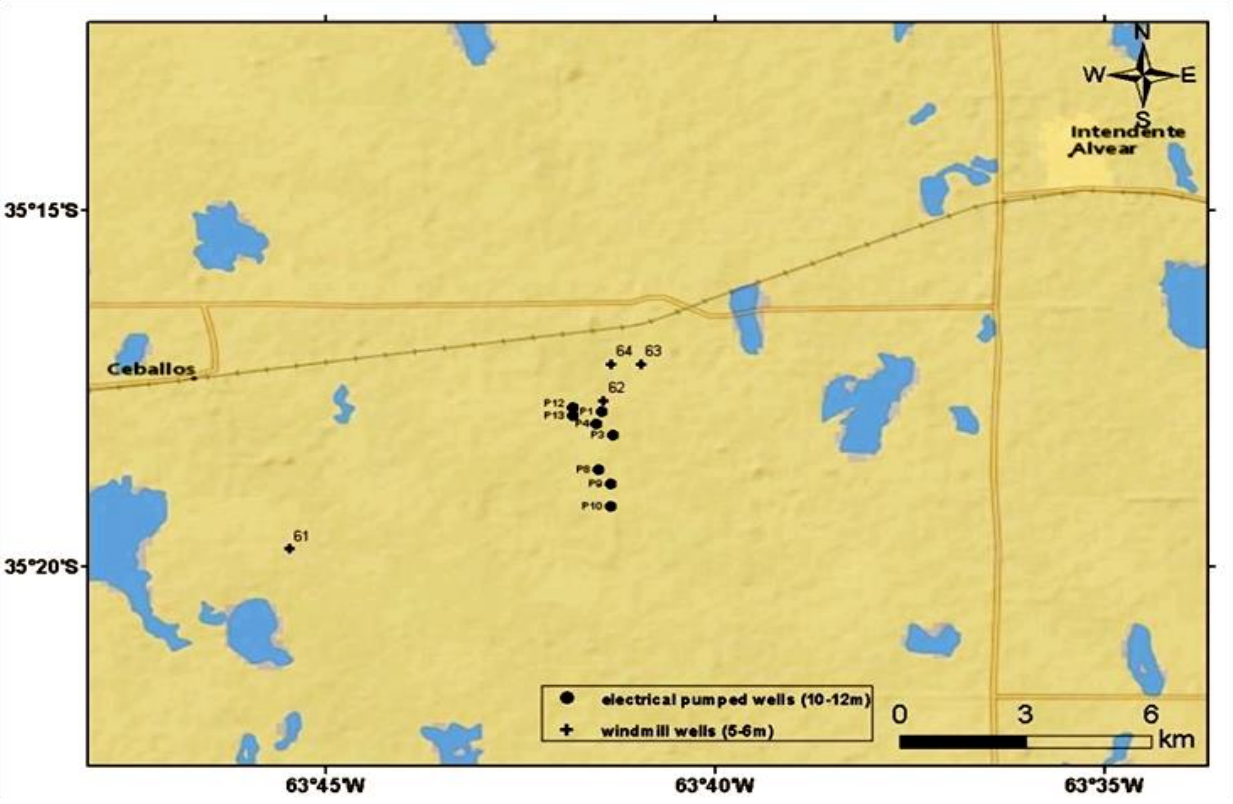

Figure 8 Map of the groundwater samples collected in Intendente Alvear study area within the aquifer Las Mercedes.

acidified to pH<2 with 7M HNO_3, to avoid undesirable secondary reactions. Immediately, the samples were labeled, stored in a portable cooler at 4ºC and sent to Sweden for further laboratory analysis.

4.1.2 Sediments sampling

A total of 10 sediment samples were collected at four different points in the area of Quemú Quemú. The samples were named according to the place where they were found: sediments M and P from the new drilled boreholes in the recharge area (Fig. 9a), sample L on the surface of the semi dry lake in discharge area (Fig. 9b) and sample A from volcanic ash placed in the cutting of the road (Fig. 9c). The sediments locations are displayed in the sampling site map of QQ (Fig. 7). All the sediments were labeled, packed in plastic bags and sent to Sweden for further experimental work and analysis.

4.2 Groundwater analysis

Groundwater samples were analyzed at the Department of Land and Water Resources Engineering at KTH and at the Stockholm University in Sweden. Hydro-chemical analyses consisted of:

- Alkalinity: as bicarbonate concentration was measured by titration following the standard protocol SS-EN ISO 9963-2, at the laboratory of Land and Water Resources Engineering, KTH.

Alkalinity is the measure of the buffer capacity of water to resist an acid and is defined as:

$$\text{Alkalinity} = [HCO_3^-] + 2[CO_3^{2-}] + [OH^-] - [H^+]$$

In natural waters when pH ranges from 5.5-8 the predominant specie is HCO_3^-. In this case all terms can be neglected and the alkalinity is equal to the concentration of bicarbonate ions: Alkalinity = $[HCO_3^-]$.

A manual titration with HCl 20.1mmol/L was performed and the end point was detected by an acid-base indicator (phenophtaleine). The alkalinity values were obtained using the following equation:

$$\text{Alkalinity} = \frac{C(V_{HCl} - V_{HClblank})}{V_s} \text{mmol} \cdot L^{-1}$$

Where,

C=concentration of HCl used in the titration (mol/L)

V_{HCl}= volume of HCl used in the titration (mL)

V_{HCl} blank= volume of HCl used for the blank (mL)

Vs= volume of groundwater sample used (mL)

To convert alkalinity from mmol/L to mg/L the result was multiplied by 61, which is the molar mass of HCO_3^-.

- Major anions: chloride (Cl^-), nitrate (NO_3^-), sulfate (SO_4^{2-}), were determined by Dionex DX-120 Ion Chromatograph. Phosphate (PO_4^{3-}) was analyzed on Aquatec 5400 analyzer at wavelength of 690 nm. Fluoride (F^-) was determined by ion-selective electrode technique. All these analyses were carried out at the Department of Land and Water Resources Engineering at KTH. Some samples were diluted 1:20 before analysis to meet the sensitivity of the equipment.
- Major cations and trace elements: were analyzed by inductively coupled plasma-optical emission spectrometry (ICP-OES), at the Department of Geology and Geochemistry at Stockholm University. This method has good sensitivity and low time consumption to determine very low concentrations from the groundwater samples.

Figure 9 Sediments samples collected in the area of QQ in the following sites: a)from the new boreholes, b) on the surface of the dry lake and c) on the cutting of the road for volcanic ash sampling.

- Ionic Charge Balance: is required to show the accuracy of the results for major ions. Ion concentrations were calculated in meq/L. In natural waters anionic charges should be equal to the catonic charges (Appelo and Postma. 2005). Ionic charge balance was calculated following the equation:

$$I.C.B(\%) = \frac{\sum\left(cations, \frac{meq}{L}\right) - \sum\left(anions, \frac{meq}{L}\right)}{\sum\left(cations, \frac{meq}{L}\right) + \sum\left(anions, \frac{meq}{L}\right)} x100$$

4.3 Geochemical modeling

The total aqueous speciation of groundwater compounds was determined on Visual Minteq 3.0 Geochemical modeling, by using the database minteqa2 (Gustafsson, JP. 2011). The five samples with the highest concentration of As were selected for a total aqueous speciation and determination of Saturation Index of minerals. This geochemical modeling was performed by PHREEQC using the database minteq.v4 (Parkhust et al. 1999). Saturation Index indicates whether or not groundwater tends to precipitate or dissolve a particular mineral and is calculated by comparing the chemical activities of the mineral ions dissolved in groundwater with their solubility product. Saturation index is defined as:

$$SI = \log\left(\frac{IAP}{K_{sp}}\right)$$

Where IAP is the ion activity product and K_{sp} is the solubility product for a given temperature.

When SI=0 (IAP=K_{sp}) the solution is in equilibrium with the mineral phase. When SI>0 the solution is supersaturated with the mineral and when SI<0 is under-saturated.

4.4 Sediment analysis

pH of leachates, Cation Exchange Capacity (CEC), and Sequential Extraction Procedure in four steps, were determined for all the sediments samples at the laboratory of LWR department, KTH. The qualitative mineralogical composition of four sediments was analyzed by X-Ray Diffraction (XRD) in Finland.

4.4.1 pH and Cation Exchange Capacity

For determination of pH, an aliquot with 25 ml of distilled water was added to 10g of sieved soil, it was kept shaken for 5 min and then settled for 30 min before to measure the pH of the supernatant.

Cation Exchange Capacity was used to measure the total amount of available sites on the surface of the sediment exchangeable with cations. Usually, the highest cation exchange capacity occurs on clay and organic matter surfaces. CEC has a buffer effect towards acidification, which means that a site with high CEC takes longer time to acidify than a site with low CEC.

For determination of CEC it was used the method of Barium Chloride–triethanolamine (TEA) suggested by professor Gunnar Jacks in the lab of KTH. Before starting the procedure, the samples were dried at 65ºC. Then, 5g of each sediment sample was mixed with 12.5 mL of buffer solution (0.5N $BaCl_2 \cdot 2H_2O$ and 0.2N TEA adjusted to pH 8.2 with HCl) and left shaking for 1 hour. The mixed solution was filtered through OOH filters and 75ml of buffer solution was added in different steps to remove the released solids in the bottle. Finally, 50mL of the replacement solution (0.5N $BaCl_2$ with 0.4ml of the buffer solution per liter) was added to each sample.

The solutions obtained were analyzed by atomic absorption spectrometry model VARIAN at the laboratory of LWR in KTH, in order to determine the concentrations of Ca^{2+}, Na^{+}, K^{+} and Mg^{2+}. The CEC values were calculated following the equation:

$$C(X_i) = \frac{12.5x\left(\frac{100}{5}\right)xc(X_i)xV}{1000xM_{X_i}}$$

$$CEC = \sum C(X_i)$$

Where, C(Xi) is the cation concentration (meq/L), c(Xi) is the cation concentration (mg/L), M_{Xi} is the molar mass (g/mol), V is the total volum of $BaCl_2$ added (50mL) and CEC is the cation exchange capacity (meq/100g).

4.4.2 Sequential Extraction Procedure

The extraction procedure employed was a modified version from Bhattacharya et al. 2006, and was used to investigate the composition of the sediment that may be potentially leached into groundwater.

Four steps sequential extraction were performed on each sediment sample by duplicate at the laboratory of LWR at KTH. The aim is to quantify the amount of trace metals released from the sediments with multiple extracting reagents. These reagents destroy the chemical bindings between metals and sediments allowing the metals to be released in the solution. The content of moisture was determined for each sediment sample before SEP. The four steps sequential extraction procedure was as follows:

- De-ionized water (DIW) extraction at pH 7: for quantifying metals on the water-soluble fraction. 4g of dry sediment from each sample were put in 250 ml aliquots together with 50 ml de-ionized water adjusted to pH 6.95 with NaOH. After shaking on a horizontal shaker for 2 hours, the solutions were filtered using 0.45 μm filters and acidified with 0.5 ml of concentrated HNO_3 and stored in 50 ml plastic bottles.
- Acetate (NaOAc) extraction at pH: to quantify metals bound to carbonate and phosphate minerals phases. The remaining contents of the aliquot from the previous step were left for decantation and the liquid fraction was removed. 200ml 1M of acetate (C_2H_3NaOs) was added to each flask. The flasks were left for another 2 hours and the solutions filtered through 00K filters, acidified and stored in 50 ml plastic bottles.
- Oxalate ($(NH_4)_2C_2O_4$) extraction at pH: to quantify the elements bound to secondary amorphous Fe, Al, Mn oxides and hydroxides. The remaining contents of the flasks from the previous steps were left for decantation and liquid fraction was removed. Then, 100 ml of 0.2 M oxalate ($(NH_4)_2C_2O_4$) were added in dark and left for 4h in the horizontal shaker. The contents of the conical flasks from these phases were left for decantation and the liquid fraction was removed. Samples were centrifuged for 15 min at 4000rpm. The supernatants were filtered through 0.45μm Sartorius filters and diluted 5 times prior to analysis.
- Residual fraction (7M HNO_3) extraction at pH<2: To quantify metals bound to more crystalline mineral phases or bound to silicates not leached in the previous steps. The remaining sediment in the conical flask was extracted with HNO_3 concentrated (to pH<2) in the digestion tubes and thereafter boiled for 2.5 hours on a digester with small glass portions to prevent eruptive boiling. Then, the solutions were left to cool down, filtered through OOK filters, and diluted to 50mL with DIW. The metals held in crystalline structures which are not expected to be released into groundwater in normal conditions in the environment.

Trace metal concentrations from the extracted solutions were determined by ICP-OES at Department of Geology and Geochemistry at Stockholm University.

4.4.3 Mineralogical analysis

X-Ray Diffraction (XRD) analysis was performed on four selected sediment samples: L3, M2, P3 and A in order to determine the qualitative mineralogical composition of the sediments. Knowing the mineralogical phases it will be possible to determine which metals are likely to be released in the aqueous phase and if they possess a high trace metal pollution problem. Around 10 g of each sediment sample was weighted and stored for further XRD analysis in the laboratories of the University of Turku in Finland. The equipment used was a Phillips P-XRD (40kV and 25mA) model. XRD spectra of the solid phases were obtained by scanning the 2theta from 5º to 75º with respect to the counts. XRD spectra were interpreted by Match 2.0.12 graphic software, and the mineral phases were identified using PDF-2 database (Match. 2.0.12).

4.5 Data processing

The following programs were used to process the data:

- Aquachem 4.0, Waterloo Hydrogeologic Inc. software: for plotting the statistical diagrams of the hydro-chemical results.
- Arc-GIS 10.0: for mapping the location of the wells sampled in the study areas.
- Surfer Golden Software 8.0: for plotting the spatial distribution maps. The statistical interpolation method applied was ordinary kriging interpolation.
- Visual Minteq 3.0 for modeling the As aqueous speciation.
- PHREEQC 2.18 software's for modeling the total aqueous speciation and saturation index.
- AutoCAD 10.0: for plotting soil profiles and the hydro-geological sketch map of the study area.
- Match! 2.0.12, phase identification from powder diffraction for interpretation of XRD results.
- Geochemist's workbench 7.0, for plotting the Eh-pH diagrams.

5 RESULTS

5.1 Groundwater chemistry

The statistical summary of the hydro-chemical analytical results is presented in table 2 for an assessment of the drinking water quality according to WHO standard guideline (WHO. 2011) and the Argentinean Food Code (CAA. 1994).

Table 2: Statistical summary of groundwater chemical characterization from the two study areas in NE of La Pampa province. *Water quality assessment according to the WHO standard limits for drinking water*, (WHO. 2011) and the Argentinean Food Code regulations** (CAA. 1994).*

			QUEMÚ QUEMÚ (n=32)						INTENDENTE ALVEAR (n=12)					
Parameter	Units	WHO limit* CAA limit**	Min	Max	Mean	Median	SD	Samples > std. limits	Min	Max	Mean	Median	SD	Samples > std. limits
pH		6.5-9.5*	7.4	9.2	8.2	8.1	0.4	0	7.7	8.8	8.3	8.3	0.3	0
		*6.5-8.5***						18%						25%
Eh	mV	-	113.6	232.6	173.4	177.3	27.4	-	136.7	202.1	167.7	167.2	19.2	-
EC	µS/cm	300*	456	11400	3274	2045	2812	100%	1160	10640	3908	2345	3123	100%
T	ºC	-	13.9	22	15.5	15.3	1.5	-	10.5	16.2	13.8	13.4	1.8	-
HCO_3^-	mg/L	-	190	1293.5	672.1	652.9	258.4	-	300.4	797	489.4	462.9	167.9	-
Cl^-	mg/L	250*	7.6	1839.2	390.9	182.9	492.6	38%	43.4	1607	546	314.3	502.6	67%
		*350***						34%						42%
NO_3^-	mg/L	11.3*	3.4	515	78.5	52.9	93.1	91%	7.6	347.3	53.7	23.9	93.5	92%
		*45**						63%						17%
SO_4^{2-}	mg/L	500*	6.7	1568.7	335.9	142.2	417.7	28%	36	1442.3	493.9	273.2	464	42%
		*400***						28%						42%
PO_4^{3-}	mg/L	-	12.6	539.1	129.9	69.6	148.6	-	19.9	467.8	112	33.7	144.3	-
Na^+	mg/L	200*	12.9	1749.2	560.3	429.9	468.9	75%	200.5	1697.5	663	417.2	497.3	100%
K^+	mg/L	-	8.7	115.9	24	11.9	25.6	-	9.4	59.4	19.8	12.8	15.6	-
Mg^{2+}	mg/L	-	1.6	161.6	43.6	33.5	43.2	-	10.1	128	41.5	31.5	34.3	-
Ca^{2+}	mg/L	-	2.4	229.8	49.8	29.9	52.5	-	14.4	83.9	34.3	29.2	20.6	-
TDS	mg/L	1200*	410	18628	1834.5	1891	4588.2	81%	839	6015	1719.6	2022	1732.7	75%
		*1500***						-						-
Al	µg/L	-	11.9	112.2	30.4	23	23.8	-	20.9	80.1	36.5	34.5	15.3	-
As	µg/L	10*	5.9	535.1	114	71.8	131.3	94%	17.5	248.4	65.3	46	64.8	100%
		*50***						56%						50%
B	µg/L	2400*	111	5483	2086.1	1643.3	1667	32%	437.3	3793	1707.8	1562.8	1102.1	25%
		*500***						75%						75%
Co	µg/L	-	1.7	2.4	2	1.9	0.3	-	1.7	3.2	2	1.9	0.5	-
Cr	µg/L	50*	0.8	12.2	4.4	2.8	3.4	0	0.5	4.7	2.4	2.3	1.5	0
Cu	µg/L	2000*	0.6	237	16.9	4.7	42.4	0	0.7	322.4	36.1	9.4	90.4	0
		*1000***						0						0
F	mg/L	1.5*	0.5	14.2	4.2	3.2	3.5	78%	1.6	7.4	3.1	2.8	1.6	100%
		0.8-1.2**						84%						100%
Fe	µg/L	-	4.4	929.5	53.9	11.8	165.8	-	6.7	1551.4	199.8	21	458.5	-
Li	µg/L	-	10.6	67.2	34.9	38.5	15.1	-	17.3	65.3	32.8	22.4	16.8	-
Mn	µg/L	400*	0.1	18.6	3.6	1.3	4.9	0	0.2	16.9	4.6	4.2	4.7	0
		100**						0						0
Mo	µg/L	70	4.1	490.3	61	36.9	94.1	25%	3.6	74.5	18.2	14.1	18.9	8%
Pb	µg/L	10*	3.8	29.5	11.9	11.5	5.9	28%	6.8	12.3	9.1	8.6	1.6	25%
		50**						0						0
Rb	µg/L	-	6.9	58.4	16.8	11.8	13.6	-	7.7	36.4	16.5	12	9.5	-
Si	mg/L	-	16.4	21.7	19	19.1	1.3	-	14.4	19.7	18.1	18.5	1.7	-
Sr	µg/L	-	58.1	4890.3	1010	861.8	1020.5	-	317.6	2571.8	955.9	1011.4	734.1	-
Ti	µg/L	-	0.2	1.8	0.4	0.3	0.3	-	0.3	2.2	0.6	0.5	0.5	-
U	µg/L	30*	5.9	47.6	17.1	15.5	10.1	10%	4.1	20	9	8.5	4.4	0
V	µg/L	-	20	1971.6	351.3	189	518.9	-	113.3	280.2	205.3	224.7	67.3	-
Zn	µg/L	-	5.4	801.1	82.2	46.9	139.2	-	22.3	482.7	76.4	40.8	128.8	-

5.1.1 Field parameters

Information of the wells sampled and results from the parameters measured in the field are presented in Appendix I.

Groundwater from QQ study area showed temperatures ranging from 13.9ºC to 22ºC (average of 15.5ºC). The pH ranged from 7.4 to 9.2 (average of 8.2) indicating circum-neutral to alkaline conditions. High salinity levels were evidenced by the high electric conductivity (EC). EC values varied from 456 to 11400 µS/cm (average of 3274.2 µS/cm), exceeding the WHO standard limit for drinking water (300 µS/cm). 50% of the wells resulted in brackish water (EC>2000µS/cm) while 25% of the wells in saline water. The redox potential (Eh) measured in the field was corrected for SHE and it ranged between 113.6 and 232.6mV (average of 173.4mV) indicating oxidizing conditions of groundwater. The depth to water table varied according to the topographic gradient from west to east, ranging from 2 to 7 m below the ground (average 3.55 m).

Groundwater from the area of Intendente Alvear (n=12) showed lower temperatures than in QQ, ranging from 10.5 to 16.2ºC (average 13.8ºC). The pH range was also under neutral to alkaline conditions, ranging from 7.7 to 8.8 (average of 8.3). EC results were higher than in QQ, ranging from 1160 to 10640µS/cm (average of 3908.3 µS/cm), with 25% of the wells being brackish water. Redox Potential (Eh) corrected by SHE showed similar oxidizing conditions and ranged from 136.7 to 202.1 mV (average of 167.7 mV). Depth to water table ranged from 2.3 to 4.5 m with an average of 3.5 m.

Total dissolved solids (TDS) showed high variability of concentrations in both study areas, varying from 410 to 18628 mg/L (average of 1834 mg/L) in the area of QQ and from 839 to 6015 mg/L (average of 4203 mg/L) in the area of IA. According to WHO standard limit groundwater above 1200 mg/L of TDS is unacceptable for drinking purpose (WHO. 2011) and therefore, 81% and 75% of samples from QQ and IA respectively exceeded the permissible limits for drinking water.

5.1.2 Major ions

Major ions concentrations, ionic charge balance and water type results are displayed in Appendix II.

The statistical distribution of major ion composition with the min, max, median, 25% and 75% of the measured ions concentrations is displayed in the box and whisker plot (Fig. 10)

The distribution of major anions in the area of QQ showed significant spatial variation, with dominance of HCO_3^- concentrations, ranging from 190 mg/L to 1293.5 mg/L (average 672.1 mg/L), followed by chlorite concentrations that ranged from 7.6 mg/L to 1839.2 mg/L (average 390.9 mg/L), and SO_4^{2-} concentrations that varied from 6.7 to 1568.7 mg/L (mean 335.9 mg/L). Phosphate levels showed high variability of concentrations ranging from 12.6 mg/L to 539.1 mg/L (average 129.8 mg/L) and nitrate concentrations were also high in some wells ranging from 3.4 mg/L to 515 mg/L (average 78.5 mg/L), probably originated from anthropogenic contamination. Major cations concentrations analyzed from QQ shallow wells showed high variability, Na showed the highest values of concentration, ranging from 12.9 to 1749.2 mg/L (average 560.3 mg/L), following

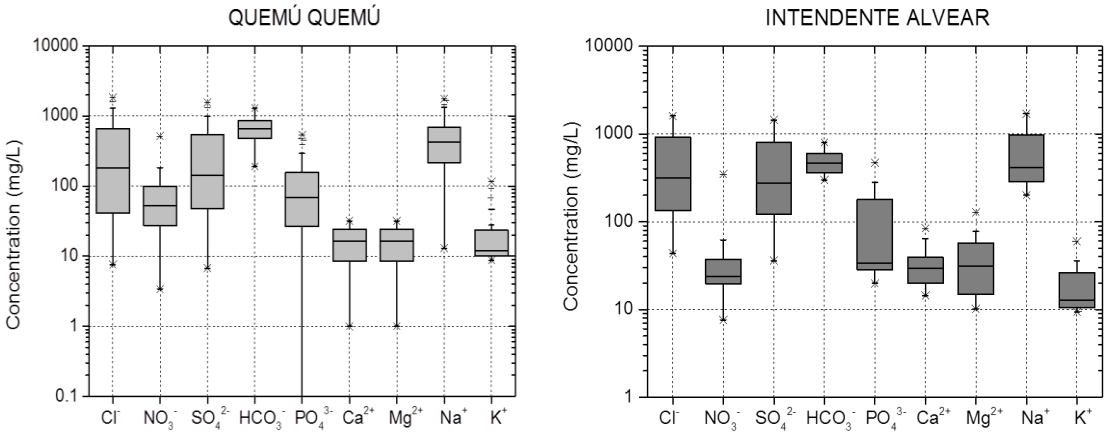

Figure 10 Box and whisker diagrams showing the statistical distribution of trace elements concentrations in groundwater sampled in QQ and IA. It is represented the min., 25% percentile, median, 75% percentile and max., of the concentrations.

was Ca^{2+} that ranged from 2.4 to 229.8 mg/L (average 49.8 mg/L), while the low range of concentrations were, Mg^{2+} that varied from 1.6 to 161.6 mg/L (average 43.6 mg/L) and K^{+} with concentrations lying between 8.7 mg/L and 115.9 mg/L (average 24 mg/L).

The major anions results of groundwater in the area of Intendente Alvear showed similar wide variation of concentrations than in the area of QQ. The predominant anions were Cl^{-} ranging from 43.4 to 1607 (average 546 mg/L), followed by HCO_3^{-} concentrations that varied from 300.4 mg/L to 797 mg/L (average 489.4 mg/L) and also SO_4^{2-} concentrations ranging from 36 to 1442.3 mg/L (average 493.9 mg/L). Phosphate levels were similar than those in QQ wells, ranging from 19.9 to 467.8 mg/L (average 112 mg/L), while nitrate concentrations decreased compared to the values from QQ ranging from 7.5 mg/L to 347.3 mg/L (average 53.7 mg/L). The variation of major cations distribution in groundwater from IA was similar than in groundwater from QQ, with dominance of Na^{+} concentrations that ranged from 200.5 to 1697.5 mg/L (average 663 mg/L), Ca^{2+} ranged from 14.4 to 83.9 mg/L (average 34.3 mg/L) and Mg^{2+} ranged from 10.1 to 128 mg/L (average 31.5 mg/L). K^{+} showed the lowest range of concentrations varying between 9.4 and 59.4 mg/L (average 19.8 mg/L).

Groundwater from both study areas, QQ and IA, exceeded the WHO standard limits for drinking water in salinity, NO_3^{-}, Cl^{-}, SO_4^{2-} and Na^{+}.

Ionic charge balance and water type

The ionic charge balance was within the acceptable error ranging between 5-10% in both areas, except one well in area of QQ (sample NO_2) that was out of range (-12.5%).

The Piper plot diagram showed that groundwater evolves from Ca^{2+} and HCO_3^{-} towards Na^{+}-HCO_3^{-}, Na^{+}-Cl^{-} and Na-SO_4^{2-}(Fig. 11). Groundwater type in the area of QQ is predominated by Na-HCO_3^{-} composition in 80% of the wells, followed by Na-Cl-SO_4^{2-} in 20% of the wells sampled. The predominant water type in IA study area is mainly composed of 50% of the wells Na-HCO_3-Cl and 50% Na-Cl-SO_4^{2-}water type. Brackish water is typically Na-Cl-SO_4^{2-} type and the highest concentrations were observed in discharge areas. Water type results are shown in Appendix II.

5.1.3 Trace Elements

Spatial variability of trace elements concentrations was observed in groundwater samples collected in QQ and in IA (Fig. 12).

Arsenic

Total Arsenic concentration ranged from 5.9 to 535.1 µg/L (average of 114 µg/L) for groundwater sampled in QQ, while in the area of IA the concentration of As ranged from 17.5 to 248.4 µg/L (average of 65.3 µg/L). 12 out of 32 groundwater samples from QQ showed As>100 µg/L while in IA only 2 out of 12 wells. According to Argentinean Food Code As limit of 50µg/L, 56.3% of the samples in the area of QQ and in 50% of the wells in IA were

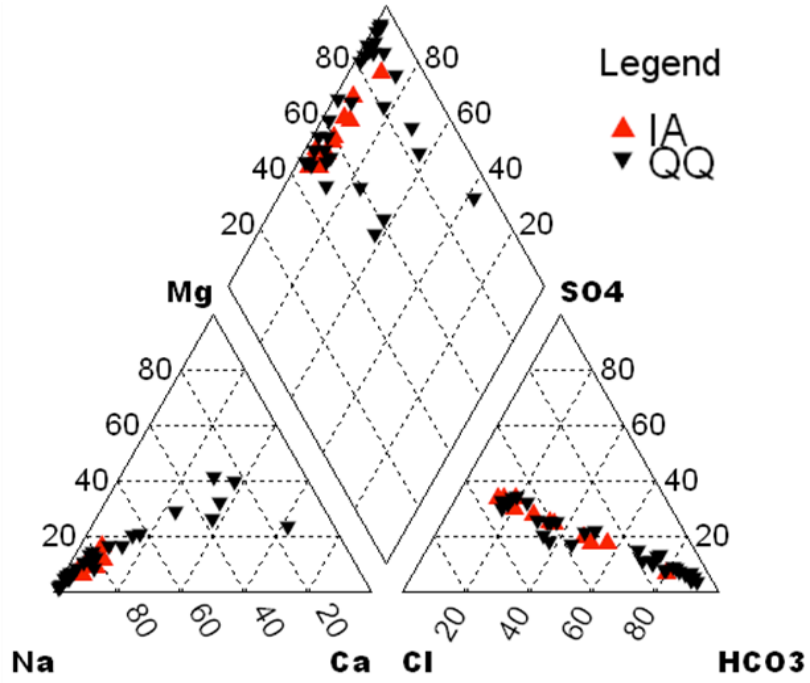

Figure 11 Piper plot of groundwater showing the distribution from saline water (Na-Cl), fresh water with cation exchange (Ca/Mg-HCO_3) and old fresh water types (Na-HCO_3).

exceeding that limit. However, based on the WHO standard limit for As of 10μg/L (WHO. 2011), 93.7% of the samples from QQ and all the samples from IA were above the limit and therefore, unsuitable for drinking purposes. The concentrations of As based on different water pumping systems at different depths, ranged from 23 to 122 μg/L (windmills), in shallow wells at 10-12 m from the saturated zone ranged from 34 to 345 μg/L and in the deeper wells of the shallow aquifer (18-25m) As ranged from 23 to 456 μg/L.

Trace elements from volcanic source

F, B, V, U and Mo are tracers of geothermal activities and they might be possible competitors of As oxyanions for sorption sites on Fe, Al and Mn mineral phases. Fluoride levels were very high in some wells, ranging from 0.5 to 14.2 mg/L (average of 4.2 mg/L) in QQ, with 78% of the wells exceeding the WHO standard limit of 1.5 mg/L. In groundwater samples from IA fluoride ranged from 1.5 to 7.4 mg/L (average of 3.1mg/L), and all the samples exceeded the WHO standard limit for drinking water. Boron, mainly as $B(OH)_3$ and $B(OH)_4$ oxyanions, showed high concentrations in saline waters. In the area of QQ, B ranged from 111 to 5483μg/L (average of 2086.1 μg/L) while in IA it varied from 437 to 3793 μg/L (average of 1708 μg/L). Since 2009 the WHO standard limit of B for safe drinking water has been established at 2.4 mg/L (WHO. 2011) and it was exceeded in 10 of 32 wells in QQ and 3 of 12 wells in IA. Vanadium occurred mainly as vanadate oxyanions and showed high concentrations in some wells similar to As levels. V showed higher levels in QQ sampled wells than in IA ranging from 20 to 1971.6 μg/L (average of 351.3 μg/L), and from 113.2 to 280.2 μg/L (average of 205.3 μg/L) in the IA study area. However, there is not any standard limit reported for Vanadium (WHO. 2011). Uranium concentrations were also high in some wells. In the area of QQ, U concentrations ranged from 5.9 to 47.6 μg/L (average of 17.1μg/L), while in groundwater samples from IA the concentrations were lower, ranging from 4.1 to 20 μg/L (average of 9 μg/L). The permissible WHO standard limit for U is 15μg/L (WHO. 2011), and it was exceeded in 15 out of 32 wells in QQ and in 1 well in IA. Mo concentrations ranged from 4.12 to 490.3 μg/L (average 61 μg/L) in the wells from QQ while in groundwater samples from IA it ranged from 3.5 to 74.5 μg/L (average of 18.2 μg/L).

Iron, Aluminium and Manganese

Total Fe concentrations in groundwater from QQ varied from 4.4 to 929.5 μg/L (average of 53.9μg/L). The average concentration of Fe decreases to 24.6μg/L, if the anomalous value of 929.5μg/L is excluded. In the wells from IA total Fe ranged from 6.7 to 1551.3μg/L (average of 199.8μg/L) and the average decreases to 23.25μg/L, if the values 1551.4 and 614 μg/L are excluded. These high concentrations of Fe might be due to the presence of Fe colloids in groundwater sample. Al concentrations ranged from 11.8 to 112.2μg/L (average of 30.4μg/L) in groundwater samples from QQ and from 20.8 to 80.1μg/L (average of 36.5μg/L) in groundwater samples from IA. Dissolved Mn concentrations were less abundant than those of Fe and Al, in groundwater samples from QQ it ranged from 0.1 to 18.6 μg/L (average 3.6 μg/L) while it ranged from 0.2 to 16.9 μg/L (average 4.6 μg/L) in IA.

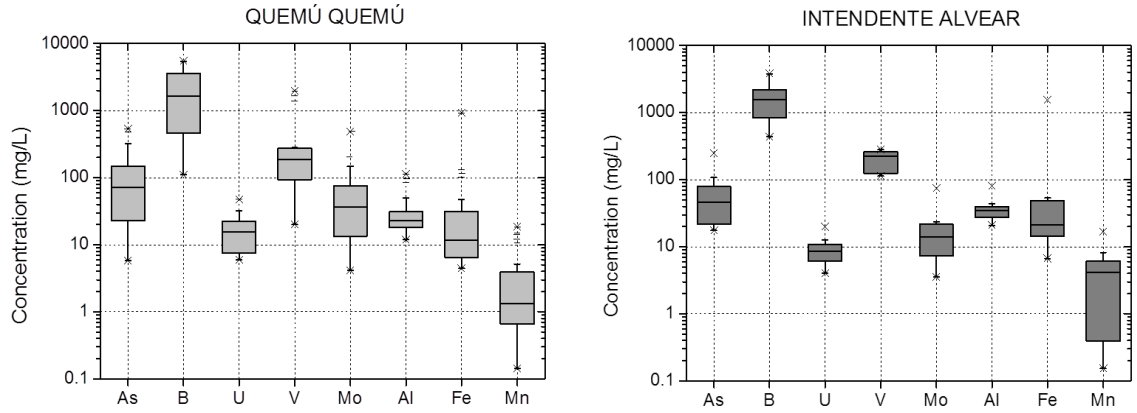

Figure 12 Box and whisker diagrams showing the statistical distribution of trace elements concentrations in groundwater sampled in QQ and IA. It is represented the min., 25% percentile, median, 75% percentile and max., of the concentrations.

Other trace elements

High concentrations of dissolved Si were found in shallow aquifers of both study areas. In the area of QQ Si ranged from 16.4 to 21.7 mg/L (average of 19mg/L) and similar concentrations of Si were found in the area of IA, ranging from 14.4 to 19.7mg/L (average of 18.1mg/L). Cu concentrations reached a maximum value of 237µg/L in the area of QQ (average 17 µg/L) and the maximum concentration of Cu was 322.4µg/L in the area of IA (average 36.1 µg/L). The concentrations of Cu were below the WHO standard limit for drinking water (2000 µg/L) in all groundwater samples. Zn concentration quite similar than those of Cu and they reached an average concentration of 82.2µg/L in the area of QQ and an average of 76.4µg/L in the area of IA. There was not any standard limit established for Zn in the WHO Standard Guideline for drinking water (WHO. 2011).

5.2 Correlations between As and other parameters

The correlation coefficient matrix between As and other hydro-chemical parameters from both study areas are presented in Appendix IV.

5.2.1 Area of Quemú Quemú

As shows positive correlations with F^- (r>0.87), V (r>0.81), HCO_3^- (r>0.64) concentrations and also weakly positive correlations with pH (r>0.55) and Eh (considering the highest As wells). It is also observed a weak positive correlation between As and B (r>0.47), U (r>0.43) and Mo (r>0.2) concentrations (Fig. 13). However, As does not show any correlation with Al, Mn, Fe, Cu and Zn concentrations. Regarding the major ions, low positive correlations are observed between As and the major cations Na^+, K^+ while negative correlation are seen with Ca^{2+} and Mg^{2+} ions. Similarly, weak positive correlation is observed between As and EC. In general, negative correlations are observed between As and PO_4^{3-}, SO_4^{2-} and NO_3^- .Other correlations can explain the hydro-geochemical composition of groundwater in shallow aquifers. Strong positive correlations are observed between Na^+ and Cl^-, and also between B concentrations and EC, Cl^-, Na^+, HCO_3^- and U. In general, no clear trend is observed between As concentrations and the depth to groundwater table collected from the different pumping systems windmills and electrical pumps.

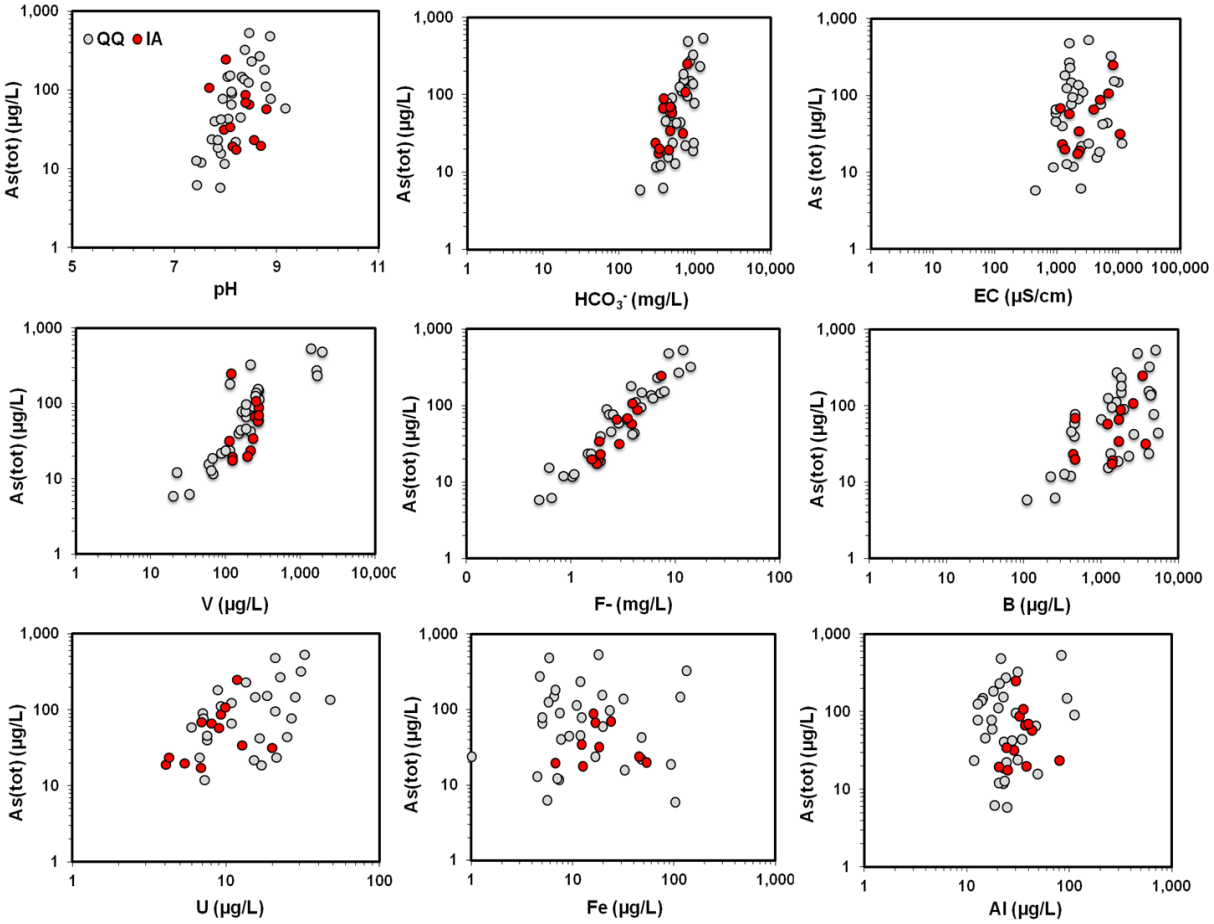

Figure 13 Scatter plots showing the correlation between As concentrations and other hydro-chemical parameters from QQ and IA study areas.

5.2.2 Area of Intendente Alvear

In general, the correlations between As and other parameters in the area of IA follow quite similar trend than results obtained in the area of QQ (Fig. 13). A very good positive correlation is observed between As and F^- ($r>0.95$), HCO_3^- ($r>0.7$) and lower with EC ($r>0.5$). In contrast with the results observed in QQ, no clear correlation is seen between As-pH and As-V in groundwater samples from IA. However, weaker positive correlation is observed between As-SO_4^{2-}, As-PO_4^{3-} while no correlation is seen between As and NO_3^-.The high salinity in As-hotspots is evidenced by the positive correlation between As-Na^+, and between As-B and As-Li even lower correlation is observed between As-Cl^-. Similar negative correlations than in QQ study area are observed between As and Al, Fe, Mn concentrations. Among other associated trace elements, B shows a wide range of positive correlations with the major ions, and also U, Li, Sr and Mo. U and Mo concentrations also show strong positive correlations with dissolved Cl^-, NO_3^-, SO_4^{2-} ions.

5.3 Spatial distribution of As and other parameters in shallow groundwater

The spatial distribution maps of As concentrations and other hydro-chemical parameters from QQ and IA are displayed in Appendix V.

5.3.1 Area of Quemú Quemú

The wells investigated in the area of QQ showed high variability of As concentrations and other trace metals in groundwater. The wells sampled in QQ were labeled according to the geographical coordinates displayed from the village QQ and the railways crossing from N to S, as a reference point. The highest As concentrations (>200 μg/L) were found in the northeast of the study area, mainly in the depressions or close to discharge areas (Fig. 14a). As concentrations>50 μg/L are widely distributed over all the study area. The concentrations of As below the WHO standard limit (<10μg/L) were found only at few wells located in the northwest side, near the municipal wells that were closed during the sampling campaigns, in the recharge area. The spatial distribution of F concentrations showed similar pattern than As. The highest F levels, over 10 mg/L, are found in the same "As-hotspots" in the northeast part of the study area (Fig. 14b). In contrast, the wells with high Ca^{2+} concentrations are found in the same wells with the lowest F^- concentrations. The spatial distribution of B shows the similar trend than As and F^-, and the highest B concentrations (>2500μg/L) are located in the same "As-F-hotspots" wells (Fig. 14c). However, high levels of B are also observed in the wells situated in the southeast side, near the lakes in discharge area. The concentrations of HCO_3^- are widely distributed over the study area, increasing towards the NE, where are found the highest As, F, V levels (Fig. 14d) and the lowest in the northwest near the village. Also, V concentrations show similar spatial distribution than "As-F and B hotspots" with the highest levels mainly placed in the NE part of the study area (Fig. 14e). Contrarily, total Fe concentrations are generally low in the NE side and higher concentrations are found in the southwest of the village, with a maximum level in the well SO41 (Fig. 14f) Al and Mn concentrations were generally low, with the maximum concentrations located in the north-northwest for Al and southwest for Mn.

5.3.2 Area of Intendente Alvear

Most of the wells sampled in this area were situated in the recharge area in the aquifer called Las Mercedes, which supplies water to the villages of Intendente Alvear and Ceballos. Groundwater samples were collected from municipal wells and from rural wells situated in the south and north of the study area. Sample ISO63 was excluded from the spatial distribution maps because it was very far from the group of wells and could create a false statistical interpolation. The highest As concentrations (>250μg/L) are found in the north all collected from rural wells, probably these wells were not functioning for long time and would have stagnant water with reducing conditions. The wells with highest As concentrations (>50 μg/L) also showed the highest levels of F^- (>7.1mg/L), B (>3.4mg/L) and HCO_3^- (>800mg/L). B concentrations are spatially distributed over the area showing a scattered trend between urban and rural wells. High Fe concentrations are observed in one municipal well, the same with high Mn concentration despite in has the highest pH value and slightly oxidizing conditions. Probably, this is due to the presence of colloids in the samples. Al concentrations were in general low in all the wells, except in one municipal well.

5.4 Geochemical modeling

Based on the geochemical modeling calculations performed in Visual Minteq software, using all groundwater analytical results (pe= 59/Eh (mV) at 25ºC), the predominant As species dissolved

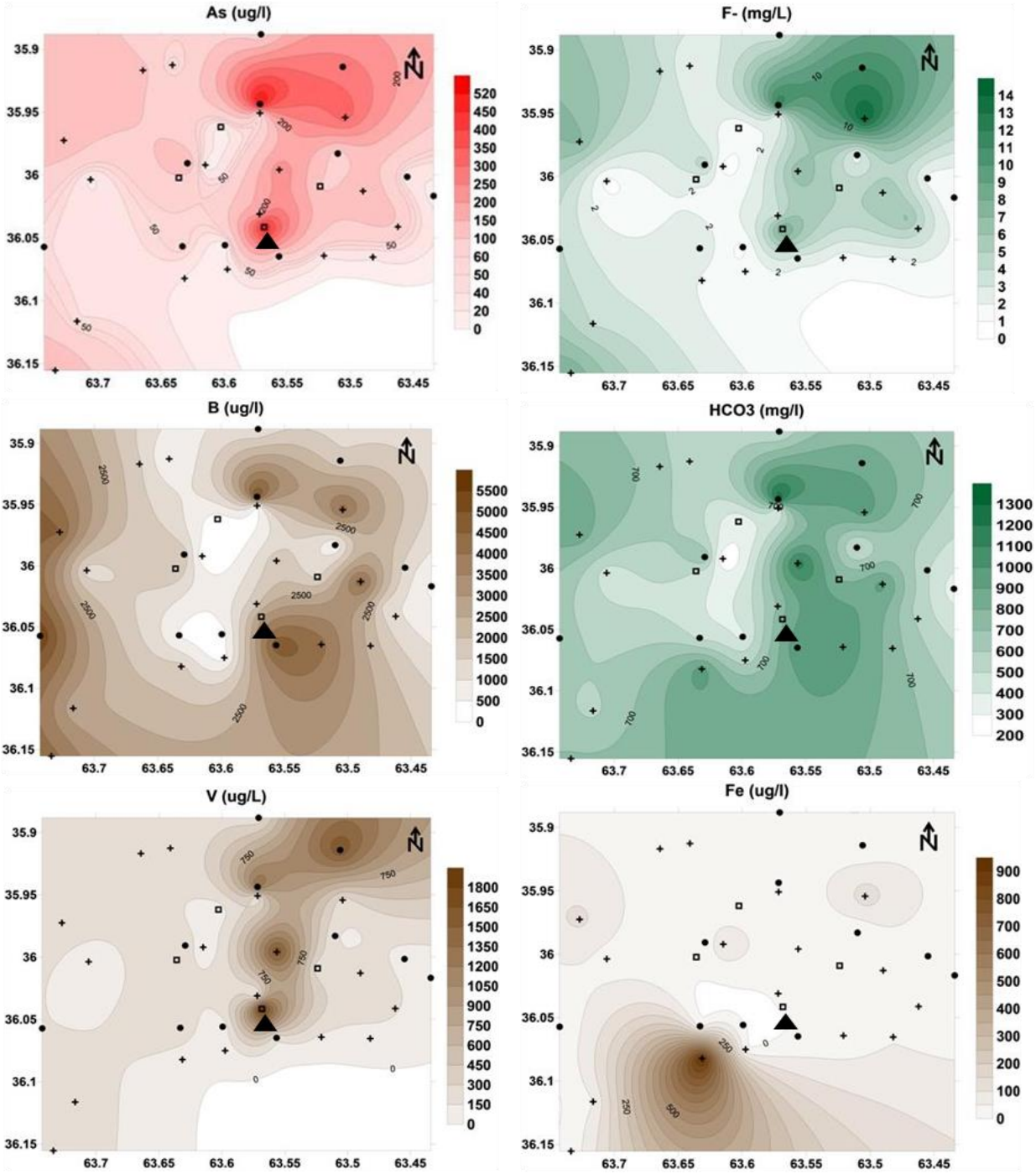

Figure 14 Spatial distribution maps showing the variation of aqueous As, F, B, HCO_3^-, V and Fe concentrations in QQ study area. The iso-curves are plotted using kriging interpolation. Note irregular scales.

in groundwater were arsenate As(V) in 99% of the samples, with the main oxyanions as $H_2AsO_4^-$ and in minor range $HAsO_4^{2-}$. Contrarily, arsenite species As(III) were not prompt to be encountered under these pH and redox potential conditions.

Five samples with high As concentrations were selected to determine the total aqueous species of groundwater in the geochemical modeling PHREEQC. The results of the main species found in groundwater are presented in Appendix XII. This geochemical modeling showed the predominant As species were also arsenate oxyanions (mainly as $HAsO_4^{2-}$). However, it was not possible to determine analytically the species As(III), As(V), Fe(II) and Fe(III) and therefore, the pe values for the redox couples could not be simulated in PHREEQC to check with the Eh

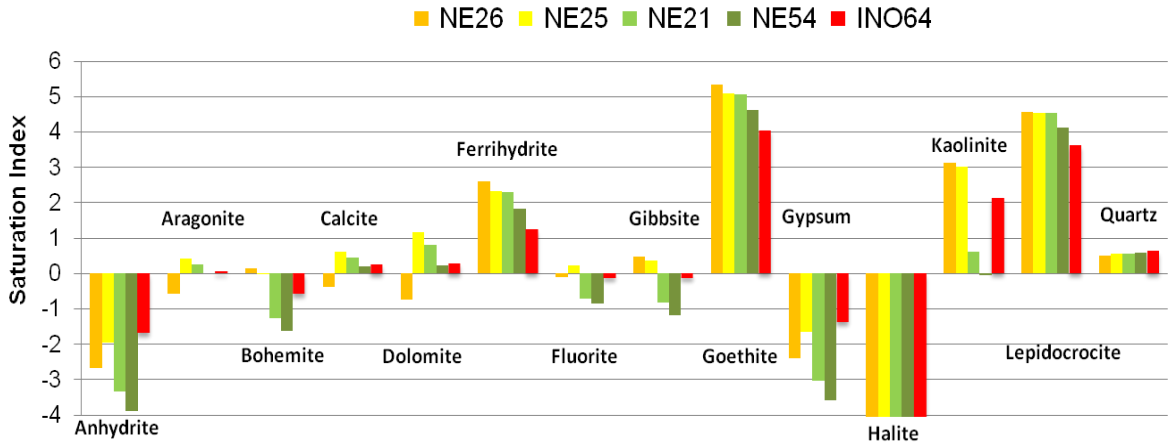

Figure 15 Saturation indices of the mineral phases for five selected groundwater samples modeled using PHREEQC code.

results measured in-situ in the field. Although, It was assumed that the probable governing redox couple in the aquifer were Fe(II)/Fe(III) and these did not reach the equilibrium.

Geochemical calculations of mineral saturation index (SI) showed that groundwater samples enriched of As are undersaturated with respect to As minerals. Different Fe mineral phases like goethite (FeOOH), ferrihydrite ($Fe(OH)_3$), and lepidocrocite (γ-FeO(OH)) are supersaturated in most of groundwater samples and likely to precipitate (Fig. 15). Al- mineral phases like kaolinite ($Al_2Si_2O_5(OH)_4$) is also supersaturated, but gibbsite is near equilibrium or undersaturated. Calcite, fluorite, quartz and aragonite are mostly in equilibrium in groundwater samples. Groundwater of selected samples is undersaturated with respect to gypsum, halite and anhydrite, and supersaturated with respect to phosphate minerals for samples NE25, NE21, NE54.

5.5 Sediments characteristics

5.5.1 Sediments descriptions

The sediments samples M and P, collected from the new drilled boreholes in the recharge area, are predominantly composed of yellowish brown coarse-medium sands in the upper sequence to light-greyish fine sands and silts in the lower sequence. Volcanic ash sample, collected at few cm from the surface, showed fine-grained glassy texture with intercalated fine loess sands. The fine texture of volcanic glass is probably an evidence of the fast cooling of the volcanic material. Volcanic ash sample was initially light greyish and became darker greyish probably due to oxidation of the sample during transportation and storage. The loess sample L1, collected from the discharge area, has a light grayish color as result of the high content of precipitated salts, while the lower sequences L2 and L3 were darker greyish to brown (Fig. 16). The color characteristics of the sediments were described according to Munsell chart color guide. Carbonate concretions were visible in the upper layer of the sandy aquifer or at 1 to 2 m depth found accumulated on the roots of the trees.

5.5.2 pH and Cation Exchange Capacity

The results of pH and cation exchange capacity (CEC) are presented in Appendix VII.

The pH values of the loess sediments and volcanic ash leachates were alkaline. The sample L3 showed the highest pH value of 10.3. Loess sediments samples M and P showed similar alkaline values, with an average of 8.86 for M and 8.83 for P, increasing with depth. Volcanic ash had a pH of 8.5. The increased pH of the leachates of the sediments is consistent with some groundwater values, and indicates the high buffering capacity of carbonates or silicates minerals found in the loess sediments and volcanic ash. The high pH of the leachate for sample L might indicate an accumulation of readily soluble salts.

The readily exchangeable cations were Ca^{2+} and Mg^{2+} for samples P, M and A, and Na^{+}/K^{+} for samples L (Fig. 17). The total CEC of the loess sediments ranged from 11.1 to 34.4meq/100g with an average of 22.1meq/100g, similar than the CEC of volcanic ash with 21.8meq/100g. However, volcanic ash showed higher amount of Ca^{2+} and Mg^{2+} exchangeable cations than the

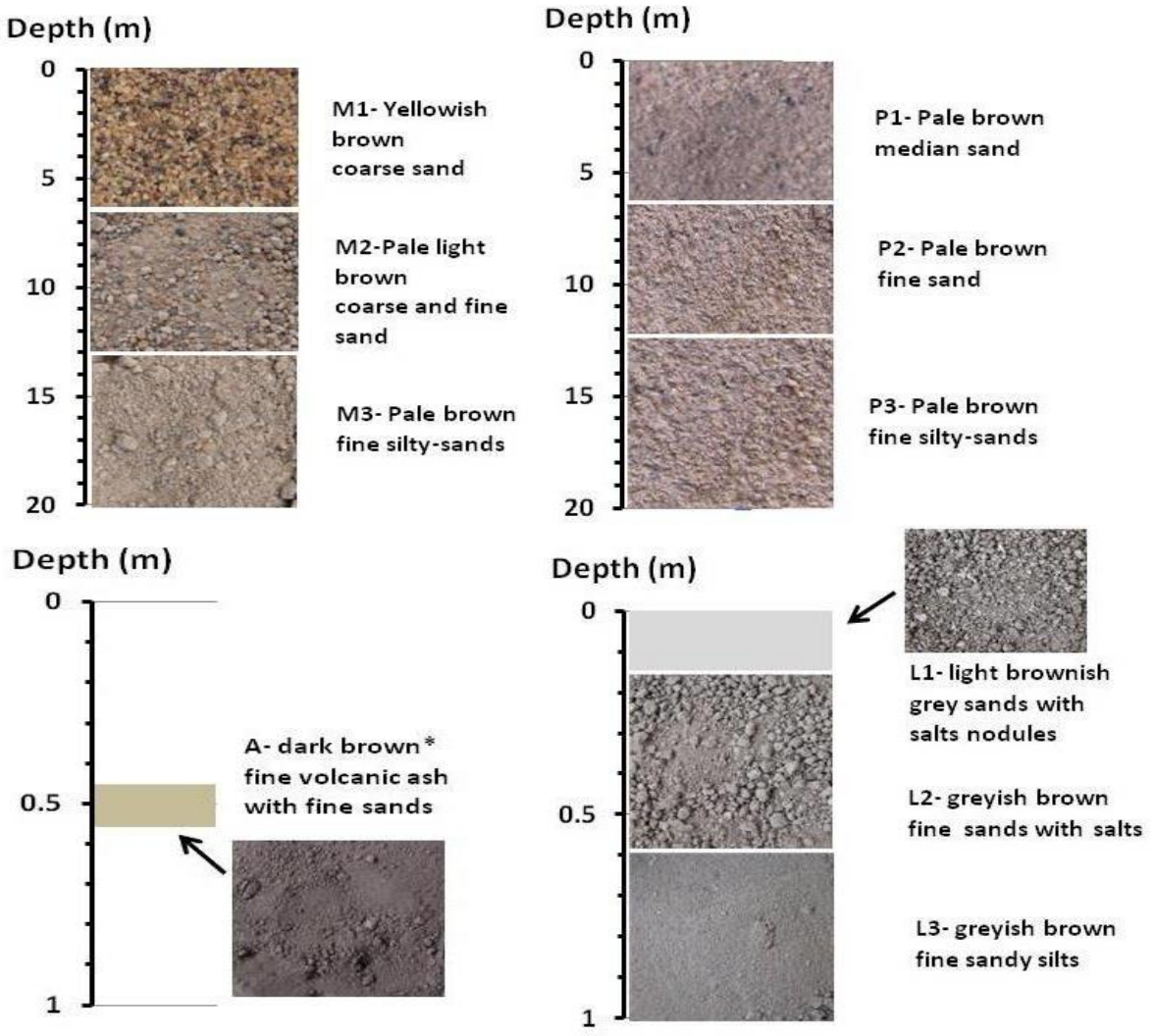

Figure 16 Description of the sediments profiles sampled in the area of QQ, with the depth to the sample, color and texture characteristics.

other sediments. Total cation exchange capacity is within the typical range of soils of high organic matter content (10-30 meq/100g).

5.5.3 Sequential extractions

The results obtained from the sediment sequential extractions performed in four steps are presented in Appendix IX.

The sequential extraction results performed in loess sediments and volcanic ash were quite similar, except for sample L collected in the discharge area. The highly mobile elements extracted from water soluble fraction (DIW) from loess sample L were: Na, K, Si, V, As, P and C, while for the other loess samples they were: Na, K, Ca and Mg and Si were mobile at lower concentrations, and for volcanic ash the readily soluble elements were Ca, K, Si, Mg and Al.

Arsenic

The amount of As released from the water soluble fraction (DIW) for sample L was extremely high (145.1 mg/kg) compared to other samples and other fractions. The extractable As concentration from the loess sediments M and P was: 0.2 mg/kg (8.6 %) in the water soluble fraction, 0.4 mg/kg (15.7 %) bound to carbonate or phosphate mineral phases, 0.1 mg/kg (5.5%) extracted from short range ordered secondary-oxide minerals, 1.50 mg/kg (62.7 %) from more crystalline Fe, Al, Mn oxy-hydroxide mineral phases. The amount of As extracted in different fractions from volcanic ash was: 0.20 mg/kg from DIW fraction, 0.7 mg/kg from carbonate and phosphate mineral phases, 0.3 mg/kg from amorphous Fe, Al, Mn oxy-hydroxides and 1.2 mg/kg from crystalline mineral phases (Fig. 18a)

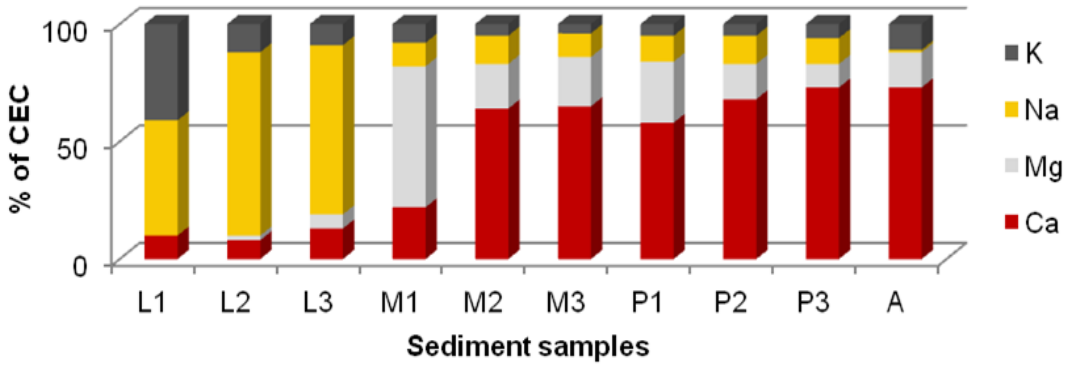

Figure 17 Concentrations of the cation exchange capacity of the sediments sampled in QQ study area.

Aluminium

The average content of extracted Al from the residual fraction was very high for all the loess sediment samples. According to the four sequential extractions steps the concentrations of Al in the leachates were: 6.3 mg/kg (0.1 %) from water-soluble fraction, 1.2 mg/kg (0.02 %) from acetate fraction, 27.2 mg/kg (0.5 %) from oxalate fraction and 4802.8 mg/kg (99.3 %) from residual fraction, which represents the crystalline mineral phases at low pH.

The amount of Al extracted from volcanic ash was higher than in the loess sediments and the concentration in each fraction was: 16.1 mg/kg (0.2 %) from water soluble fraction, 26.6 mg/kg (0.4%) bound to carbonates and phosphates, 51.5 mg/kg (0.7 %) bound to amorphous oxy-hydroxides and 7145.6 mg/kg (98.7 %) from the residual fraction bound to crystalline aluminosilicate minerals (Fig. 18b).

Iron

High concentrations of Fe were also extracted from the loess sediments and volcanic ash. The extractable Fe concentrations from loess sediments were: 9.6 mg/kg from water-soluble fraction, 1.8 mg/kg from acetate fraction representing the amount bound to carbonate minerals, 11.4 mg/kg from oxalate fraction representing the amount bound to secondary amorphous minerals and 4260 mg/kg (representing the 99.4 %) from residual fraction which represents the amount extracted from crystalline minerals. The amount of Fe extracted from volcanic ash was similar than in the loess sediments with: 12.5 mg/kg (0.2 %) from water soluble fraction, 27.3 mg/kg (0.4 %) from acetate (carbonates and phosphates), 79.3 mg/kg (1.1 %) from oxalate fraction (secondary amorphous oxy-hydroxides) and the highest proportion (98.4%) was extracted from the residual fraction, where Fe is bound to the crystalline phases with 7342.5 mg/kg (Fig. 18c). The low amount of Fe in the 3rd extraction may indicate low content of amorphous phases and possible transformation or ageing of Fe oxy-hydroxide to more crystalline minerals.

Manganese

The concentrations of Mn extracted from the loess sediments were low compared to those of Fe and Al extractions, being 0.37 mg/kg (0.3 %) from the soluble fraction (soluble phases), 3.3 mg/kg (2.2 %) from acetate fraction (carbonates and phosphates phases), 2.5 mg/kg (2.9 %) from oxalate fraction (amorphous Mn oxy-hydroxides minerals) and 73.9 mg/kg (91.4%) from the most acid fraction (crystalline Mn minerals). The extractable Mn from volcanic ash was similar than in the loess with: 0.5 mg/kg from water soluble fraction (soluble minerals), 1.2 mg/kg from acetate (carbonates and phosphates phases), 13.8mg/kg from oxalate (amorphous Mn oxides) and 90 mg/kg from more crystalline Mn oxide minerals (Fig. 18d).

5.5.4 Total extractions

Total extractions were calculated by the sum of each sequential extraction step according to:

$$TE = E_{Diw} + E_{Acetate} + E_{Oxalate} + E_{RF}$$

The loess sediments from recharge area, samples M and P, contain an average As concentration of 2.24 mg/kg, very similar to the amount of As extracted from volcanic ash of 2.26 mg/kg. However, the loess sample from discharge area L, contain an average As concentration of 52.6 mg/kg with the higher As content in the top layer of 149 mg/kg.

The total extracted Fe in loess of recharge area has an average of 4624 mg/kg, in loess of discharge area has a lower average of 3602 mg, while in volcanic ash the amount of Fe is higher 7462 mg/kg. Total extracted Al concentration in loess of recharge area has an average of 4867

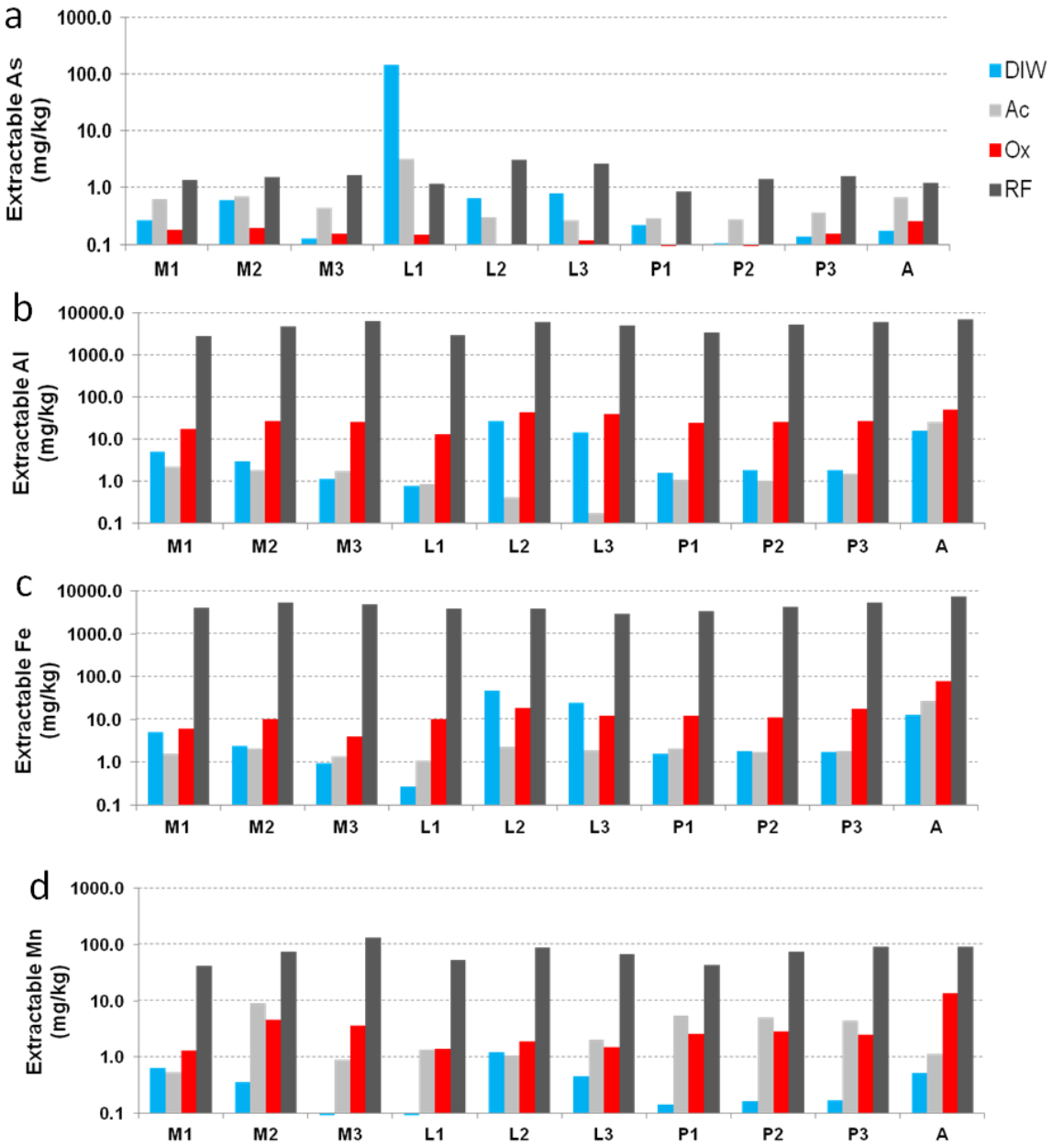

Figure 18 Analytical results from the sequential extraction procedure in four steps, showing in a) the extractable As, b) the extractable Al, c) the extractable Fe and d) the extractable Mn released from the sediments.

mg/kg, in loess of discharge has 4777 mg/kg and volcanic ash has a higher amount of Al, 7240 mg/kg. Manganese concentrations were lower than those of Fe and Al. Loess sediments from recharge area contain an average of Mn of 83.4 mg/kg, loess from the lake has an average of 73.4, while volcanic ash has a total Mn concentration of 105.5 mg/kg.

The higher concentrations of Fe, Al and Mn extracted from volcanic ash than in the loess sediments is subsequent with the observed fine material in volcanic ash sample, which represent the secondary Fe, Mn, Al oxy-hydroxides that could be binding As.

Total phosphorous concentration extracted from the loess sediments was extremely high, with concentrations ranging from 14075 to 47136 mg/kg for loess sediments and volcanic ash. These high concentrations of P may indicate an external source of phosphates based on the fertilizers added into the soil.

The total V content extracted from loess sample L was significantly high with 196 mg/kg, and similar to As. The loess sediments samples collected in the recharge area (P and M) showed an average of V of 17.1 mg/kg and volcanic ash sample showed the lowest V concentration of 11.9 mg/kg. The high concentration of trace

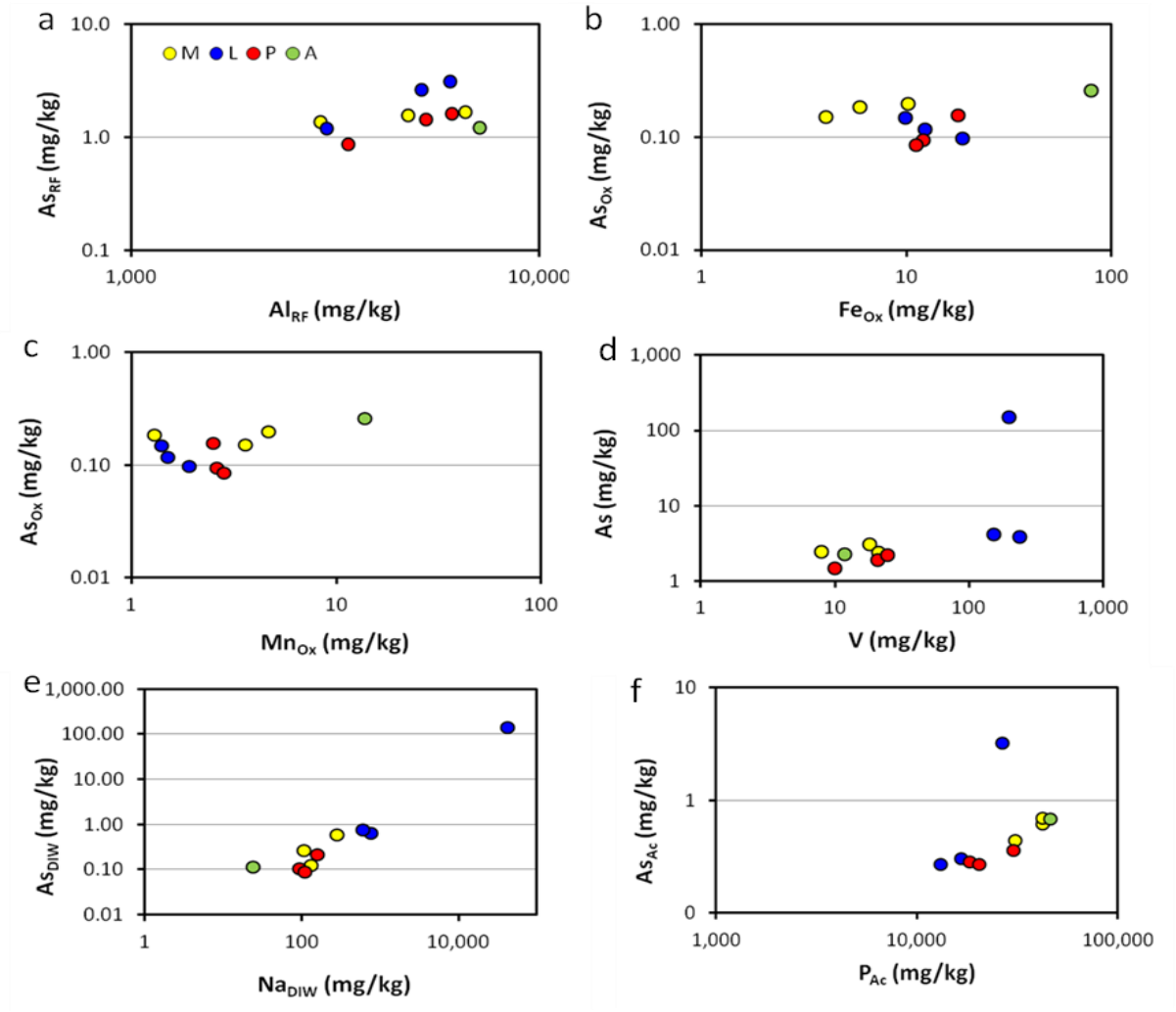

Figure 19 Correlations between extractable As and other elements from different fractions of the sediments: a) As-Al from the RF, b) As-Fe from the oxalate fraction, c) As-Mn from oxalate fraction, d) total As-V, e) As-Na from the water soluble fraction and f) As-P from the acetate fraction.

elements near at the shallowest levels and near the lakes may indicate the accumulation of salts by high evaporative concentration. Total extractions results are displayed in Appendix X.

5.5.5 Correlations between As and other elements extracted from the sediments

The Al extracted from the residual fraction shows positive correlation with As from the residual fraction (most insoluble fraction), which indicates that As is adsorbed or co-precipitated into crystalline Al minerals (Fig. 19a). The amount of Fe extracted from the oxalate fraction shows good correlation with extractable AsOx for all the samples except for sample L (Fig. 19b). Low amounts of Fe and Al were released by oxalate reagent, which indicates that the main Fe, Al oxy-hydroxides are found as crystalline minerals rather than amorphous. Therefore, most of the As is released from the residual fraction. No clear correlation can be observed between As from oxalate fraction and amorphous Mn oxy-hydroxide minerals. This indicates that amorphous Mn minerals are not a sink for As.

Sediment sample L1 showed extremely high As concentration and this sample is far from the main distribution. However, positive correlations are observed between total As and total V concentrations extracted from samples M, P and A, which may indicate that V can be a possible competitor of As for adsorption sites (Fig. 19d).

The Na^+ extracted from the readily soluble salts correlates very well with As from DIW fraction, which may indicate that As is mixed in the readily soluble salts, mostly in the sample L from the discharge area (Fig. 19e). Importantly, As extracted from the acetate fraction shows very well correlation with P, which may indicate that

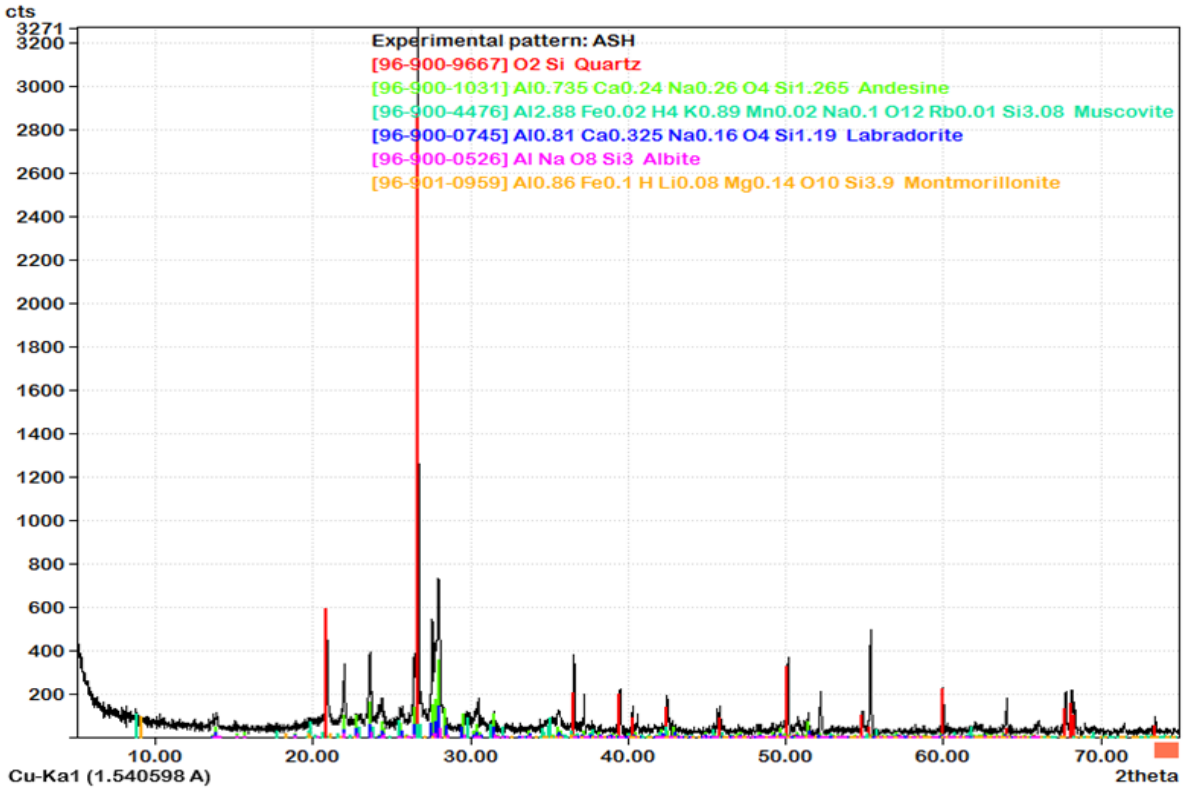

Figure 20 XRD spectra showing the qualitative mineralogical composition of volcanic ash.

both phosphates and arsenates are bound to the same carbonates or phosphates minerals and these are possible sinks for As (Fig. 19f).

5.5.6 Mineralogical results

The results of the qualitative XRD analysis showed similar mineralogical composition for the loess sediments and volcanic ash. The minerals observed in the loess sediments were based on a mixture of granites and granitoides like quartz, plagioclase (albite and anarthite), alkali-feldspars minerals (K-feldspar) and micas. Fe- oxy hydroxide minerals were not detected in the XRD spectra, probably due to their amorphous nature. Al mineral phases like gibbsite were observed in loess, and others phases of Al bearing compounds such as U, F and As. The spectra of volcanic ash showed similar composition of aluminosilicates minerals than the loess sediments, with quartz, muscovite, andesite, albite, as the main minerals (Fig. 20).

The mineralogical composition of the other sediments samples and each XRD patterns are presented in Appendix IX.

6 DISCUSSION

6.1Groundwater quality assessment

High demand of freshwater exists in the NE of La Pampa province, especially for farming and agriculture but also to supply drinking water to the rural population. Groundwater from the shallow aquifers is in the region of NE of La Pampa province the only available drinking water resource for small villages and settlements, including the areas of Quemú Quemú and Intendente Alvear. Both areas belong to the regional Pampean aquifer with an interconnected network of small aquifers and aquitards within the close basin. Groundwater composition displayed similar water types in both study areas with the dominant group type of Na-HCO_3^- for fresher waters and Na-Cl-SO_4^2 for more saline waters. Other similar characteristics found in both areas were the high levels of salinity in some wells, circum-neutral to alkaline pH and moderate oxidizing conditions (Eh~180mV). High concentrations of toxic trace elements including As, F, V, B and minor range of U and Mo, were also present in some wells in both sites.

The analytical results of groundwater indicate that high As enriched wells are found in both study areas, with 94 % of the groundwater samples in QQ and 100% of the samples in IA exceeding the WHO standard limit for As in drinking water (10 µg/L). Also, 56% of the groundwater samples in QQ and 50% of the samples in IA were exceeding the provisional Argentinean Standard limit for As of 50 µg/L according to the Argentinean Food Code. The maximum concentration of As in QQ reached up to 535µg/L, about 50 times the WHO

standard limit, and it was measured in the northeastern site of QQ study area. Whereas, groundwater from IA had 248.4 μg/L of As, exceeding by a factor of 20 the WHO Standard limit for safe drinking water. Groundwater from these wells is contaminated and unsuitable for human consumption. Remediation strategies should be applied in these wells in order to remove the pollutants and ensure safe groundwater quality. A clear correlation was observed between groundwater samples with high As concentrations and other trace elements concentrations such as F-, B, V, U and Mo, that may indicate a possible common source from volcanic origin, such as volcanic ash layers or the volcanic material that constitutes the loess sediments itself.

The spatial distribution of As, F, HCO_3^-, V and B concentrations in the area of QQ was scattered. However, the highest concentrations of toxic elements were found in the wells situated over northeastern part of QQ and one near the village. The high As contaminated wells were referred as "As hotspots" because of the pointed source contamination along the area. Moreover, possible trends to target "As hotspots" are the water type composition of Na-HCO_3^-, high alkalinity conditions, closed wells with stagnant water, and the location of the well towards discharge areas placed in the low lying area of the basin. Importantly, in the area of IA, the most contaminated well in the area of IA was found in an abandoned windmill site, characterized by high EC and high salinity, usually with Na-Cl-SO_4^{2-} water types and also high pH values. The promotion of stagnant waters with lots of organic matter and brackish waters are typical in abandoned wells. Natural organic matter would consume all the oxygen in reaching anoxic conditions and favoring the reductive dissolution of minerals binding As and other toxic metals.

Some wells in both study areas were enriched with dissolved PO_4^{3-} and NO_3^- ions, which may occur due to anthropogenic contamination from the use of fertilizers and pesticide in agriculture and also by the untreated sewage water discharged near the village. Nitrogen is not a significant product of mineral weathering, usually the primary sink of nitrogen in soil is from the biodegradation of dead animals and plants, hydrolyzed to NH_4^+ and oxidized to NO_3^- by the action of bacteria (Appelo and Postma. 2005). Moreover, inorganic nitrogen from fertilizers can be lost by leaching. In the area of QQ some wells exceeded the recommended standard limits for NO_3^- in drinking water and therefore, groundwater is considered not suitable for human consumption. High phosphate concentrations dissolved in groundwater may be originated by prolonged use of NKP fertilizers in agriculture. As a consequence, orthophosphate ions leached from fertilizers in alkaline soils may react with calcium carbonate to form hydroxyapatite. Geochemical modeling results showed that groundwater is supersaturated with respect to calcium phosphate $Ca_3(PO_4)_2$ and octa-calcium phosphate $Ca_4H(PO_4)_3 \cdot 3H_2O$ minerals, that would explain the presence of phosphates in the solid phase. Besides this, other aqueous phosphates can be abundant due to the reduced adsorption capacity of sandy sediments with large particle size, resuspension caused by wind, continuous intake from anthropogenic source, competition with other ions like As and accumulation in closed basins. Not only phosphate but also bicarbonate ions are important competitors with As for soption sites on Fe, Al and Mn oxy-hydroxides.

Ion chloride is used as a conservative tracer in groundwater and therefore, high Cl^- levels in shallow waters indicate mixing of waters from deep to shallow aquifers being more salty in the deep aquifer. Also, high chloride groundwater occurs due to the accumulation of solutes by the high evaporation rates in low areas. High salinity levels were found in groundwater in both study areas and they are evidenced by the high EC and high TDS values. EC values correlated well with Cl^-, SO_4^{2-}, Na^+, B and Li concentrations. Brackish water is frequently found in wells situated near the low-laying areas. Floodplain areas in the depressions are used as discharged areas. If low-laying basin has no outlet, the water incoming from floods that evaporates during the dry season inside the basin and consequently dissolved salts accumulate in the lowest parts. The first salts to precipitate are calcile and dolomite, further is gypsum and when the lake is almost dry halite and other highly soluble salts and heavy metals accumulate on the surface. The salty lakes indicate that annual average evapotranspiration is greater than the sum of precipitation and incoming flood water.

In addition, the presence of dissolved solids affect the water taste and also, certain components of TDS like Cl^-, SO_4^{2-}, Mg^{2+}, Ca^{2+} and HCO_3^-, may affect with corrosion or incrustations on water distribution systems.

The toxicity and availability of As depends on its speciation. According to the results obtained in the geochemical modeling, the estimated As species dissolved in shallow groundwater are arsenate As(V) oxyanions in 99% of the samples, while the mobile form arsenite As(III) would be expected in deep aquifers under more reducing conditions. Arsenate oxyanions are more strongly bound to Fe oxides than arsenites, but when the pH increases above 8.5, PZC of common Fe oxides, arsenate is weakly bound and may be easily released or displaced by other ions into groundwater.

The increase of pH in shallow groundwater is mainly controlled by the weathering of carbonates and silicates minerals. These reactions are driven by cation exchange and redox reactions. The Pampean aquifer has an abundance of carbonate minerals present at shallow depths (1 to 2 m below the ground), visible as calcrete layers, affecting the roots of the trees and causing environmental damage. The predominant carbonate minerals are calcite and dolomite. Carbonate calcium minerals have high buffering capacity because they consume protons according to the following equation:

$$CaCO_{3\,(s)} + CO_2 + H^+ \rightarrow Ca^{2+} + 2HCO_3$$

According to the saturation index results groundwater from both areas is supersaturated with respect to calcite, dolomite and aragonite as carbonate minerals.

Cation exchange reactions are the predominant in that soils the total CEC of the loess was cation exchanger of loess sediments is dominated by Ca^{2+} in fresh water, however for water with high salinity and Na-Cl water type, Na^+ ions are the dominating cation exchangers. If fresh water flushes salt water from the deep sequences of the aquifer then the sediments adsorb Ca^{2+} while Na^+ is released resulting in Na-HCO_3^- water type.

The weathering of silicates is also a key process important for the generation of high pH in groundwater however the dissolution kinetic rates for aluminosilicates are slower than carbonates.

The concentrations of aqueous Fe, Al and Mn were generally low in both study areas because under oxidizing conditions and neutral pH, Fe, Al, Mn oxy-hydroxides are stable precipitated.

Based on geochemical simulation groundwater is undersaturated with respect to the common As minerals (As-sulfide and iron sulfate minerals) which indicate that As minerals may not be present in the system. But it is supersaturated with respect to ferrihydrite, goethite and gibbsite minerals (in decreasing order of SI), which means under favorable conditions for secondary precipitation and transformation to more stable structures. Although, some wells showed high levels of Fe, like the well SO46 situated in the SW of QQ (SO46) and the municipal well INOP12 in IA. This might be probably due to the presence of low size Fe-colloids with a diameter <0.45μm that were not removed during filtrations or the presence of Fe reducing bacteria.

Similar groundwater characteristics and sources of contaminations were observed in other regions of the semi-arid Chaco-Pampean plain. For example, Smedley et al. (2002, 2005) reported very high concentrations of As (<10-5300 μg/L) associated with other trace elements such as F, V, Mo and U, in shallow aquifers under oxic and alkaline conditions, in the Eduardo Castex study area in northeast of La Pampa province. Here, As concentrations and correlated trace elements were also accumulated near the surface due high evaporation rates and very the slow flow in low laying areas. Nicolli et al. (2010) also reported similar high levels of As, F, V, B and Mo mainly in shallow groundwater of the Salí River basin in Tucumán Province. Bhattacharya et al. (2006) found high As levels in similar geochemical conditions (salty and alkaline aquifers) in the shallow aquifer of Río Dulce alluvial cone in the arid region of Santiago del Estero. Farías et al. 2003 found As yielding levels of 600 μg/L in shallow groundwaters of four Argentine provinces: South of Córdoba, West of Buenos Aires, South of Santa Fe and NE of San Luis.

Health symptoms related to drinking water were observed in both study areas, mostly oamong the people living in agricultural settlements. Dental fluorosis was the most common symptom related to the contamination of drinking water with F^-. In some groundwater samples in QQ study area, F exceeded by 10 times the WHO drinking water standard limit. High fluoride concentrations in groundwater might be sourced from the dissolution of fluorite and fluorapatite minerals, because according to the geochemical modeling, groundwater is supersaturated with respect to these minerals. Most of the fluoride adsorbed in the body comes from water, while the intake from food and toothpaste is less significant because is excreted. For this reason, long term exposure of fluoride concentrations in

water above 1.5 mg/L can lead to dental fluorosis problems and other severe diseases like osteofluorosis.

The primary arsenicosis symptoms, skin pigmentation, hyperkeratosis and black foot disease were not manifested among the rural areas investigated. However, some cases of cancers occurred in the area among the adult people but the causes could be related to other. One possible reason for the absence of As symptoms even though the high levels in groundwater, could be the good nutritional status with a diet mostly rich in proteins from meat and milk consumption. (J. Tulio, September 2011. personal communication). In general terms, the quality of groundwater from shallow aquifers in the study areas in NE of La Pampa province is poor for an extended area and therefore, low cost mitigation technologies would be required in order to remove salts and toxic trace metals from groundwater.

Some people of the region with lack of information have tried to reduce the pollutants by boiling tap water. However they are increasing the concentration of salts and consequently the exposure of human health to toxic trace elements.

6.2 Release of As and water-sediment interactions

The selection of the sediments samples was done strategically in order to investigate the different hydrological areas, recharge and discharge areas, as well as the composition of volcanic ash as a possible primary source of As. However, the concentrations of As could not be measured in-situ due to the lack of a portable hatch equipment. Samples M and P were were collected in the recharge area of the aquifer near the municipal wells of QQ. Sample L was collected from the surface of the dry lake to explore the discharge area. Sample A volcanic ash was collected to identify the possible primary source of As. Previous research from Nicolli et al. 1989 reported that the primary source of As in groundwater in the province of Córdoba was from the weathering of volcanic ash deposits. However, in some cases volcanic ash has already been depleted and trace elements like As released.

Sequential extraction procedure of loess and volcanic ash sediments was used to quantify the As bound in different mineral phases. The amount of total As extracted from loess sediments M, P and A was lower compared to the amount of As reported in Tucumán province (7-14 mg/kg) (Nicolli et al. 2010), and compared to the 2.5-7 mg/kg reported in Santiago del Estero (Bhattacharya et al. 2006) and also compared to the average of 8 mg/kg reported in Eduardo Castex, La Pampa (Smedley et al. 2005). Despite the low concentrations of As extracted from the loess sediments and volcanic ash, these are enough to contaminate groundwater with thousands of μg/L of As far exceeding the drinking water standard limits. Importantly, sediment sample L from the discharge area showed the highest concentration of As (average of 145 mg/kg) increasing towards the surface level, where are visible the incrustations of salts. These high As concentrations on the top of the lowland surface areas which were previously flooded confirms the hypothesis of solute accumulation by evaporative concentration during the dry season. Positive correlation was observed between total extracted V and As, which indicates that V oxyanions are possible competitors with As for sorption sites on Fe, Al oxy-hydroxides. Our results are consistent with previous studies from Bundschuh et al. 2011a that suggested the principal oxyanion species competing with As(V) and As(III) for sorption sites are vanadates and phosphates (Bundschuh et al. 2011a).

The high concentrations of Fe and Al extracted from the loess sediments and volcanic ash, indicated the presence of aluminosilicates and more crystalline Fe, Al oxy-hydroxide minerals than amorphous. Fe concentrations were in the same order of magnitude in volcanic ash than in the loess sediments. However, total extracted Al was higher in volcanic ash than in the loess, maybe due the presence of clay minerals in volcanic ash. These results are consistent with the XRD results confirming the presence of aluminosilicates as the main minerals even though, amorphous oxy-hydroxides minerals were not identified in the spectra. It is expected that secondary hydroxide minerals would be present in deeper aquifer, in more silty clay fractions, and would become more crystalline with depth as a result of sediment ageing (Smedley et al. 2005). Mn concentrations were two orders of magnitude lower than those of Al and Fe and also the higher amounts were bound to Mn crystalline minerals. However, in volcanic ash sample the concentration of Mn in oxalate fraction was significant compared to the loess sediments. This could indicate the presence of amorphous Mn oxy-hydroxides in volcanic ash.

Extremely high phosphate concentrations were extracted from the loess sediments and volcanic ash from the recharge area (samples M and P) and even higher from loess sediments from the discharge area (sample L) which may indicate that phosphates are probably originated from the use of KNP fertilizers in the agriculture added in the field. The natural constituents of the loess are around 90% in abundance plagioclase, quartz and K-feldpars, but phosphate minerals are not that abundant.

The solutions extracted from the loess sediments and volcanic ash soils samples were all alkaline, with pH higher than 8.5 (ZCP of Fe hydroxides) which may indicate that As(V) would be weakly bound to Fe, Al oxy-hydroxides and by the presence of other competitor ions such as HCO_3^- and PO_4^{3-} for the sorption sides, As could be desorbed easily. The pH of the saturation extracts increase slightly with depth for M and P due to the carbonates and silicates weathering.

The cations Ca^{2+} and Mg^{2+} were easily exchangeable for the loess sediments samples M and P and volcanic ash sample A, while in the sample L the readily exchangeable cation was Na^+. This sample was placed in the discharge area and is mainly constituted of high content of readily soluble salts and toxic trace elements bound to them. They are outcoming from thee deep aquifer to the surface due to the dry periods with high evaporation rates. This may explain the equilibrium of carbonates and high pH values in groundwater.

6.3 Mobilization and accumulation of As in shallow aquifers

A conceptual model of the hydrological and geochemical cycles affecting the mobility of As in shallow aquifers is explained below.

Groundwater is recharged by rainwater which is infiltrated in the shallow aquifer. That happens in the recharge areas in the highlands sandy dunes. The beginning of rainfall periods generates excess of water. Then, the water table arises and the subsequent groundwater and surface water fluxes predominate. If it continues raining the water body grows and the excess of water is deposited in the lowland areas creating closed lagoons. At that stage groundwater and surface water are exchanged. Long term flooding period induces groundwater in saturated zone and anaerobic conditions. Consequently, under these conditions is promoted the reductive dissolution of secondary Fe oxy-hydroxides, which can be accompanied by the release of As, organic matter (humic acids) and other trace elements (Fendorf et al. 2010). During the dry period high evaporation rates restore the water levels and after some years groundwater returns to the initial state and lagoons start to dry. The soils that were previously inundated are now drained and groundwater is found under oxidizing conditions. The shift in the redox conditions promotes precipitation of secondary Fe, Al or Mn oxy-hydroxide minerals and the oxidation of arsenite (AsIII) to arsenate (AsV) which is strongly adsorbed on the newly formed minerals.

High evaporation rates can induce to vertical capillarity flow and salty groundwater from deep aquifer is transported to the shallow aquifer. Ion exchange reactions take place and consequently there is an increase of ionic concentrations and the pH rises. The pH is mainly controlled by the dissolution of carbonate and silicate minerals, as explained before. When pH increases above 8.5 which is the zero point charge for many amorphous Fe oxides like ferrihydrite, goethite, etc., As can be weakly adsorbed and easily released into groundwater, especially when other ions like phosphates, bicarbonates and vanadates are competing for the same sorption sites.

The flat topography of the area restricts the groundwater flow and favors the residence time of groundwater in the aquifer where many geochemical reactions occur at the same time in order to reach the equilibrium.

The high pH of groundwater also favors the dissolution of volcanic glass (Nicolli et al. 2010), which can be quickly depleted, when As oxyanions and other complexes are released into groundwater. That explains the low content of As found in volcanic ash sample which was similar than in loess sediments from the recharge area.

The large variability of groundwater composition with different range of toxic ions and trace elements that occurs within short distances can be explained by natural and human contribution. The main impact of the aquifer is the use of the land for agriculture and pastures, and the soils have high nutrients inputs, large amounts of organic matter, agriculture products added in the field crops, abstraction of groundwater for irrigation, untreated sewage water discharged into the field, etc. For these reasons, some "As hotspots" were observed in the study area.

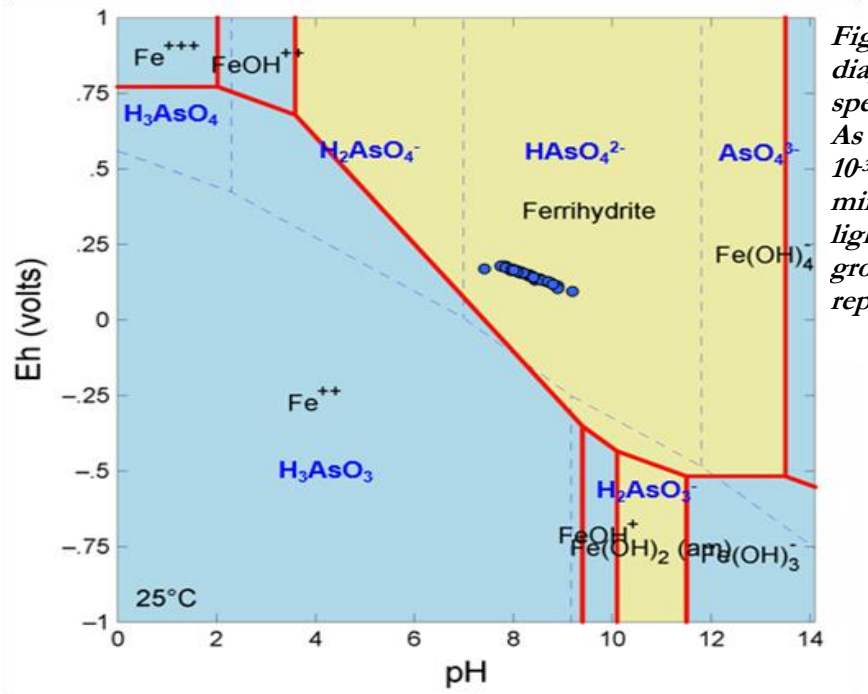

Figure 21 Eh-pH stability diagram for As and Fe species at 25ºC with the total As 10^{-6}mol/L and total Fe 10^{-3}mol/L. Solid species and minerals are plotted in the light brown area and groundwater samples are represented as blue dots.

Usually the transition from As(III) to As(V) occurs in the same Eh zone as the oxidation of iron Fe^{2+} to Fe^{3+}. Based on Visual Minteq modeling, arsenate As(V) is the predominant specie of As in 99% of the groundwater samples, and the main oxyanions are $HAsO_4^{2-}$ with a little contribution of $H_2AsO_4^-$. This is consistent with the Eh-pH measured in groundwater samples from both areas (Fig. 21). As oxyanions have usually negative charge but this it can be changed when As form complexes with other solutes, such as Mg^{2+} and Ca^{2+}. Although Mn concentrations extracted from the sediments were lower than those of Al and Fe, these minerals might be involved in the oxidation of As(III) to As(V) species.

Arsenic can be more abundant in deep aquifers, in the deep soil profile rich in silty-clays sediments. These sediments are mainly composed of oxy-hydroxides minerals with different structure ordered range. As can be found co-precipitated in the mineral structure or adsorbed on the surface of the minerals. Usually, short ordered range of Fe oxy-hydroxides can be potential secondary sources of As under favorable redox conditions for their mobilization.

The mechanisms responsible for the mobilization of As in shallow aquifers are already described as: 1) reductive dissolution of Fe oxy-hydroxide minerals binding As, 2) desorption of As under oxidizing conditions due to rise of pH above 8.5, 3) release of As due to the presence of competitive ions for sorption sites such as HCO_3^-, PO_4^{3-} and vanadates, 4) accumulation of salts and toxic elements concentrations in lowland areas due to the high evaporation rates during the dry season.

In shallow aquifers aqueous As is mainly occurring in Na-HCO_3^- water types at high pH values under oxic conditions. The presence of abundant phosphates from fertilizers in agriculture may also limit the adsorption on Fe minerals, being competitors with As and bring a pointed source contamination of groundwater.

Finally, carbonate minerals distributed over the loess sediments as a calcrete layers could be also potential sinks for As where it can be weakly adsorbed on the surface and desorbed during dissolution of these minerals (Welch and Ullman. 1999).

6.4 Targeting safe aquifers in low As zones

Targeting low As aquifers and safe wells might be difficult in the study area of NE La Pampa. These are the main reasons: 1) the complex hydrogeological system with the presence of small sub-aquifers with different amounts of volcanic ash at different depths that may trigger to changes on geochemical conditions of groundwater. 2) use of fertilizers and organic matter added to the soil that may also effect with changes on the geochemistry of the aquifer and the mobility of As by competition of organic acids (humic acids). 3) Strong and fast seasonal oscillations, with very dry and wet periods may also change the hydrogeochemical conditions, and bring to episodes of high and low As concentrations in the shallow aquifers. 4) an

important aspect to know is the use and managing of the wells and the pumping systems. Importantly, in those agricultural areas where groundwater is the only water source for irrigation the field crops if there is an excessive pumping groundwater from different aquifers (deep and shallow) can be mixed. Contrarily, abandoned wells resulting in stagnant waters can trigger to reducing conditions and mobilize large concentrations of toxic trace elements to the aquifer.

However, it might be suggested that the wells sampled on the sand dunes or near the recharge areas showed better groundwater quality with low toxic trace elements concentrations than the wells situated near the discharge areas. For example in QQ study area the lowest As-concentration well (NO12-Cobrero) is situated in the NW from QQ in sandy slope area. The measured depth to water table is 7m. This well points out good quality of groundwater and safe conditions for human use.

7 CONCLUSIONS

Groundwater from the shallow aquifers of the northeast of La Pampa province is highly enriched with As and other associated trace elements, like F, V, B, U and Mo in some wells. These elements are hosted in the sedimentary Quaternary loess and fine textured sandy silty aquifer with calcareous layers and some volcanic ash visible as thin layers. The highest As "hotspots wells" are localized near discharge areas and mainly in Na-HCO_3^- water types. Most of the wells have high salinity levels, and high As and associated toxic elements exceeding the WHO standard limits for safe drinking water. Those contaminated wells are unsuitable for human consumption. However, safe wells with low As concentration in fresh groundwater are encountered in sandy dunes zones acting as recharge areas.

Key factors that trigger to the mobilization of As are: the rise of pH in groundwater induced by carbonate and silicate weathering processes which are produced by cationic exchange reactions. Also, from redox variations due to bacteriological activity and climatic factors with changes in the water table can produce changes in the chemical composition of groundwater. Geochemical processes like oxidation/reduction, cation exchange, adorption-desorption, co-precipitation and surface complexation on As-bearing minerals can trigger to the mobilization of As in shallow groundwater.

There is no evidence of high amount of As in the loess sediments and in volcanic ash, despite the high concentrations of As in groundwater. Furthermore, other anthropogenic activities should be considered as important factors for the mobilization of As in groundwater. For example, adding high amounts of fertilizers and pesticides in the field and enrich the soils with significant amounts of organic matter, are some examples that they have been extensively used for many years in La Pampa. The sequential extractions might suggest that the volcanic ash samples used in this study has already been depleted. However, good correlations between As and other trace elements, F, V, B, U and Mo were found in the extractions, and this might suggest that the primary source is from volcanic material found in volcanic ash or spread in the loess sediments.

The mineralogical composition of the loess sediments is typical of volcanic composition with more crystalline minerals like plagioclase, k-feldspars and quartz, but also other more reactive Fe, Al or Mn amorphous minerals, that were not detected in the qualitative XRD analyses, are key factors to understand the geochemistry of As and the mechanisms for its mobility in such environments.

Other hydro-geochemical factors and characteristics of the aquifer like low flow velocities, low permeability of silts and clays, mixing of water from deep to shallow aquifers, higher vertical flows than horizontal flows, lack of runoff, etc. can trigger to the mobilization and accumulation of As in the shallow aquifers of NE of La Pampa region. In addition, further work would be required to carry out in this area in order to understand the variations and predictions over time and the human effects of As and F contaminated groundwater.

8 RECOMMENDATIONS AND FURTHER WORK

Further research should be carried out in the study area focusing on the suggested approach:

- Quantify the concentrations of As in the aqueous and solid phase of the deep aquifer. Importantly, determine the pH and redox conditions and the main species of As dissolved in groundwater.
- Analyze As concentrations and other correlated trace elements during the wet season in order to evaluate the hypothesis of dilution and understand the climatic

variations affecting the geochemistry of As in the shallow aquifers.

- Evaluate other possible minerals adsorbents for As like carbonates and phosphates, determine the sorption capacity and kinetics of these minerals as possible secondary source of As at shallow levels.
- Determine the impact of anthropogenic contaminants, such as fertilizers and organic matter added into the field, in the lab scale, by investigating the competition between phosphates and humic acids with As under similar conditions than in shallow aquifers.
- Investigate the mineralogical composition of the clays from the deep aquiferDevelop a surface complexation model to calculate the effect of competitor ions on the mineral surfaces, and the behavior of As like the speciation, during the adsorption-desorption or co-precipitation processes.
- Perform an epidemiological study with hair and urine samples from the rural population in both study areas in order to estimate the impact of As and F after long term consumption of contaminated drinking.

Perform a hydrological study to determine the water table variations during the wet and dry season by installing piezometers to evaluate the impact of redox oscillations on the mobilization and attenuation of As.

9 REFERENCES

Alarcón-Herrera, M.T., Bundschuh, J.,Nath, B., Nicolli, H.B., Gutierrez, M., Reyes-Gómez, V. M., Nuñez, D., Martín-Domínguez, I.R. (2012) Co-occurrence of arsenic and fluoride in groundwater of semi-arid regions in Latin America: Genesis, mobility and remediation. *Journal of Hazardous Materials, In press.*

Appelo, C.A.J. & Postma, D. Geochemistry, groundwater and pollution, 2n edition (2005), Balkerma publishers. Amsterdam. 649 pp.

Bejarano Sifuentes, G. & Nordberg, E. (2003) Mobilization of arsenic in the Río Dulce Alluvial Cone, Santiago del Estero Province, Argentina. Department of Land and Water Resources Engineering KTH, Stockholm, Sweden. TRITA-LWR-Degree Project 03-06.

Bennet, W.W., Teasdale, P.R., Panther, J.G., Welsh, D.T., Zhao, H., Jolley, D.F. (2012) Investigating Arsenic Speciation and Mobilization in sediments with DGT and DET: A Mesocosm Evalutation of Oxic-Anoxic Transition. *Environmental Science and Technology*, 46, 3981-3989.

Bhattacharya, P., Jacks, G., Frisbie, S.H., Smith, E., Naidu, R., Sarkar, B. (2002) Arsenic in the environment: a global prespective. Heavy metals in the environment. Marcel Dekker Inc., New York, 147-215 pp.

Bhattacharya, P., Claesson, M., Bundschuh, J., Sracek, O., Fagerberg, J., Storniolo, A.R., Thir, J.M. (2006) Distribution and mobility of arsenic in the Rio Dulce Aluvial Aquifer in Santiago del Estero Province, Argentina.*Science of the total Environment* 358, 97-120.

Blanco, M.C., Paoloni, J.D., Morrás, H.J.M., Fiorentino, C.E., Sequeira, M. (2006) Content and distribution of arsenic in soils, sediments and groundwater environments of the Southern Pampa region, Argentina. *Environmental Toxicology*, 21, 561-574.

Boyle, R.W. & Jonasson, I.R. (1973) The Geochemistry of arsenic and its use as an indicator element in geochemical prospecting. *Journal of Geochemical Exploration* 2, 251-296.

Blouet, B.W. & Blouet, O.M. (2009) Latin America and the Caribbean, A systematic and Regional Survey. 6th edition. New York. Ed. John Willey & Sons. 500 pp.

Bundschuh, J., Farías, B., Martin, R., Storniolo, A., Bhattacharya, P., Cortes, J., Bonorino, G., Albouy, R. (2004) Groundwater arsenic in the Chaco-Pampean Plain, Argentina: case study from Robles county, Santiago del Estero Province.*Applied Geochemistry* 19, 231-143.

Bundschuh, J., Bhattacharya, P., Sracek, O., Mellano, M.F., Ramírez, A.E., Storniolo, A.R., Martín, R.A., Cortés, J., Litter, M.I., Jean, J.S. (2011a) Arsenic removal from groundwater of hte Chaco-pampean plain (Argentina) using natural geological materials as adsorbents.*Journal of Environmental Science and Health*. 46, 1298-1311.

Bundschuh, J., Litter, M.I., Parvez, F., Román-Ross, G., Nicollis, H.B., Jean, J.S., Liu, C.W., López, D., Armienta, M.A., Guilerme, L.R.G., Gomez Cuevas, A., Cornejo, L., Cumbal, L., Toujaguez, R. (2011b) Review, One century of Arsenic exposure in Latin America: a review of history and occurrence from 14 countries. *Science of the total environment*.

Camilión, M. C. (1993) Clay mineral composition of Pampean Loess (Argentina). *Quaternary International* 17, 23-31.

Carabante, Ivan (2012) Arsenic adsorption of Iron Oxide, Implications for soil remediation and water purification. Doctoral Thesis, Department of Civil, Environmental and Natural Resources Engineering. Luleå University of Technology, Sweden.

Casentini, B., Pettine M., Millero F, J. (2010) Release of Arsenic from Volcanic Rocks through Interactions with Inorganic Anions and Organic Ligands. *Aquatic Geochemistry* 16, 373-393.

Castro, C. E. (2008) Analisis hidrogeologico y modelo conceptual del funcionamiento del acuifero de Intendente Alvear. La Pampa. Argentina. Doctoral thesis in Ciencias hídricas. Universidad Nacional de la Pampa (UNLap), Santa Rosa.

Claesson, M. & Fagerberg, J. (2003) Arsenic in groundwater of Santiago del Estero- sources mobility patterns and remediation with natural materials. Department of Land and Water Resources Engineering, KTH, Stockholm, Sweden. TRITA-LWR-Degree Project 03-05.

Farías, S.S., Casa, V.A., Vázquez, C., Ferpozzi, L., Pucci, G.N., Cohen, I.M. (2004) Natural contamination with arsenic and other trace elements in groundwater of Argentine Pampean Plain. *Sciences of the Total Environment* 309, 187-199.

Fendorf, S., Nico, S.N., Kocar, B.D., Masue, Y., Tufano, K.J. (2010) Arsenic Chemistry in Soils and Sediments. *Developments in Soil Science*. 34, 357-371.

Ferguson, J.F. & Gavis, J. (1972) A review of the arsenic cycle in natural waters- Baltimore, Maryland, U.S.A: Water Research Pergamon Press, 6, 1259-1274.

Fernandez-Turiel J.L, Galindo, G., Parada, M.A., Gimeno, D., Garcia-Vallés, M., Saavedra, J. (2005) Estado actual del conocimiento sobre el arsenico en el agua de Argentina y Chile: origen, movilidad y tratamiento. Digital CSIC. - Barcelona. 11-32.

Galindo, G., Sainato, C., Dapeña, C., Fernández-Turiel, J.L., Gimeno, D., Pomposiello, M.C., Panarello, H.O. (2007) Surface and groundwater quality in the northeastern region of Buenos Aires Province, Argentina. *Journal of South American Earth Sciences*, 23, 336-345.

Giai, S. B. & Tullio, J. O. Características de los principales acuíferos de la provincia de la Pampa. Facultad de Ciencias Humanas UNLpam y Dirección de Aguas de la Pampa, Santa Rosa.

Gitari, W.M., Petrik, L.F., Key, D.L., Okujeni, C. (2010) Partitioning of major trace inorganic contaminants in fly ash acid mine drainage derived solid residues. *Int. J., Env. Science Tech.* 7, 519-534.

Goldberg, S. & Johnston, T.C. (2001) Mechanisms of arsenic adsoprtion on amorphous oxides evaluated using macroscopic measurments, vibrational spectroscopy, and surface complexation modeling. *Journal of colloid and interface science*. 204-216.

Harvey, C.F., Swart, C.H., Badruzzaman, A.B.M., Keonblute, N. (2002) Arsenic mobility and groundwater extraction in Bangladesh, *Science*, 298, 1602.

Henke R., Kevin (2009) Arsenic: Environmental Chemistry, health threats and waste treatment. Kentucky. John Wiley and sons Ltd. 559 pp.

Jain, C.K. & Ali, I. (2000) Arsenic: Occurrence, Toxicity and Speciation Techniques. *Water Resources*. 34, 4304-4312.

Lindback, K. & Sjölin, A.M. (2006) Arsenic in groundwater in the south western part of the Río Dulce Alluvial conce, Santiago del Estero Province, Argentina. Department of Land and Water Resources Engineering KTH, Stockholm, Sweden. TRITA-LWR-Degree Project 06-26.

Litter, M.I., Morgada, M.E., Bundschuh, J. (2010) Possible treatments for arsenic removal in Latin America waters for human consumption. *Environmental Pollution*. 158, 1105-1118.

Litter, M.I., Alarcón-Herrera, M.T., Arenas, M.J., Armienta, M.A., Avilés, M., Cáceres, R.E., Cipriani, H.N., Cornejo, L., Dias, L.E., Fernández Cirelli, A., Farfán, E.M., Garrido, S., Lorenzo, L., Morgada, M.E., Olmos-Márquez, M.A., Pérez-Carrera, A. (2011) Small-scale and household methods to remove arsenic from water for drinking purposes in Latin America. *Science of the Total Environment.*

Lizama, K. A., Fletcher, T. D., Sun G. (2011) Removal processes for arsenic in constructed wetlands. *Chemosphere* 84, 1032-1043.

Mariño, E. & Schulz, C.J. (2008) Importancia de los acuíferos en ambiente medanoso en la región semiarida pampeana. Heullas 12, 113-127.

Mohan, D. & Pittman Jr, C.U. (2007) Arsenic removal from water/wastewater using adsorbents-A critical review. *Journal of Hazardous Materials*. 1-53.

Nicolli, H.B., Suriano, J.M., Gomez Peral, M.A., Ferpozzi, L.H., Baleani, O.A. (1989) Groundwater Contamination with Arsenic and other trace elements in an area of the Pampa, Province of Cordoba, Argentina. *Environmental Geology Water Science*. 14, 3-16.

Nicolli, H.B., Bundschuh, J., García, J.W., Falcón, C.M., Jean, J.S. (2010) Sources and controls for the mobility of arsenic in oxidizing groundwaters from loess-type sediments in arid/semi-arid dry climates: Evidence from the Chaco-Pampean plain, Argentina. *Water Research* 44, 5589-5604.

Nicolli, H.B., Bundschuh, J., Blanco, Maria del C., Tujchneider O.F., Panarello Héctor O., Dapeña, C., Rusansky J.E. (2012) Arsenic and associated trace elements in groundwater form the Chaco Pampean Plain, Argentina: Results from 100 years of research. *Science of the Total Environment.*

O'Reilly, M.J., Watts, M.J., Shaw, R.A. Marcilla, A.L., Ward, N.I. (2010) Arsenic contamination of natural waters in San Juan and La Pampa, Argentina. *Environmental Geochemistry and Health*. 25, 491-515.

Otero, N., Vitória, L., Soler, A., Canals, A. (2005) Fertiliser characterization: Major, trace and rare earth elements. *Applied Geochemistry*. 20, 1473-1488.

Parkhurst, D.L. and CAJ Appelo. (1999) User´s guide to PHREEQC (Version 2) – A computer program for speciation, batch reaction, one dimensional transport, and inverse geochemical calculations. U.S.G.S. Water-Resources Investigations Report 99-4259.

Pimparkar B.D. (2011) Bhave A. Arsenicosis: a review of recent advances.*J. Assoc. Physicians India*. 59-335

Ramos O.E., Cáceres, L.F., Ormachea, M.R., Bhataccharya, P., Quino, I., Quintanilla, J., Sracek, O., Thunvik, R., Bundshuh, J., García, M.E. (2011) Sources and behaviour of arsenic and trace elements in groundwater and surface water in the Poopó Lake Basin, Bolívian Altiplano. *Enviro. Earth Sci*. (In press).

Rodriguez, M. (2011) Simulación numerica preliminar del flujo de agua subterránea en un sector aldeaño a Quemú Quemú, La Pampa. Degree Project Natural Resources Engineering. Facultad de Ciencias Exactas y Naturales. Universidad Nacional de La Pampa (UNLaP).

Smedley, P.L., Macdonald D.M.J., Nicolli, H.B., Barros, A.J., Tullio, J.O., Pearce, J.M. (2000) Arsenic and other Quality problems in Groundwater from Northern La Pampa Province, Argentina. *Technical Report from the British Geological Survey*.Overseas Geology Series.

Smedley, P.L., Nicolli H.B., Macdonald, D.M.J., Barros, A.J., Tullio, J.O. (2002) Hydrogeochemistry of arsenic and other inorganic constituents in groundwaters from La Pampa, Argentina. *Applied Geochemistry*. 17, 259-284.

Smedley, P.L. & Kinniburgh D.G. (2002) A review of the source, behaviour and distribution of arsenic in natural waters. *Applied Geochemistry*. 17, 517-568.

Smedley, P.L., Kinniburgh, D.G., Macdonald, D.M.J., Nicolli, H.B., Barros, A.J., Tullio, J.O., Pearce, J.M., Alonso, M.S. (2005)Arsenic associations in sediments from the loess aquifer of La Pampa, Argentina. *Applied Geochemistry*. 20, 989-1016.

Sracek, O., Bhattacharya, P., Jacks, G., Gustafsson, J.P., Von Brömssen, M. (2004) Behaviour of arsenic and geochemical modeling of arsenic enrichment in aqueous environment. *Applied Geochemistry*. 19, 169-180.

Stewart, C., Johnston, D.M., Leonard, G.S., Horwell, C. J., Thordarson, T., Cronin, S.J. (2006) Contamination of water supply by ashfall: A literature review and simple impact modeling. *Journal of volcanology and geothermal research*. 158, 296-306.

Tullio, J.O. & Giai, S.B. (1990) Ubicación y reservas de los principales acuíferos de La Pampa. Inédito. Administración Provincial del Agua de La Pampa. Santa Rosa.

Tullio, J.O., Pearce, J.M., Alonso, A.M. (2005) Arsenic associations in sediments from the loess aquifer of La Pampa, Argentina. *Applied Geochemistry*, 20, 989-1016.

Welch, S.A. & Ullman, W. (1999) The effects of microbial glucose metabolism on bytownite feldspar dissolution rates between 5 and 35ºC. Aquatic cycles at the earth surface. *Geochim. and Cosmochim. Acta*. 63, 3247-3259.

WHO. (1993) Guidelines for drinking water quality. Vol. 1, recommendations 2nd edition. World Health Organization. Geneva, Switzerland.

WHO. (2004) Guidelines for drinking water quality. third edition. Geneva Switzerland, Arsenic in drinking water, background document for preparation of WHO guidelines for drinking-water quality.

WHO. (2011) Guidelines for drinking water quality, fourth edition. World Health Organization, Geneva, Switzerland.

Zhang, H. & Selim, H.M. (2008) Reaction and Transport of Arsenic in Soils: Equilibrium and Kinetic Modeling. *Advances in Agronomy* 98, 45-115

10. OTHER REFERENCES

APA, Administración Provincial del Agua. 2001. Ministerio de Obras y Servicios Públicos. Govierno de la Pampa. http://www.apa.lapampa.gov.ar/acuiferos.html (accessed on December 2011) [in Spanish]

Código Alimentario Argentino. 1994. Chapter XII http://www.msal.gov.ar/argentina-saludable/pdf/CAPITULO_XII.pdf (accessed on 8 February, 2012) [in Spanish]

Gustafsson, J.P. (2011) Visual Minteq, a free equilibrium speciation model. http://www2.lwr.kth.se/english/oursoftware/vminteq (accessed on 15 December, 2012)

Match, version 2.0.12, Face identification from powder diffraction. Crystal impact: http://www.crystalimpact.com/match(accessed on May 2013)

IGN, National Institute of Geography of the Republic Argentine. Website: http://www.ign.gob.ar/sig250 (accessed on November 2011).

Tullio, J. Professor at the National University of La Pampa and manager at the Agencia Provincial del Agua. Personal communication September 2011.

APPENDIX I: Information of the wells sampled and results of the parameters measured in the field.

Sample ID	Location	Owner	Date of sampling	Water table (m)	Latitude (S)	Longitude (W)	T(ºC)	pH	EC (µS/cm)	Eh (mV)	TDS (mg/L)
NO5	QQ	La Celia	13-sep	3.1	-35.973	-63.727	14.4	8.1	9880	181.5	18628
NO6	QQ	R. Rodriguez	13-sep	3.5	-36.004	-63.706	16.4	7.9	4480	187.7	9443
NO1	QQ	San Ramón	13-sep	5.2	-35.917	-63.664	15.3	8.8	2660	137.8	4294
NE15	QQ	Escuela Trilí	13-sep	4.5	-35.913	-63.641	14.3	7.8	1227	197.2	1921
NO35	QQ	Bataglia	14-sep	4.0	-36.002	-63.636	13.9	8.1	2270	176.0	4365
NO9	QQ	San Leopoldo	14-sep	4.4	-35.991	-63.629	14.0	8.3	1730	165.3	2669
NE19	QQ	La Alicia	14-sep	4.3	-35.962	-63.603	15.1	7.9	894	185.0	1646
SO39	QQ	Aeroclub	14-sep	2.7	-36.057	-63.633	14.0	9.2	965	113.6	1353
SO20	QQ	Sol de Mayo	14-sep	5.7	-36.057	-63.743	16.4	8.1	6540	181.4	12644
SO40	QQ	Ricosa	14-sep	2.8	-36.155	-63.734	15.2	8.1	8580	176.7	15143
SO41	QQ	Escuela Huelén	14-sep	3.5	-36.116	-63.717	15.0	7.9	5620	189.7	10613
SO46	QQ	Quinta Barbulo	14-sep	3.6	-36.082	-63.631	15.7	7.8	4970	200.0	9270
NE27	QQ	San Alberto	15-sep	3.7	-35.951	-63.572	14.3	8.3	984	168.6	1787
NE26	QQ	El Arreador San Alberto	15-sep	4.3	-35.944	-63.572	15.2	8.5	3320	155.9	5597
NE24	QQ	Las Gambetas	15-sep	2.7	-35.914	-63.506	15.6	8.7	1620	146.3	1361
NE28	QQ	La Carpa casa	15-sep	3.2	-35.888	-63.571	14.2	8.1	976	178.3	817
NE25	QQ	Chacón	15-sep	3.5	-35.954	-63.504	16.1	8.4	7580	162.4	4555
NE22	QQ	Velázquez	15-sep	4.5	-35.983	-63.510	17.3	8.9	1730	131.7	1187
NE21	QQ	Don Juan Perez	15-sep	2.8	-35.996	-63.556	15.4	8.5	1660	154.3	1830
SE49	QQ	Rambarger	15-sep	2.0	-36.031	-63.572	15.5	8.8	1356	139.1	1083
SE50	QQ	Club de caza	16-sep	3.4	-36.065	-63.557	15.7	7.9	5170	185.5	3313
SE63	QQ	La Enriqueta	16-sep	3.6	-36.009	-63.524	15.8	8.1	1830	177.9	1526
SE62	QQ	San Miguel	16-sep	3.8	-36.065	-63.482	15.3	8.2	2510	172.6	1923
SE64	QQ	Castro	16-sep	3.0	-36.064	-63.521	15.1	7.7	11400	199.8	6590
SE83	QQ	Don Alfredo	16-sep	3.9	-36.013	-63.490	17.5	8.4	2230	163.4	1779
SE53	QQ	Tambo Garraham	16-sep	4.8	-36.001	-63.455	22.0	7.8	3270	193.7	2093
SE61	QQ	La Pampita	16-sep	3.4	-36.017	-63.434	15.6	7.5	1860	213.2	1281
SE60	QQ	Montserrat	16-sep	2.0	-36.033	-63.471	15.3	8.4	1451	152.0	1108
SE48	QQ	Moralejo	16-sep	3.2	-36.075	-63.597	15.0	7.4	1464	217.7	1105
SE54	QQ	Club de Pesca	17-sep	3.4	-36.041	-63.568	14.8	8.9	1600	120.7	1297
NO12	QQ	Cobrero	17-sep	7.0	-35.992	-63.615	15.6	7.9	456	232.6	410
SO2	QQ	Nito Bataglia	17-sep	5.1	-36.056	-63.599	16.1	7.4	2490	189.8	1861
ISO61	IA	Ea.San Antonio	21-sep	3.2	-35.329	-63.758	13.5	7.9	10640	186.7	6015
ISEP10	IA	Petisco	21-sep	4.2	-35.319	-63.689	12.7	8.1	2370	176.6	1597
INEP9	IA	Las Mercedes	21-sep	4.1	-35.314	-63.689	16.1	8.2	2190	173.2	1471
INEP8	IA	Las Mercedes	21-sep	3.6	-35.311	-63.691	16.2	8.1	2320	180.0	1617
INEP1	IA	Las Mercedes	21-sep	3.7	-35.297	-63.691	15.9	8.5	4000	156.8	2427
INEP3	IA	Las mercedes	22-sep	3.0	-35.302	-63.688	14.9	8.6	1241	150.8	839
INOP4	IA	Las mercedes	22-sep	2.9	-35.300	-63.692	13.1	8.7	1358	144.9	972
INOP12	IA	Las Mercedes	22-sep	4.5	-35.296	-63.697	10.5	8.8	1610	136.7	2718
INOP13	IA	Las Mercedes	22-sep	4.1	-35.298	-63.697	14.2	8.4	5040	161.2	2914
INO62	IA	Suc. Hércoli	22-sep	2.3	-35.294	-63.690	13.2	8.4	1160	159.1	890
INO63	IA	Suc. Hercoli	22-sep	3.1	-35.286	-63.682	11.8	7.7	6850	202.1	4734
INO64	IA	Suc. Hercoli	22-sep	3.3	-35.286	-63.689	12.9	8.0	8120	184.1	4780

APPENDIX II: Major ions concentrations (mg/L), ion balance (%) and water type of groundwater samples.

Sample ID	HCO_3^-	Cl^-	NO_3^-	SO_4^{2-}	PO_4^{3-}	∑Anions (meq/L)	Na^+	K^+	Mg^{2+}	Ca^{2+}	∑Cations (meq/L)	Ion balance	Water type
NO5	870.5	1604.9	98.4	1319.2	62	89.6	1670.9	47.1	80.8	55.2	83.3	-3.63%	Na-Cl-SO_4
NO6	447.5	742.8	116	615.5	539.1	48.7	647.6	68.4	80.6	107.8	41.9	-7.42%	Na-Cl-SO_4
NO1	662.1	320.4	76.4	192	86.8	26.2	562.6	21.7	14.6	13	26.9	1.20%	Na-HCO_3-Cl
NE15	502.7	75.3	46.1	59.2	13.4	12.6	190.1	10.2	33.5	46	13.6	3.82%	Na-HCO_3
NO35	496.6	370.2	72.4	220.7	28.4	24.7	475.8	17.1	33.6	30.6	25.4	1.37%	Na-HCO_3-Cl
NO9	711.1	71.1	52.8	95.3	57.2	17.4	361.1	11.9	11.7	9.3	17.4	0.25%	Na-HCO_3
NE19	306.5	29.5	90.8	23.1	0	7.9	57.4	10.3	42.7	51.7	8.9	5.97%	Na-HCO_3
SO39	472	42.9	20.3	36	150	11.8	238.9	9.6	1.6	2.4	10.9	-3.80%	Na-HCO_3
SO20	643.7	986.4	30.9	935.9	19.5	58.7	1228.3	19.3	45.6	39.3	59.6	0.75%	Na-Cl-SO_4
SO40	717.3	1289.9	183.3	969.7	77.2	72.5	1468.5	25	55.7	29.2	70.6	-1.33%	Na-Cl-SO_4
SO41	576.3	788.6	29.7	780.9	16.1	48.8	928.3	27.9	46.6	87.9	49.3	0.55%	Na-Cl-SO_4
SO46	950.2	639.7	45.9	527.6	390.2	49.5	505.4	115.9	161.6	229.8	49.7	0.19%	Na-HCO_3-Cl
NE27	410.7	25.6	80.4	30.8	119.8	10.8	130.8	45.6	21.1	26.7	9.9	-4.12%	Na-HCO_3
NE26	1293.5	197.4	105.9	224.3	266.3	36.6	731.4	11.3	19	11.5	34.2	-3.29%	Na-HCO_3
NE24	864.4	25	31	25.9	96.5	17.5	381.2	9.3	3.9	3.9	17.3	-0.48%	Na-HCO_3
NE28	490.4	29.8	25.6	31.4	24.8	10.4	190.4	10.4	14.8	15.4	10.5	0.70%	Na-HCO_3
NE25	950.2	1025.6	11.9	987.5	159	67.6	1346.1	21	42.4	23	63.7	-2.98%	Na-Cl-SO_4-HCO_3
NE22	435.3	168.4	35.4	154.6	36.9	16.2	369.8	8.7	3	4.4	16.8	1.80%	Na-HCO_3-Cl
NE21	1164.8	39.6	8.5	69.1	156.1	23.8	497.7	12	12	7	23.3	-1.03%	Na-HCO_3
SE49	705	21.9	3.4	31.2	102.7	14.2	287.3	9.9	7.9	5.8	13.7	-1.69%	Na-HCO_3
SE50	980.9	690.7	11.4	560.9	28.6	47.8	913.9	14.9	77.5	47.5	48.9	1.09%	Na-HCO_3-Cl-SO_4
SE63	797	71.9	84.5	107.8	58	19.6	384	11.5	24	17.2	19.8	0.68%	Na-HCO_3
SE62	747.9	242.7	60.6	254	159.3	27.1	484.8	13.7	39.5	30.9	26.2	-1.67%	Na-HCO_3-Cl
SE64	962.5	1839.2	100.7	1568.7	481.1	107	1749.2	93.7	160.8	96.9	96.5	-5.14%	Na-Cl-SO_4
SE83	938	115.2	48.2	107.9	56.8	22.6	496.2	11.6	15.5	8.6	23.6	2.23%	Na-HCO_3
SE53	508.8	428.6	164.2	330.8	12.6	30.2	526.2	14.8	59.8	57.9	31.1	1.49%	Na-HCO_3-Cl-SO_4
SE61	349.4	236	168.3	129.8	0	17.8	167.9	11.4	62.8	147.9	20.1	6.06%	Na-Ca-HCO_3-Cl
SE60	625.3	42.7	53	51.4	60.6	14.3	297.2	8.9	10	7.2	14.3	0.00%	Na-HCO_3
SE48	551.7	66.9	111.9	56.2	449.9	18.7	104.1	46.9	55.6	106.5	15.6	-8.99%	Ca-Na-HCO_3-PO_4
SE54	803.1	38.7	8.4	44.3	292.6	18.8	368.9	9.3	4.8	4.1	16.9	-5.50%	Na-HCO_3
NO12	190	7.6	19.6	6.7	153.3	5.4	12.9	9.2	11.2	49.4	4.2	-12.86%	Ca-Mg-HCO_3
SO2	380.1	232.6	515	201.2	0	25.3	155.9	11.1	139.7	219.4	29.5	7.66%	Ca-Na-HCO_3-NO_3
ISO61	692.7	1607	347.3	1442.3	250.4	95	1697.5	34.9	77.5	63.8	84.3	-6.00%	Na-Cl-SO_4
ISEP10	453.7	316	38.4	275.1	19.9	23	394.6	10.4	31.6	29.3	21.5	-3.38%	Na-HCO_3-Cl
INEP9	331	312.5	36.3	271.3	20.8	20.8	391	13.6	31.5	29.6	21.4	1.54%	Na-HCO_3-Cl
INEP8	472	300.6	21.9	262.8	30.7	22.5	439.9	11.9	26.8	29.1	23.1	1.42%	Na-HCO_3-Cl
INEP1	380.1	616.7	23.4	547.1	33	35.9	726.3	13.9	36.2	26.8	36.3	0.55%	Na-Cl-SO_4
INEP3	300.4	105.9	18.4	84.3	28	10.4	203.3	9.5	12.4	18.5	11	3.14%	Na-HCO_3-Cl
INOP4	337.2	133.3	14.8	113.2	41.5	12.4	247.1	9.4	10.1	14.4	12.5	0.57%	Na-HCO_3-Cl
INOP12	496.6	132.3	7.6	128.8	34.3	15.2	325.9	10.5	13.1	16.4	16.3	3.53%	Na-HCO_3-Cl
INOP13	392.4	761	21	703.2	28.9	43.4	865	17.4	57.2	40.5	44.8	1.60%	Na-Cl-SO_4
INO62	472	43.4	24.5	36	107.5	11.4	200.5	10.4	16.8	21.3	11.4	0.03%	Na-HCO_3
INO63	747.9	1060	29	894.6	467.8	66.3	1077	59.4	128	83.9	63.1	-2.52%	Na-Cl-SO_4
INO64	797	1163.8	61.6	1168.4	281.5	74.5	1388.2	36	56.5	37.9	67.8	-4.68%	Na-Cl-SO_4

APPENDIX III: Trace elements concentrations (µg/L) and As speciation (M) modeled in PHREEQC.

Sample ID DL	Al 679	As(tot) 5.6	As(III) (M) *	As(V) (M) *	B 3.6	Co 1636	Cr 481	Cu 341	F^- (mg/L)	Fe 803	Li 1776	Mn 116
NO5	95.7	147.3	1.77E-16	1.96E-06	4523.8	<DL	10.6	4.8	7.2	114.5	67.2	2.3
NO6	49.3	15.6	4.41E-17	2.08E-07	1251.2	1.7	2	2	0.6	32.2	45.7	18.6
NO1	20.5	112.1	9.12E-18	1.49E-06	1587.9	<DL	<DL	52.3	4.2	10.8	30.6	0.4
NE15	23.2	40.4	2.21E-16	5.38E-07	459.6	1.9	1.4	2.9	1.9	7.6	38.7	1.1
NO35	112.2	90.2	1.15E-16	1.20E-06	1999	<DL	4.3	2.5	2.2	7.4	22.8	5.1
NO9	14.3	148.6	9.03E-17	1.98E-06	1838	<DL	2.4	1	4.8	6.5	17	4.4
NE19	22.9	11.7	3.06E-17	1.56E-07	222.9	<DL	<DL	1.4	1	7.3	18.8	0.5
SO39	17.9	59.4	1.53E-18	7.92E-07	457.4	<DL	<DL	10.4	2.9	19.7	10.6	0.6
SO20	34.9	43.9	5.40E-17	5.86E-07	5483	2.2	12.2	2.5	4.1	9.2	45.8	0.5
SO40	22.7	154.6	1.85E-16	2.06E-06	4208.1	2.4	8.5	24.5	7.9	19.5	39.4	1.9
SO41	28	42.7	9.91E-17	5.69E-07	2675.4	<DL	5.8	9.9	3.9	47.3	47.3	0.9
SO46	23.1	18.6	3.52E-17	2.48E-07	1669.3	<DL	3.2	237	1.9	929.5	45.5	12.2
NE27	15.2	45.5	2.78E-17	6.06E-07	417.7	2.1	<DL	12.2	2.4	11.8	30.1	0.5
NE26	84.4	535.1	3.10E-16	7.16E-06	5122.5	<DL	<DL	4.6	12	17.9	28.8	5.2
NE24	24.1	270.9	3.49E-17	3.61E-06	1617.2	1.7	<DL	1.7	10.9	4.7	19.9	2.4
NE28	47.1	65.9	9.21E-17	8.79E-07	1021.4	<DL	<DL	1.1	3.4	5	18.1	0.6
NE25	31.7	324.3	2.07E-16	4.35E-06	4262.3	<DL	6.3	18.9	14.2	132.2	51.4	0.7
NE22	12.9	77.9	4.85E-18	1.04E-06	468.1	1.7	<DL	0.6	2.3	5	17.2	0.1
NE21	21	231.8	1.76E-16	3.09E-06	1841.8	1.8	<DL	8	6.8	11.9	23.3	1
SE49	18.4	182.4	1.84E-17	2.435E-06	1856.3	<DL	2.2	4.5	3.8	6.7	21.1	3.4
SE50	17.4	77.7	1.95E-16	1.04E-06	4862.2	2	<DL	3.2	2.5	12.2	63.2	10.6
SE63	30.4	96.1	1.22E-16	1.28E-06	1384.8	<DL	<DL	6.2	4.8	22.9	40.3	1.1
SE62	24.6	22	1.95E-17	2.93E-07	2298.3	2.4	4.9	42.5	1.7	47.3	46.2	1.5
SE64	31.6	23.7	1.01E-16	3.16E-07	4142.5	<DL	2.2	6.5	1.5	16.6	60.3	14.2
SE83	14.1	137.5	5.87E-17	1.83E-06	4400.1	<DL	<DL	10.9	6	31.6	39.4	0.9
SE53	11.9	23.6	7.67E-17	3.15E-07	1342	<DL	<DL	1.6	1.6	<DL	46.1	2.4
SE61	20.7	12	1.65E-16	1.60E-07	405.8	<DL	<DL	1.3	0.9	7	41.6	1.4
SE60	13	125	7.29E-17	1.67E-06	1248.5	1.7	1.7	3.8	6.2	5.7	20.4	1
SE48	23.4	12.9	3.11E-16	1.72E-07	336.6	1.8	<DL	7.2	1.1	4.4	38.3	2.4
SE54	21.8	485.6	1.67E-16	6.48E-06	2985.5	<DL	2	0.7	8.7	5.8	19.7	0.5
NO12	24.9	5.9	8.20E-19	7.81E-08	111	2.2	<DL	49.6	0.5	102.7	15.7	1.2
SO2	18.9	6.2	1.13E-15	8.29E-08	255.3	1.7	0.8	5.7	0.7	5.6	45	15.1
ISO61	29.2	31.8	5.11E-17	4.24E-07	3793	<DL	4.7	22.8	2.9	18.2	52.7	0.5
ISEP10	20.9	19.3	2.19E-17	2.57E-07	1428.2	2	0.5	1.6	1.8	6.7	21.6	0.2
INEP9	25.3	17.5	1.41E-17	2.33E-07	1403.4	2	3.1	4	1.8	12.6	21.4	0.3
INEP8	24.7	34.3	4.62E-17	4.57E-07	1697.3	<DL	<DL	0.7	1.9	12.1	23.1	0.2
INEP1	37.1	66.4	1.75E-17	8.85E-07	1709.3	<DL	2	7.2	2.8	16.8	35	4
INEP3	80.1	23.4	5.44E-18	3.13E-07	437.3	1.7	<DL	8.5	1.9	45.2	17.3	6
INOP4	38.5	19.9	2.31E-18	2.65E-07	465.5	1.7	<DL	10.4	1.6	53.3	17.9	4.1
INOP12	43.3	57.8	4.81E-18	7.71E-07	1219.8	3.2	<DL	12.8	3.8	1551.4	20.9	16.9
INOP13	33.1	87.9	2.85E-17	1.17E-06	1795.1	1.9	2.6	8.2	4.4	15.9	43.7	4.5
INO62	40.3	69.3	3.69E-17	9.24E-07	467.5	<DL	<DL	19.9	3.5	23.8	21.3	6.3
INO63	35.9	107.5	7.37E-16	1.43E-06	2615.7	<DL	<DL	322.4	3.9	614	65.3	8.2
INO64	30.1	248.4	3.67E-16	3.32E-06	3461.8	1.8	1.5	15.1	7.4	28	53.4	4.2

Sample DL	Mo 1761	P 15872	Pb 2301	Rb 6731	Si 5123.0	Sr 0.011	Ti 0.117	U 3132	V 987	Zn 1116
NO5	62	83.6	3.8	20.8	17984.0	1909.2	0.4	28.2	275.4	113.6
NO6	57.9	<DL	<DL	26.8	19718.5	2147.9	<DL	<DL	59.5	36.1
NO1	13.4	85.3	<DL	8.7	19116.2	495.2	0.3	9.3	280.7	73.8
NE15	4.3	<DL	<DL	6.9	21162.9	1157.6	0.2	7.5	151.5	97.5
NO35	39.8	38.7	<DL	10.4	19893.3	<DL	0.6	7.1	234.3	30.9
NO9	18.9	30.5	<DL	7.3	20471.7	311.3	0.3	15.5	279.9	28.8
NE19	<DL	<DL	<DL	<DL	19759.4	891.7	0.2	<DL	68.4	45.1
SO39	4.1	46.1	<DL	<DL	18637.3	58.1	0.7	5.9	278.5	46.1
SO20	204.9	<DL	<DL	14.5	21658.8	1235.4	0.3	25	159.4	30.3
SO40	110.1	45.9	<DL	20.8	18338	1192.3	0.2	18.6	274.6	28.1
SO41	125.6	<DL	<DL	16.5	19390.5	1260.4	0.2	16.5	217.5	88.5
SO46	120.8	<DL	7.8	55.7	19531.3	2830.8	0.3	17.1	67.5	801.1
NE27	4.8	136.6	<DL	21	18599.1	490.1	0.2	7.5	190	158
NE26	76.2	195.9	11.5	15.8	18299.5	424.2	0.8	32.4	1390.1	54.1
NE24	10.9	40.8	<DL	<DL	18824.7	130.7	0.4	22.5	1652.3	23.4
NE28	22.1	<DL	<DL	11.5	19733.0	410.3	0.4	10.8	190.3	33.2
NE25	490.3	101.7	<DL	17.6	16690.1	1170.4	1.8	30.9	215.6	67.7
NE22	59.2	22	<DL	7.1	17932.7	122	0.4	7.1	166.5	21.4
NE21	15.1	121.8	<DL	11.6	17185.8	590	0.6	13.5	1673.5	61.3
SE49	15.7	62.9	<DL	7.3	18168.1	232.9	0.6	8.9	114.2	29.2
SE50	63.7	22.5	11.5	12.1	20545.8	1604.7	0.2	26.7	186.6	245.1
SE63	28.8	54.7	13.1	10.5	19629.5	402.8	0.5	21	188	35.9
SE62	36.4	208.7	12.7	7.6	17053.5	861.8	0.5	15.3	87.8	65.9
SE64	146.6	1121.1	12.9	58.4	16416.8	4890.3	0.3	21.3	115.7	66.1
SE83	53.3	35.2	10.3	<DL	18261.3	317.2	0.9	47.6	259.4	56.9
SE53	76.8	<DL	<DL	7.3	18026.5	1138.4	<DL	6.7	100.7	5.4
SE61	37.4	<DL	9.8	<DL	20869.0	1558.6	0.3	7.2	22.5	31.6
SE60	8	34.2	7.8	<DL	19274.6	329.7	0.5	10.8	251.9	59.5
SE48	5.4	936.3	29.5	19.9	20216.7	1203.6	0.2	<DL	64.7	22.6
SE54	29.6	63	8.2	<DL	19055.4	152.5	0.3	21	1971.6	28.1
NO12	<DL	199.1	11.6	7.9	20532.9	272.4	0.3	<DL	20	96.9
SO2	9.6	<DL	16.9	<DL	18164.9	2526.3	0.2	<DL	33	47.8
ISO61	74.5	638.6	12.3	25.9	15351.3	2001.1	0.3	20	113.3	57
ISEP10	23.3	52.5	8.7	<DL	19576.8	1018.2	0.3	4.1	124.6	26.6
INEP9	23.1	155	7.4	9	19633.5	1011.4	0.5	6.9	123.4	27.9
INEP8	20.2	53.1	8.5	10.2	19025.3	910.5	0.4	12.8	231.4	22.7
INEP1	14.4	32.6	9.3	15.3	18262.7	<DL	0.7	8	246.5	22.3
INEP3	5.7	59.5	8	12	19747.3	317.6	2.2	4.3	217.9	54.4
INOP4	8.9	73.3	10.7	7.7	18972.0	322.8	0.8	5.4	198.1	41.6
INOP12	4.8	104.1	6.8	10.7	14423.6	345.3	0.8	9	272.2	67.6
INOP13	11.7	84	8.2	13.2	18180.9	1308.7	0.4	9.3	280.2	27.2
INO62	3.6	165.6	8.4	12	18750.3	371.9	0.6	7	280.1	39.9
INO63	13.7	1207.4	11.4	36.4	17829.3	2571.8	0.4	9.9	255.7	482.7
INO64	15.3	367.4	9.2	29.3	17235.6	1291.1	0.4	11.8	120	47.2

<DL samples below detection limit

APPENDIX IV: Correlation coefficients of total hydro-chemical parameters analysed in groundwater samples from Quemú Quemú (n=32).

	T	pH	EC	Eh	F	Cl	NO3	SO4	HCO_3	PO4	Ca	Mg	Na	K	As	B	U	V	Mo	Cu	Li	Si	Sr	Zn	Al	Fe	Mn
T	1.00	-0.12	0.06	0.12	-0.08	0.05	0.20	0.05	-0.02	-0.09	0.11	0.12	0.04	-0.05	-0.12	0.05	0.10	-0.12	0.19	0.00	0.24	-0.20	0.05	-0.06	-0.30	0.10	0.06
pH	-0.12	1.00	-0.26	-0.94	0.48	-0.30	-0.52	-0.28	0.25	-0.10	-0.73	-0.68	-0.08	-0.36	0.55	0.08	-0.06	0.49	-0.08	-0.11	-0.58	-0.31	-0.64	-0.18	-0.09	-0.16	-0.42
EC	0.06	-0.26	1.00	0.21	0.23	0.99	0.09	0.99	0.41	0.25	0.23	0.61	0.97	0.54	0.02	0.71	0.43	-0.15	0.62	0.11	0.76	-0.33	0.70	0.16	0.29	0.19	0.35
Eh	0.12	-0.94	0.21	1.00	-0.49	0.26	0.30	0.25	-0.29	0.12	0.62	0.55	0.04	0.36	-0.57	-0.11	0.05	-0.51	0.12	0.19	0.47	0.37	0.53	0.22	0.09	0.22	0.31
F	-0.08	0.48	0.23	-0.49	1.00	0.12	-0.25	0.16	0.66	-0.03	-0.47	-0.34	0.38	-0.23	0.87	0.56	0.64	0.64	0.45	-0.12	-0.05	-0.36	-0.32	-0.14	0.20	-0.06	-0.30
Cl	0.05	-0.30	0.99	0.26	0.12	1.00	0.10	0.99	0.29	0.24	0.25	0.63	0.94	0.56	-0.08	0.64	0.33	-0.22	0.57	0.09	0.75	-0.28	0.73	0.15	0.32	0.17	0.37
NO3	0.20	-0.52	0.09	0.30	-0.25	0.10	1.00	0.07	-0.26	-0.08	0.61	0.52	-0.04	0.04	-0.24	-0.19	-0.10	-0.23	-0.14	-0.08	0.27	-0.11	0.40	-0.12	0.01	-0.09	0.44
SO4	0.05	-0.28	0.99	0.25	0.16	0.99	0.07	1.00	0.32	0.25	0.24	0.61	0.95	0.55	-0.05	0.67	0.37	-0.20	0.63	0.08	0.76	-0.29	0.71	0.14	0.30	0.17	0.35
HCO_3	-0.02	0.25	0.41	-0.29	0.66	0.29	-0.26	0.32	1.00	0.27	-0.19	0.09	0.51	0.18	0.64	0.72	0.71	0.54	0.29	0.16	0.30	-0.43	0.12	0.24	0.18	0.21	0.11
PO4	-0.09	-0.10	0.25	0.12	-0.03	0.24	-0.08	0.25	0.27	1.00	0.29	0.38	0.17	0.71	0.11	0.07	0.20	0.14	0.10	0.32	0.16	-0.21	0.44	0.27	0.08	0.32	0.53
Ca	0.11	-0.73	0.23	0.62	-0.47	0.25	0.61	0.24	-0.19	0.29	1.00	0.85	-0.01	0.59	-0.47	-0.20	-0.07	-0.38	0.06	0.50	0.47	0.13	0.72	0.53	-0.04	0.55	0.64
Mg	0.12	-0.68	0.61	0.55	-0.34	0.63	0.52	0.61	0.09	0.38	0.85	1.00	0.41	0.75	-0.39	0.15	0.14	-0.36	0.24	0.44	0.71	-0.12	0.95	0.52	0.08	0.51	0.76
Na	0.04	-0.08	0.97	0.04	0.38	0.94	-0.04	0.95	0.51	0.17	-0.01	0.41	1.00	0.38	0.17	0.81	0.50	-0.01	0.63	0.68	0.68	-0.37	0.53	0.04	0.33	0.06	0.21
K	-0.05	-0.36	0.54	0.36	-0.23	0.56	0.04	0.55	0.18	0.71	0.59	0.75	0.38	1.00	-0.27	0.12	0.08	-0.23	0.20	0.61	0.48	-0.14	0.75	0.65	0.12	0.66	0.60
As	-0.12	0.55	0.02	-0.57	0.87	-0.08	-0.24	-0.05	0.64	0.11	-0.47	-0.39	0.17	-0.27	1.00	0.47	0.43	0.81	0.19	-0.16	-0.22	-0.30	-0.36	-0.16	0.24	-0.12	-0.20
B	0.05	0.08	0.71	-0.11	0.56	0.64	-0.19	0.67	0.72	0.07	-0.20	0.15	0.81	0.12	0.47	1.00	0.81	0.22	0.54	-0.05	-0.22	-0.22	0.22	0.03	0.33	0.01	0.08
U	0.10	-0.06	0.43	0.05	0.57	0.33	-0.10	0.37	0.71	0.20	-0.07	0.14	0.50	0.08	0.43	0.81	1.00	0.22	0.41	0.00	0.43	-0.18	0.13	0.06	0.17	0.07	0.16
V	-0.12	0.49	-0.15	-0.51	0.64	-0.22	-0.23	-0.20	0.54	0.14	-0.38	-0.36	-0.01	-0.23	0.81	0.22	0.22	1.00	-0.13	-0.15	-0.32	-0.21	-0.33	-0.14	0.10	-0.13	-0.18
Mo	0.19	-0.08	0.62	0.12	0.45	0.57	-0.14	0.63	0.29	0.10	0.06	0.24	0.63	0.20	0.19	0.54	0.41	-0.13	1.00	0.14	0.43	-0.26	0.28	0.11	0.08	0.23	0.02
Cu	0.00	-0.11	0.11	0.19	-0.12	0.09	-0.08	0.08	0.16	0.32	0.50	0.44	-0.01	0.61	-0.16	-0.05	0.00	-0.15	0.14	1.00	0.12	0.01	0.27	0.91	-0.10	0.95	0.24
Li	0.24	-0.58	0.76	0.47	-0.05	0.75	0.27	0.76	0.30	0.16	0.47	0.71	0.68	0.48	-0.22	0.52	0.43	-0.32	0.43	0.12	1.00	-0.15	0.72	0.25	0.15	0.21	0.43
Si	-0.20	-0.31	-0.33	0.37	-0.36	-0.28	-0.11	-0.29	-0.43	-0.21	0.13	-0.12	-0.37	-0.14	-0.30	-0.22	-0.18	-0.21	-0.26	0.01	-0.15	1.00	-0.17	0.09	0.00	-0.06	0.02
Sr	0.05	-0.64	0.70	0.53	-0.32	0.73	0.40	0.71	0.12	0.44	0.72	0.95	0.53	0.75	-0.36	0.22	0.13	-0.33	0.28	0.27	0.72	-0.17	1.00	0.36	0.18	0.34	0.73
Zn	-0.06	-0.18	0.16	0.22	-0.14	0.15	0.27	0.14	0.24	0.27	0.53	0.52	0.04	0.65	-0.16	0.03	0.06	-0.14	0.11	0.91	0.25	0.09	0.36	1.00	-0.06	0.94	0.35
Al	0.10	-0.09	0.29	0.09	0.20	0.32	0.01	0.30	0.18	0.08	-0.04	0.08	0.33	0.12	0.24	0.33	0.17	0.10	0.08	-0.10	0.15	0.00	0.18	0.20	1.00	-0.01	0.14
Fe	0.10	-0.16	0.19	0.22	-0.06	0.17	-0.09	0.17	0.21	0.32	0.55	0.51	0.06	0.66	-0.12	0.01	0.07	-0.13	0.23	0.95	0.21	0.01	0.34	0.03	0.94	1.00	0.30
Mn	0.06	-0.42	0.35	0.31	-0.30	0.37	0.44	0.35	0.11	0.53	0.64	0.76	0.21	0.60	-0.20	0.08	0.16	-0.18	0.02	0.24	0.43	-0.06	0.73	-0.17	0.35	0.14	1.00

APPENDIX V: Correlation coefficients of total hydro-chemical parameters analysed in groundwater samples from Intendente Alvear (n=12).

	T	pH	EC	Eh	F-	Cl-	NO_3	SO_4	HCO_3	PO_4	Ca^{2+}	Mg^{2+}	Na^+	K^+	As	B	U	V	Mo	Cu	Li	Si	Sr	Zn	Al	Fe	Mn
T	1.00	-0.04	-0.14	0.06	-0.40	-0.10	-0.03	-0.11	-0.48	-0.42	-0.19	-0.22	-0.13	-0.33	-0.27	-0.12	-0.01	-0.12	0.10	-0.37	-0.23	0.59	-0.11	-0.41	-0.02	-0.68	-0.67
pH	-0.04	1.00	-0.67	-0.99	-0.25	-0.68	-0.39	-0.66	-0.70	-0.74	-0.83	-0.81	-0.65	-0.78	-0.34	-0.72	-0.49	0.39	-0.48	-0.58	-0.72	-0.03	-0.87	-0.54	0.48	0.27	0.45
EC	-0.14	-0.67	1.00	0.67	0.54	0.99	0.74	0.99	0.79	0.72	0.79	0.78	0.99	0.78	0.50	0.95	0.80	-0.38	0.69	0.33	0.90	-0.50	0.82	0.31	-0.31	-0.11	-0.20
Eh	0.06	-0.99	0.67	1.00	0.24	0.69	0.40	0.66	0.69	0.72	0.83	0.80	0.65	0.77	0.33	0.73	0.50	-0.41	0.50	0.56	0.71	0.04	0.87	0.52	-0.50	-0.29	-0.48
F-	-0.40	-0.25	0.54	0.24	1.00	0.51	0.03	0.56	0.69	0.53	0.29	0.39	0.57	0.50	0.95	0.56	0.32	0.02	-0.10	0.17	0.63	-0.46	0.30	0.17	-0.10	0.18	0.32
Cl-	-0.10	-0.68	0.99	0.69	0.51	1.00	0.72	0.99	0.76	0.71	0.81	0.80	0.99	0.79	0.48	0.95	0.78	-0.38	0.70	0.35	0.91	-0.47	0.85	0.33	-0.33	-0.13	-0.23
NO_3	-0.03	-0.39	0.74	0.40	0.03	0.72	1.00	0.71	0.45	0.35	0.49	0.37	0.72	0.36	-0.06	0.67	0.79	-0.52	0.95	-0.03	0.43	-0.48	0.48	-0.04	-0.21	-0.18	-0.33
SO_4	-0.11	-0.66	0.99	0.66	0.56	0.99	0.71	1.00	0.77	0.70	0.77	0.77	0.99	0.77	0.53	0.96	0.78	-0.40	0.67	0.30	0.90	-0.47	0.81	0.28	-0.33	-0.14	-0.22
HCO_3	-0.48	-0.70	0.79	0.69	0.69	0.76	0.45	0.77	1.00	0.87	0.71	0.72	0.79	0.84	0.69	0.83	0.65	-0.24	0.38	0.52	0.81	-0.55	0.71	0.51	-0.33	0.18	0.09
PO_4	-0.42	-0.74	0.72	0.72	0.53	0.71	0.35	0.70	0.87	1.00	0.85	0.87	0.70	0.97	0.56	0.68	0.48	-0.11	0.27	0.80	0.86	-0.34	0.80	0.80	-0.12	0.12	0.10
Ca^{2+}	-0.19	-0.83	0.79	0.83	0.29	0.81	0.49	0.77	0.71	0.85	1.00	0.98	0.76	0.92	0.28	0.74	0.57	-0.12	0.50	0.77	0.89	-0.27	0.98	0.75	-0.28	0.01	-0.12
Mg^{2+}	-0.22	-0.81	0.78	0.80	0.39	0.80	0.37	0.77	0.72	0.87	0.98	1.00	0.76	0.95	0.39	0.74	0.50	-0.07	0.80	0.80	0.93	-0.26	0.97	0.78	-0.28	0.03	-0.06
Na^+	-0.13	-0.65	0.99	0.65	0.57	0.99	0.72	0.99	0.79	0.70	0.76	0.76	1.00	0.76	0.54	0.96	0.80	-0.38	0.68	0.29	0.89	-0.51	0.80	0.27	-0.33	-0.11	-0.19
K^+	-.336	-0.78	0.78	0.77	0.50	0.79	0.36	0.77	0.84	0.97	0.92	0.95	0.76	1.00	0.53	0.75	0.51	-0.13	0.32	0.82	0.92	-0.33	0.90	0.81	-0.18	0.11	0.05
As	-0.27	-0.34	0.50	0.33	0.95	0.48	-0.06	0.53	0.69	0.56	0.28	0.39	0.54	0.53	1.00	0.54	0.24	-0.04	-0.17	0.22	0.62	-0.27	0.31	0.21	-0.12	0.04	0.19
B	-0.12	-0.72	0.95	0.73	0.56	0.95	0.67	0.96	0.83	0.68	0.74	0.74	0.96	0.75	0.54	1.00	0.81	-0.45	0.68	0.28	0.85	-0.51	0.80	0.27	-0.45	-0.04	-0.22
U	-0.01	-0.49	0.80	0.50	0.32	0.78	0.79	0.78	0.65	0.48	0.57	0.50	0.80	0.51	0.24	0.81	1.00	-0.22	0.76	0.09	0.61	-0.64	0.58	0.08	-0.35	0.01	-0.15
V	-0.12	0.39	-0.87	-0.41	0.02	-0.38	-0.52	-0.40	-0.24	-0.11	-0.12	-0.07	-0.38	-0.13	-0.04	-0.45	-0.22	1.00	-0.61	0.23	-0.09	-0.06	-0.22	0.23	0.36	0.39	0.61
Mo	0.18	-0.48	0.69	0.50	-0.10	0.70	0.95	0.67	0.38	0.27	0.50	0.39	0.68	0.32	-0.17	0.68	0.76	-0.61	1.00	-0.05	0.39	-0.35	0.54	-0.06	-0.38	-0.25	-0.50
Cu	-0.37	-0.58	0.33	0.56	0.17	0.35	-0.03	0.30	0.52	0.80	0.77	0.80	0.29	0.82	0.22	0.28	0.09	0.23	-0.05	1.00	0.63	-0.09	0.70	0.99	-0.00	0.29	0.26
Li	-0.23	-0.72	0.90	0.71	0.63	0.91	0.43	0.90	0.81	0.86	0.89	0.93	0.89	0.92	0.62	0.85	0.61	-0.09	0.39	0.63	1.00	-0.40	0.90	0.61	-0.26	0.00	-0.01
Si	0.59	-0.03	-0.50	0.04	-0.46	-0.47	-0.48	-0.47	-0.55	-0.34	-0.27	-0.26	-0.51	-0.33	-0.27	-0.51	-0.64	-0.06	-0.35	-0.09	-0.40	1.00	-0.24	-0.12	0.08	-0.04	-0.56
Sr	-0.11	-0.87	0.82	0.87	0.30	0.85	0.48	0.81	0.71	0.80	0.98	0.97	0.80	0.90	0.31	0.80	0.58	-0.22	0.54	0.70	0.90	-0.24	1.00	0.67	-0.41	-0.05	-0.22
Zn	-0.41	-0.54	0.31	0.52	0.17	0.33	-0.04	0.28	0.51	0.80	0.75	0.78	0.27	0.81	0.21	0.27	0.08	0.23	-0.06	0.99	0.61	-0.12	0.67	1.00	0.04	0.35	0.31
Al	-0.02	0.48	-0.31	-0.50	-0.10	-0.33	-0.21	-0.33	-0.33	-0.12	-0.28	-0.28	-0.33	-0.18	-0.12	-0.45	-0.35	0.36	-0.38	-0.00	-0.26	0.08	-0.41	0.04	1.00	0.14	0.44
Fe	-0.68	0.27	-0.11	-0.29	0.18	-0.13	-0.18	-0.14	0.18	0.12	0.01	0.03	-0.11	0.11	0.04	-0.04	0.01	0.39	-0.25	0.29	0.01	-0.67	-0.05	0.35	0.14	1.00	0.88
Mn	-0.67	0.45	-0.20	-0.48	0.32	-0.23	-0.33	-0.22	0.09	0.10	-0.12	-0.06	-0.19	0.05	0.19	-0.22	-0.15	0.61	-0.50	0.26	-0.01	-0.56	-0.22	0.31	0.44	0.88	1.00

APPENDIX VI: Spatial distribution of As and other elements analysed in QQ study area, using kriging interpolation for mapping the results. ▲ village of Quemú Quemú.

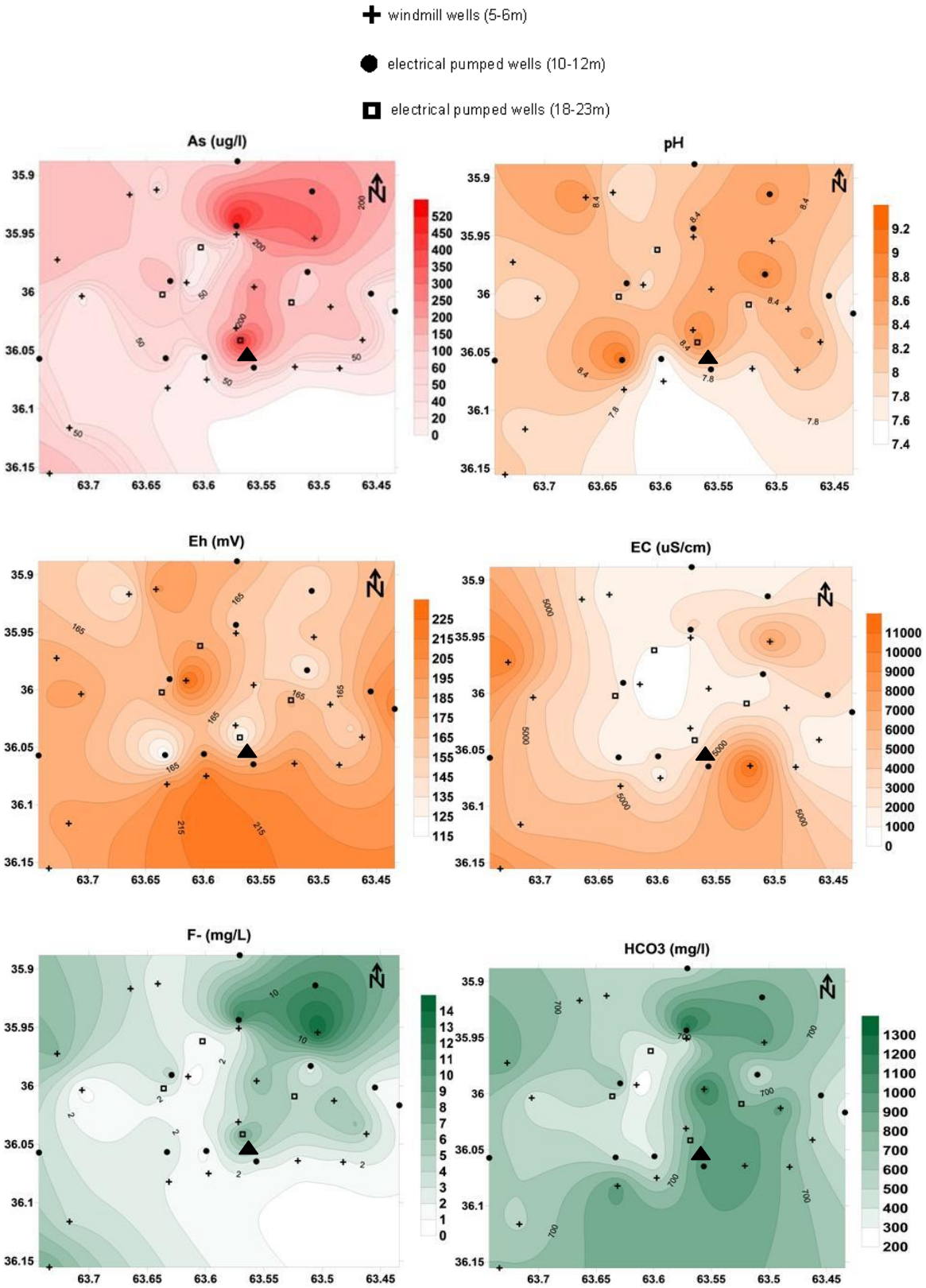

Appendix VI (cont.) Spatial distribution of As and other elements analysed in QQ study area, using kriging interpolation for mapping the results. ▲ village of Quemú Quemú.

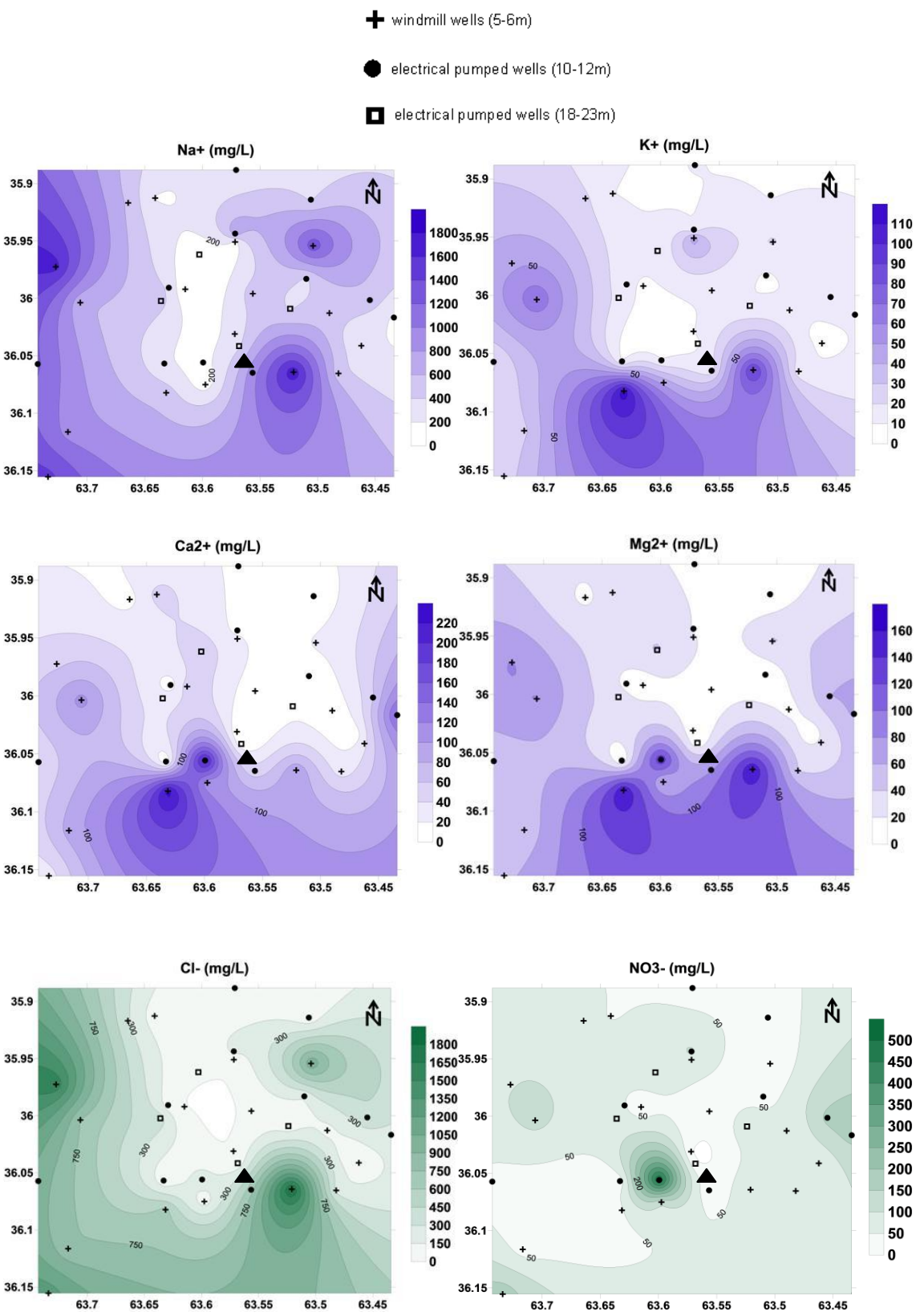

Appendix VI (cont.): Spatial distribution of As and other elements analysed in QQ study area, using kriging interpolation for mapping the results. ▲ village of Quemú Quemú.

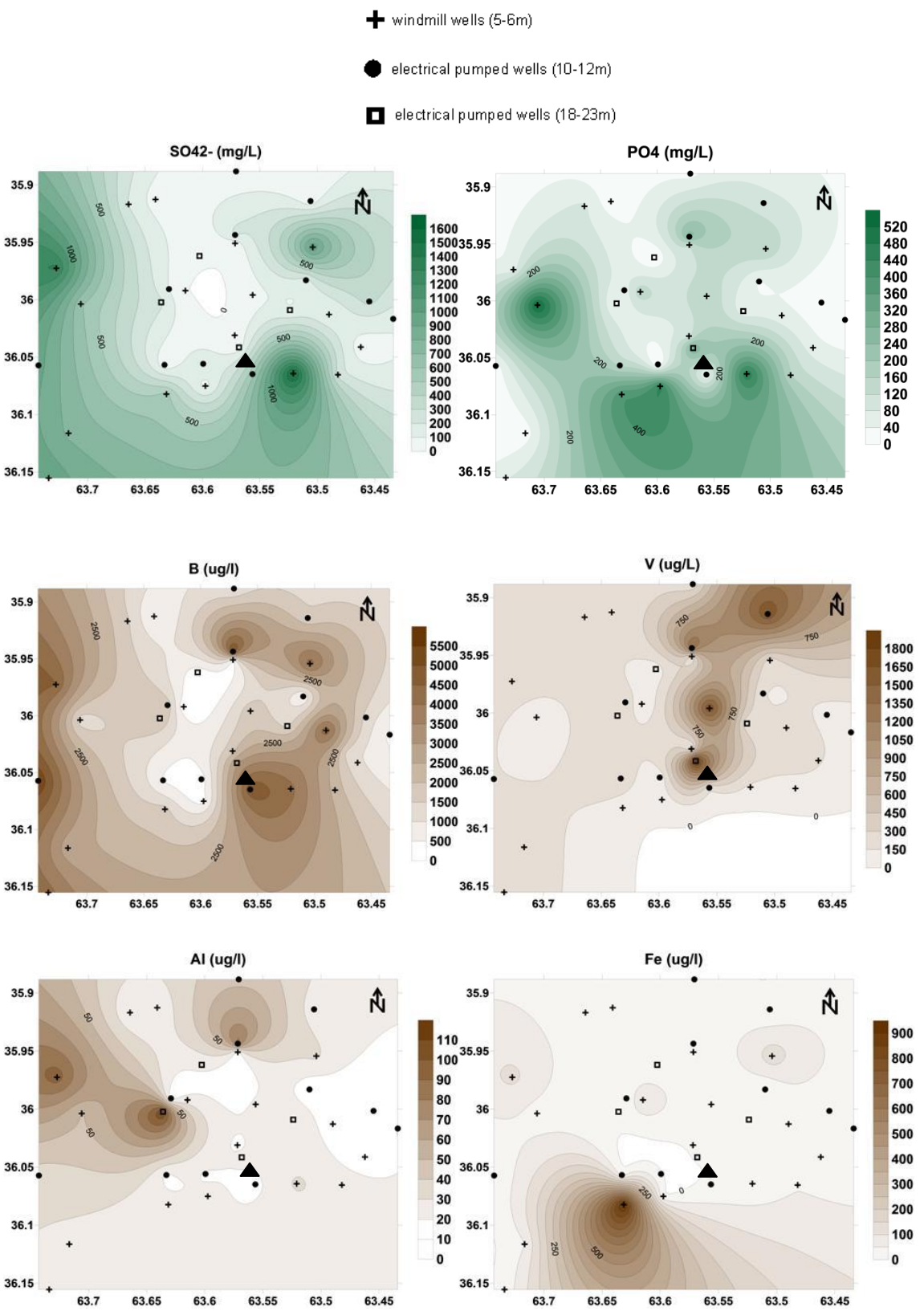

Appendix VI (cont.): Spatial distribution of As and other elements analysed in QQ study area, using kriging interpolation for mapping the results. ▲ village of Quemú Quemú.

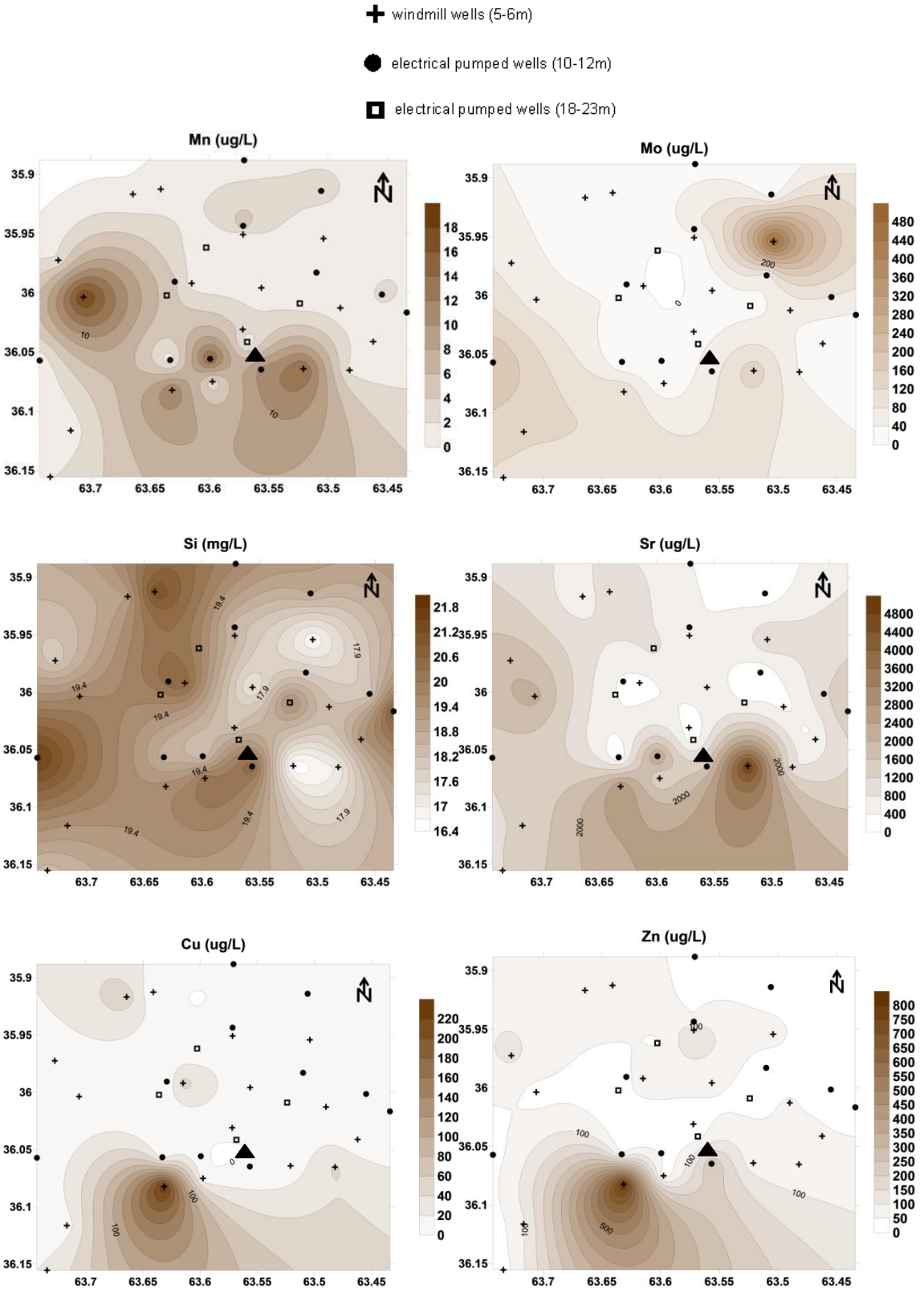

APPENDIX VII: Spatial distribution of As and other elements analysed in IA study area, using kriging interpolation for mapping the results.

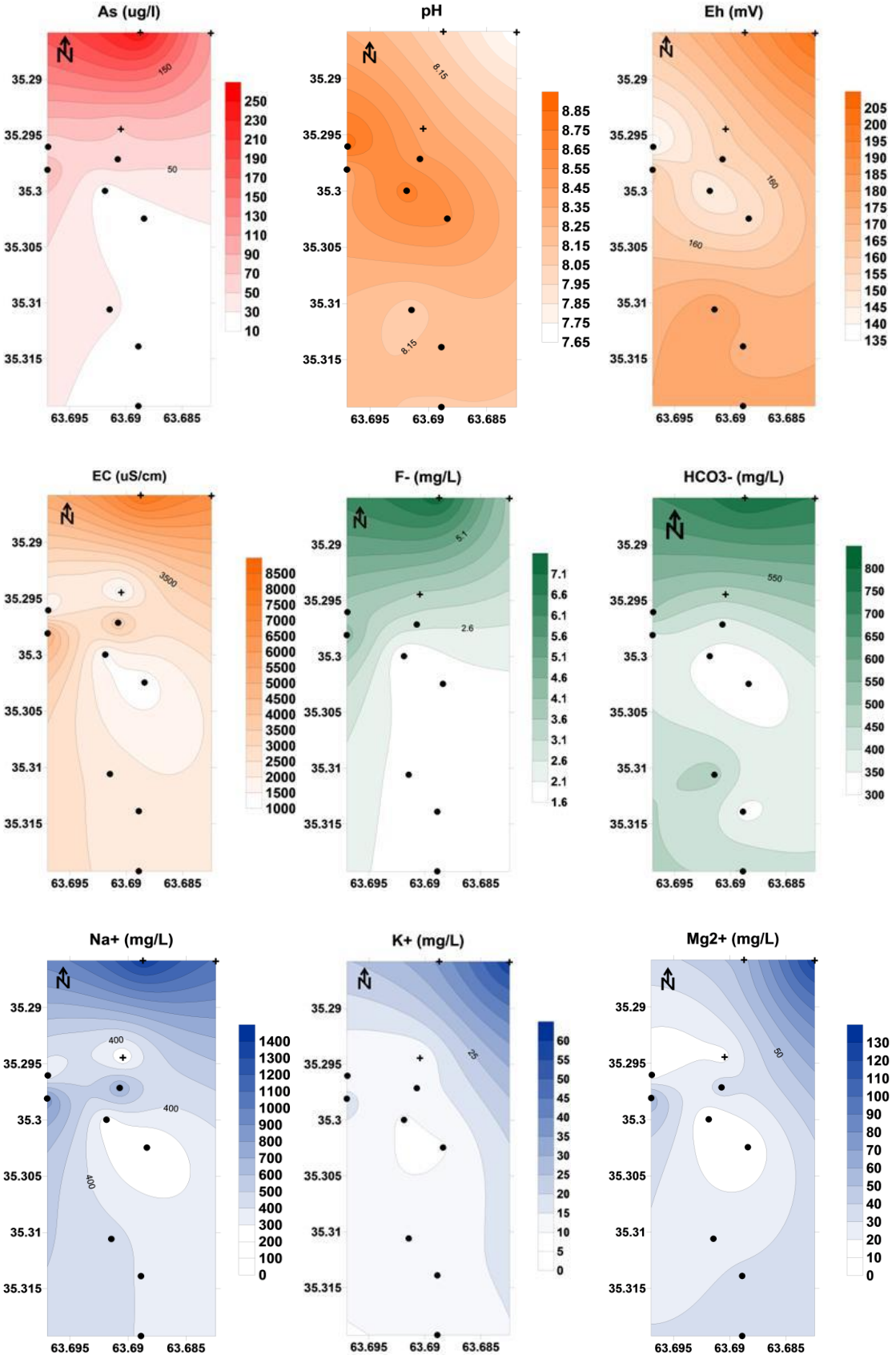

Appendix VII (cont.): Spatial distribution of As and other elements analysed in IA study area, using kriging interpolation for mapping the results.

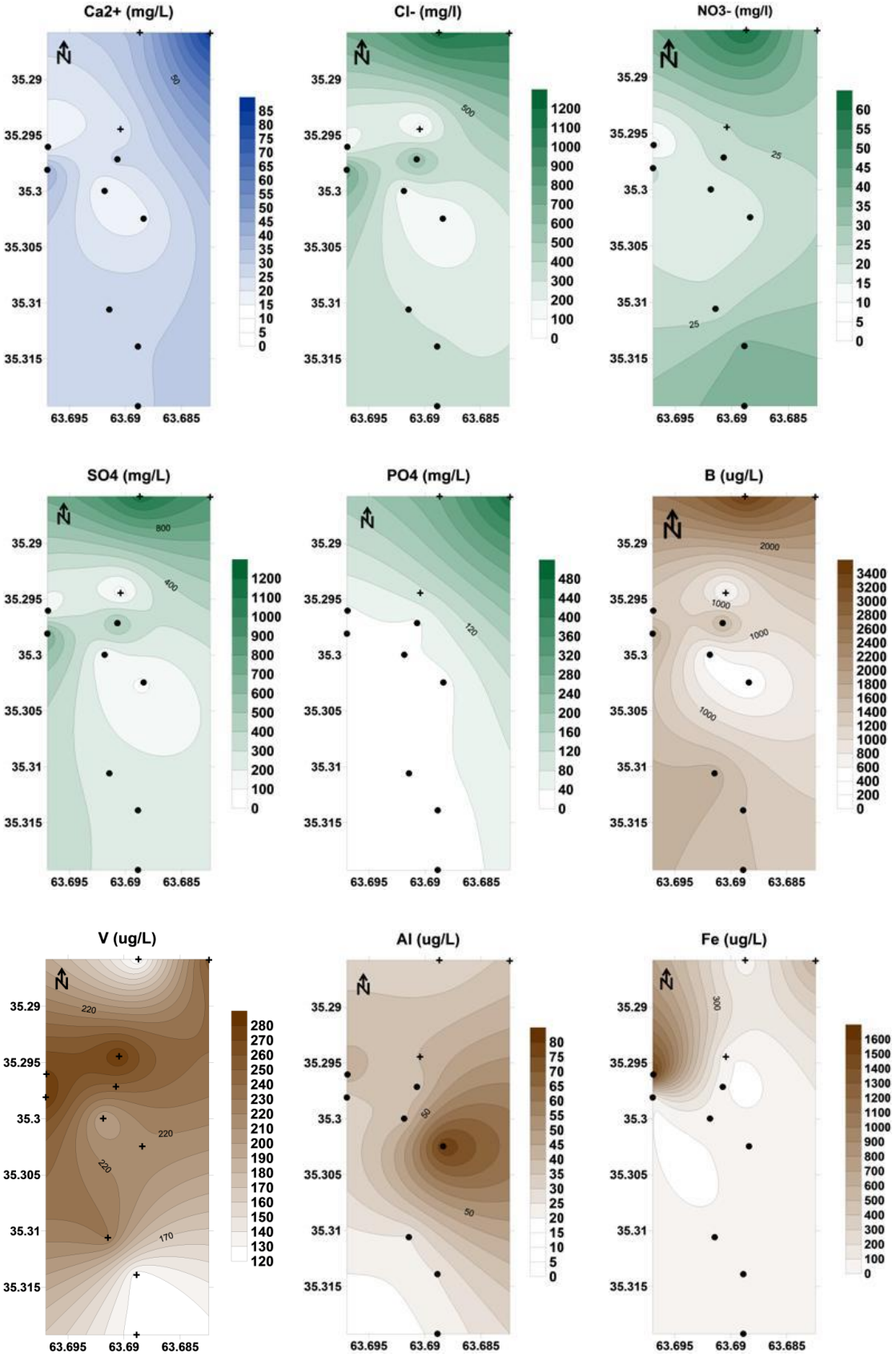

Appendix VII (cont.): Spatial distribution of As and other elements analysed in IA study area, using kriging interpolation for mapping the results.

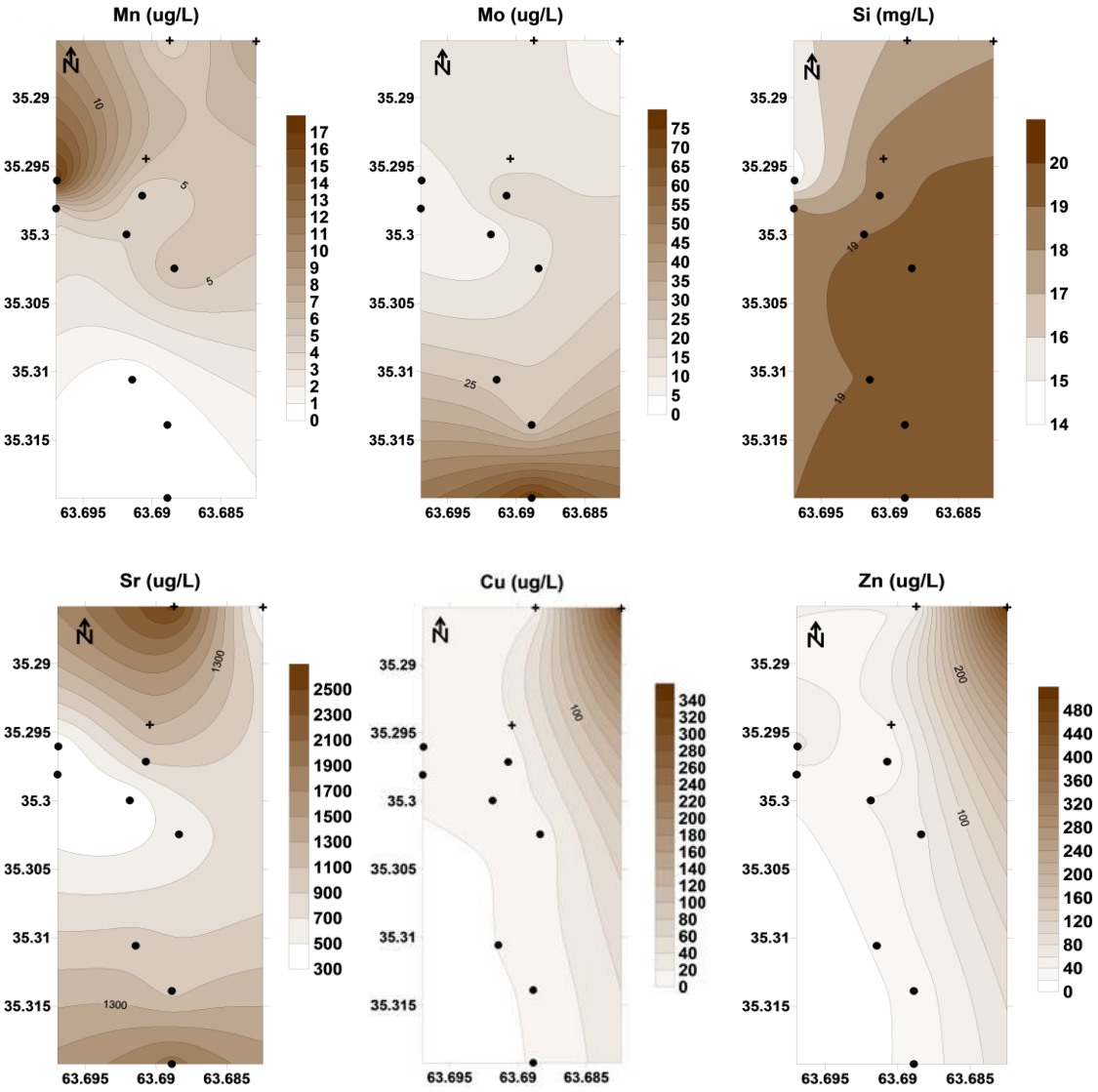

APPENDIX VIII: Main characteristics of the sediments samples collected in the area of QQ and results of pH and CEC analysed on the sediments leachates.

Sample	Sediment type	Depth (m)	pH	Munsell Color and code
M1	coarse sand	0 to 6	8,57	light yellowish brown 10YR-6/4
M2	fine sand	6 to 12	8,96	pale brown 10YR-6/3
M3	fine sand	12 to 18	8,97	pale brown 10YR-6/3
P1	fine sand	0 to 6	8,82	pale brown 10YR-6/3
P2	fine sand with silt	6 to 12	8,71	very pale brown 10YR-7/3
P3	fine sand with silt	12 to 18	8,95	pale brown 10YR-6/3
L1	fine sand with salts nodules	0 to 0.03	9,78	light browish grey 10YR-6/2
L2	fine silty sand	0.03 to 0.06	10,22	greyish brown 10YR-5/2
L3	fine silty sand	0.06 to 0.09	10,26	greyish brown 10YR-5/2
A	volcanic ash	0,05	8,52	very dark greyish brown 10YR-3/2

Sample	Ca^{2+} (meq/100g)	Mg^{2+} (meq/100g)	Na^{+} (meq/100g)	K^{+} (meq/100g)	Total CEC
L1	2	0.04	4.97	4.10	11.11
L2	3.36	0.96	15.5	2.36	22.18
L3	5.7	2.44	15.1	2.36	25.6
M1	2.74	7.4	0.64	0.48	11.26
M2	14.08	4.24	1.30	0.54	20.16
M3	24	7.86	1.87	0.64	34.37
P1	16.48	7.4	1.58	0.64	26.1
P2	19.32	4.4	1.67	0.67	26.06
P3	17.88	2.4	1.30	0.75	22.33
Ash	16.92	3.52	0.06	1.34	21.84

APPENDIX IX: Results of the four steps sequential extractions applied on the sediments samples (in mg/kg).

Sample	Al	As	B	Ba	Ca	Cd	Co	Cr	Cu	Fe	K	Li	Mg
DIW													
M1	5.14	0.26	0.75	0.14	12.43	<DL	<DL	0.04	0.05	5.11	70.01	0.34	2.69
M2	3.03	0.60	1.21	0.07	57.31	<DL	<DL	0.04	0.03	2.34	28.70	0.35	18.51
M3	1.14	0.12	0.41	0.04	48.35	<DL	0.03	0.04	0.02	0.95	17.85	0.26	17.19
L1	0.79	145.07	<DL	0.55	168.97	0.02	0.04	0.05	0.23	0.27	1517.51	0.22	0.60
L2	27.38	0.64	5.58	0.47	17.90	<DL	0.04	0.03	0.11	47.79	72.76	0.19	50.27
L3	14.39	0.78	3.29	0.33	16.72	<DL	0.02	0.03	0.14	24.38	45.32	0.14	29.92
P1	1.59	0.22	1.26	0.47	30.44	<DL	<DL	0.01	0.01	1.61	20.98	0.16	4.40
P2	1.85	0.11	0.66	0.04	38.01	<DL	<DL	0.03	0.02	1.84	14.47	0.18	9.17
P3	1.85	0.14	0.71	0.11	47.58	<DL	<DL	0.02	0.02	1.74	17.20	0.26	15.75
ASH	16.12	0.17	0.54	0.59	139.89	<DL	<DL	0.06	0.04	12.53	110.14	0.39	22.17
ACETATE													
M1	2.21	0.62	0.59	7.50	204.01	0.06	0.04	0.14	0.30	1.56	509.34	0.30	38.48
M2	1.87	0.70	0.56	6.43	606.44	0.06	0.10	0.13	0.30	2.11	403.38	0.31	113.36
M3	1.78	0.44	0.39	5.71	335.78	0.04	<DL	0.06	0.26	1.38	426.73	0.21	181.75
L1	0.87	3.24	8.19	1.07	85.69	0.04	<DL	0.07	0.19	1.10	598.64	0.20	3.74
L2	0.42	0.30	0.45	2.04	205.45	0.04	<DL	0.05	0.28	2.28	676.79	0.13	44.40
L3	0.18	0.27	0.47	2.99	157.20	0.02	<DL	0.05	0.25	1.92	574.28	0.10	86.08
P1	1.12	0.28	0.19	5.85	200.50	0.04	0.04	0.04	0.17	2.06	323.95	0.14	55.27
P2	1.05	0.27	0.25	5.78	228.20	0.04	0.07	0.05	0.14	1.74	366.18	0.16	92.34
P3	1.57	0.36	0.33	6.72	441.89	0.05	0.10	0.06	0.21	1.82	464.27	0.22	133.87
ASH	26.58	0.68	0.36	14.99	818.08	0.07	0.06	0.13	0.61	27.29	878.57	0.33	103.29
OXALATE													
M1	17.58	0.18	0.31	0.40	1.47	0.03	0.02	0.03	0.04	5.96	9.96	0.36	2.99
M2	26.95	0.20	0.27	0.30	1.43	<DL	0.09	0.03	0.06	10.21	13.21	0.38	73.74
M3	25.77	0.15	0.21	0.33	1.07	0.01	0.08	0.03	0.07	4.07	18.33	0.28	177.99
L1	13.17	0.15	1.04	0.20	1.04	0.02	<DL	0.03	0.06	9.92	18.07	0.24	8.36
L2	43.35	0.10	0.37	0.27	0.55	0.01	0.02	0.02	0.13	18.88	56.51	0.19	55.64
L3	39.75	0.12	0.25	0.19	0.53	0.24	0.01	0.02	0.16	12.34	52.67	0.16	72.03
P1	24.72	0.09	0.11	0.31	0.63	<DL	0.04	0.02	0.05	12.12	13.77	0.17	9.65
P2	26.05	0.08	0.10	0.24	0.69	0.01	0.05	0.02	0.05	11.16	14.25	0.19	9.63
P3	26.99	0.15	0.14	0.36	1.06	0.01	0.07	0.03	0.07	17.86	14.51	0.27	67.31
ASH	51.47	0.26	0.20	2.53	2.24	0.13	0.16	0.05	0.23	79.35	25.22	0.42	8.80
RF													
M1	2914.64	1.36	1.63	186.06	2362.35	0.09	1.70	1.83	2.08	4121.68	527.18	2.07	966.11
M2	4771.12	1.56	2.92	163.88	13979.59	0.26	2.10	2.96	2.64	5339.26	1028.60	3.40	1533.24
M3	6566.95	1.67	4.11	52.60	27397.64	1.60	2.58	2.93	2.90	5001.00	1251.50	5.58	5217.28
L1	3016.51	1.19	3.60	25.96	1952.44	0.09	1.79	2.13	1.12	3908.46	731.97	2.11	1167.24
L2	6047.21	3.13	6.86	39.09	6755.09	0.17	2.98	3.61	2.52	3831.34	2176.43	15.35	4503.36
L3	5129.14	2.63	4.79	42.93	8483.59	0.44	2.41	2.64	2.50	2947.78	1989.65	15.37	5009.24
P1	3405.01	0.87	1.35	30.67	6465.60	0.31	1.76	1.68	2.10	3415.99	665.62	2.86	1665.10
P2	5275.58	1.43	2.35	40.89	7570.82	0.60	2.42	3.15	3.10	4344.23	1149.12	4.73	1774.24
P3	6095.05	1.62	3.24	41.53	14050.13	0.95	2.68	3.40	3.03	5437.74	1115.86	4.45	2672.63
ASH	7145.56	1.20	1.94	45.36	2801.32	0.92	2.96	3.95	2.88	7342.54	1183.17	3.65	1361.23

Appendix IX (cont.): Results of the four steps sequential extractions applied on the sediments samples (in mg/kg).

	Mn	Mo	Na	Ni	P	Pb	Rb	Si	Sr	Ti	V	Zn	Zr
DIW													
M1	0.65	0.04	107.26	<DL	3.44	0.10	0.10	17.82	0.08	0.26	0.44	0.84	0.03
M2	0.36	<DL	283.39	<DL	1.57	<DL	0.14	35.55	0.37	0.14	1.10	0.38	0.04
M3	0.08	<DL	134.14	<DL	0.60	0.04	0.10	46.32	0.50	0.05	0.43	0.41	0.02
L1	0.08	<DL	41959.66	0.76	120.82	0.06	0.76	190.45	4.02	0.06	176.95	0.87	0.04
L2	1.22	0.09	759.85	0.04	4.91	0.05	0.12	180.13	0.36	2.28	11.16	0.39	0.03
L3	0.46	0.06	615.04	0.03	4.21	0.04	0.08	112.31	0.32	1.32	9.40	0.37	0.02
P1	0.14	0.37	158.65	<DL	0.87	<DL	0.06	29.55	0.16	0.09	0.58	0.26	0.02
P2	0.17	0.02	93.58	<DL	1.26	0.03	0.06	37.60	0.25	0.11	0.36	0.11	0.02
P3	0.17	<DL	110.52	<DL	0.85	0.04	0.07	42.10	0.57	0.10	0.31	0.26	0.07
ASH	0.52	<DL	24.00	<DL	2.05	0.06	0.17	42.85	0.76	0.66	0.08	21.41	0.06
ACETATE													
M1	0.55	0.04	147923.34	0.04	42203.12	0.13	4.97	22.16	1.95	0.09	0.11	0.56	0.11
M2	9.04	0.03	150004.62	0.09	42506.50	0.16	3.03	29.42	3.31	0.31	0.21	0.76	0.12
M3	0.89	0.03	109186.07	<DL	30844.27	0.09	1.27	36.04	6.83	0.09	0.14	6.71	0.08
L1	1.33	0.27	94535.98	0.04	26612.04	0.12	1.34	53.73	1.78	0.13	4.55	0.44	0.06
L2	1.06	0.02	58235.27	<DL	16618.47	0.08	1.10	32.93	9.10	0.13	0.42	0.34	0.04
L3	2.03	0.03	47532.11	<DL	13152.01	0.06	0.58	32.77	12.15	0.14	0.97	0.22	0.03
P1	5.37	<DL	67606.19	0.06	18425.49	0.07	0.82	24.69	2.28	0.24	0.11	0.37	0.06
P2	5.15	0.03	75877.10	0.05	20574.43	0.08	0.45	26.68	3.23	0.22	0.12	0.33	0.07
P3	4.51	0.05	112011.25	0.04	30365.50	0.11	0.81	34.65	6.96	0.20	0.11	0.53	0.08
ASH	1.15	<DL	171417.53	0.14	46453.89	0.17	1.96	39.10	3.89	1.38	0.14	0.68	2.05
OXALATE													
M1	1.29	<DL	537.89	0.05	138.77	0.05	0.08	3.47	0.05	0.38	0.06	0.11	0.09
M2	4.67	<DL	875.98	0.08	326.21	0.05	0.10	7.30	0.02	1.24	0.15	0.15	0.21
M3	3.60	<DL	916.12	0.06	375.35	0.02	0.12	9.95	0.02	0.56	0.12	0.14	0.19
L1	1.40	<DL	591.92	0.04	146.53	0.07	0.06	7.33	0.05	0.58	0.24	0.14	0.22
L2	1.92	<DL	990.01	0.03	349.56	0.05	0.15	28.81	0.07	1.15	0.65	0.15	0.24
L3	1.51	<DL	1006.23	0.02	463.04	0.02	0.15	29.65	0.05	0.85	1.07	0.29	0.22
P1	2.62	<DL	703.16	0.05	301.57	0.04	0.09	8.09	0.01	0.87	0.10	0.07	0.14
P2	2.84	<DL	688.38	0.04	302.10	0.04	0.10	8.20	0.01	0.99	0.12	0.08	0.19
P3	2.50	<DL	762.83	0.05	268.37	0.06	0.10	8.84	0.04	1.33	0.16	0.13	0.19
ASH	13.80	<DL	1298.17	0.11	353.85	0.22	0.22	16.48	0.06	6.97	0.30	0.31	0.84
RF													
M1	41.71	0.28	846.47	2.51	406.33	2.08	3.25	15.22	11.83	98.14	7.28	12.26	2.02
M2	73.43	0.57	1132.98	2.90	450.46	2.52	6.69	71.14	30.96	309.53	16.67	12.75	7.67
M3	132.53	0.35	1508.97	3.17	482.36	2.45	11.57	25.13	77.66	364.38	20.65	14.46	10.68
L1	53.22	0.04	628.82	2.14	172.17	1.54	4.00	13.71	11.95	99.55	16.52	12.27	1.61
L2	88.69	14.21	1032.17	3.50	372.05	2.37	12.38	34.97	49.67	254.16	140.95	12.36	6.05
L3	67.27	0.07	1114.75	3.04	455.82	2.15	10.53	39.26	92.13	172.40	227.05	9.94	1.65
P1	43.25	0.77	617.14	2.58	324.67	1.97	5.14	25.25	15.94	121.33	9.23	10.72	0.34
P2	74.87	0.29	766.09	3.13	349.00	2.28	8.62	48.43	23.66	322.13	20.33	10.92	6.63
P3	90.19	7.12	999.87	3.49	375.81	2.44	8.25	22.23	60.46	388.80	23.94	15.89	8.71
ASH	89.99	0.18	661.17	4.59	326.50	3.25	10.12	20.05	16.93	232.33	11.33	25.21	6.39

APPENDIX X: Results of the total extractions concentrations (in %) from the sediments samples.

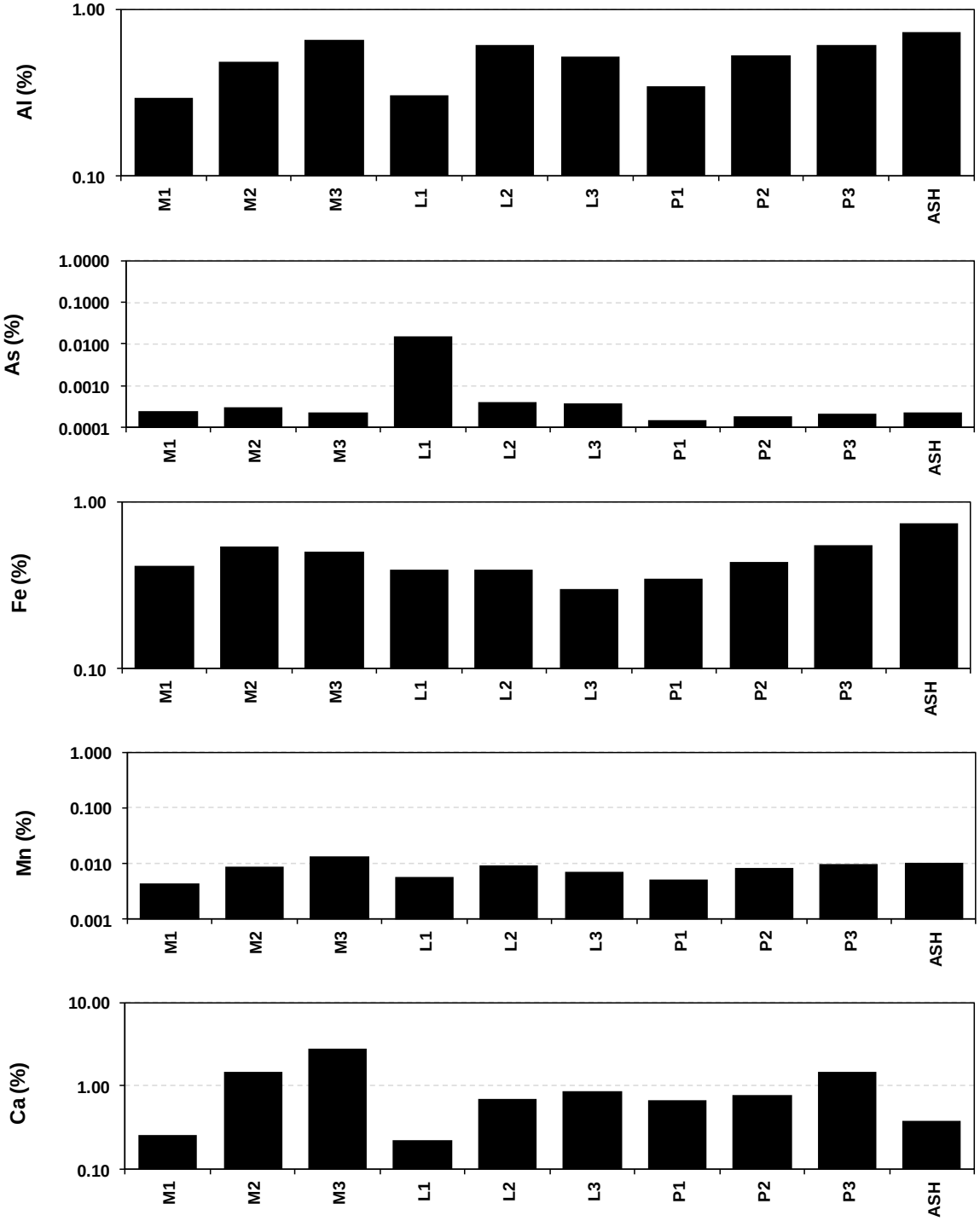

Appendix X (cont.): Results of the total extractions concentrations (in %) from the sediments samples.

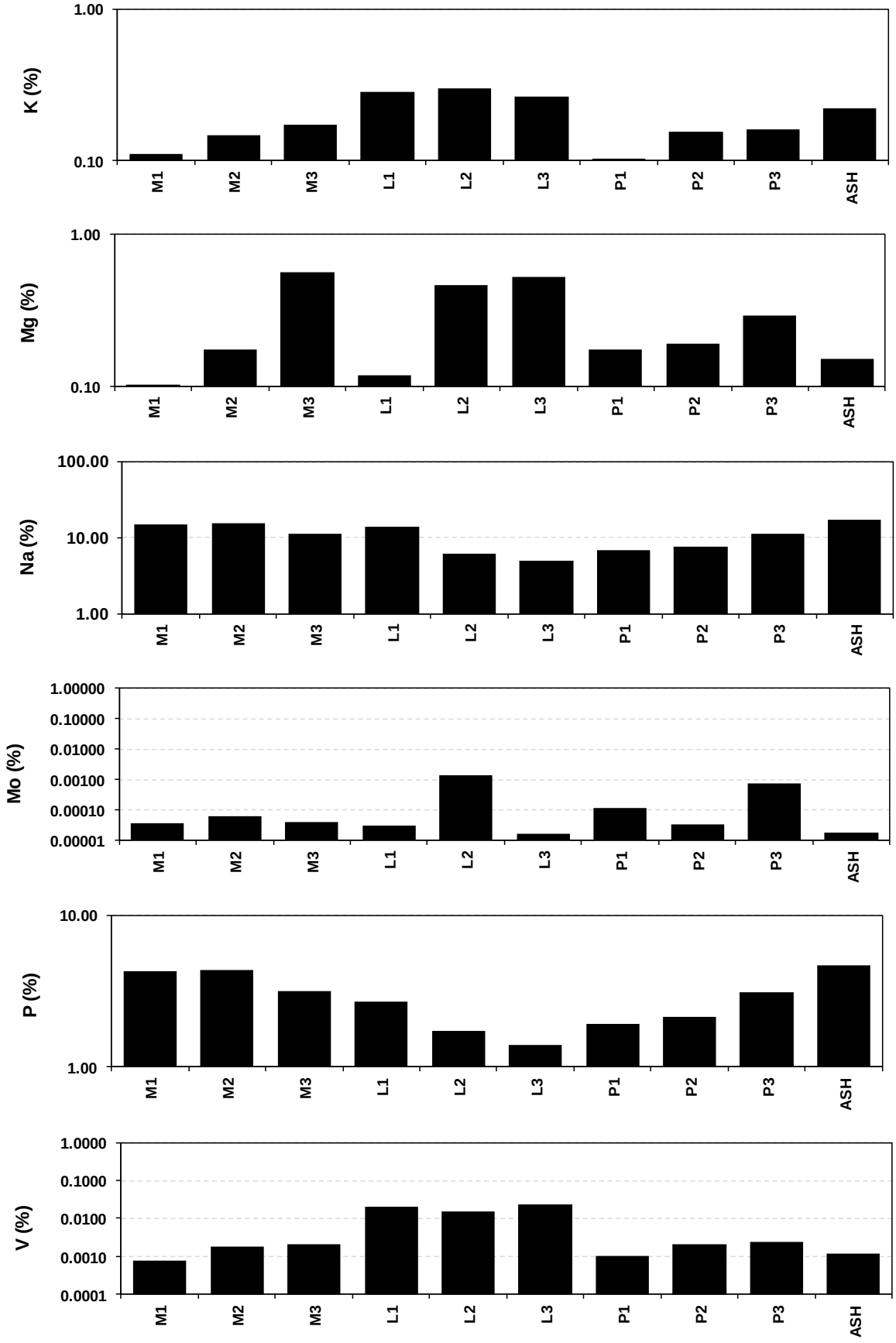

APPENDIX XI: X-Ray Diffraction spectra showing the qualitative mineralogical results for the sediment samples volcanic ash and L3.

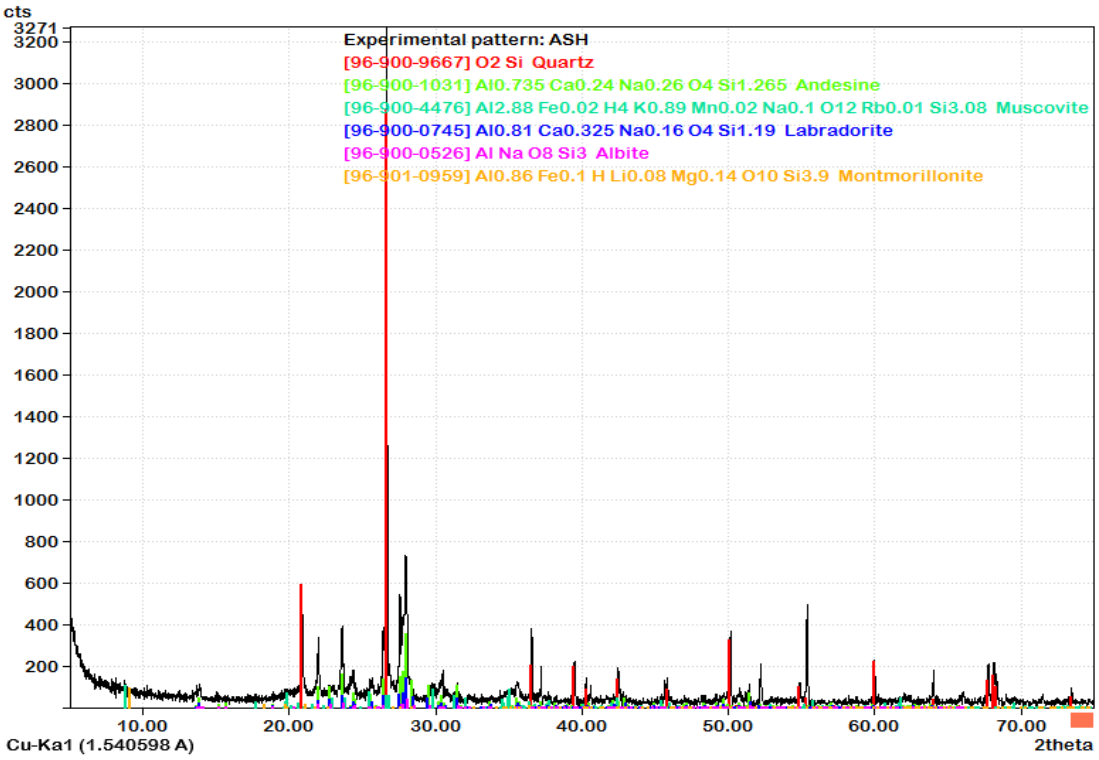

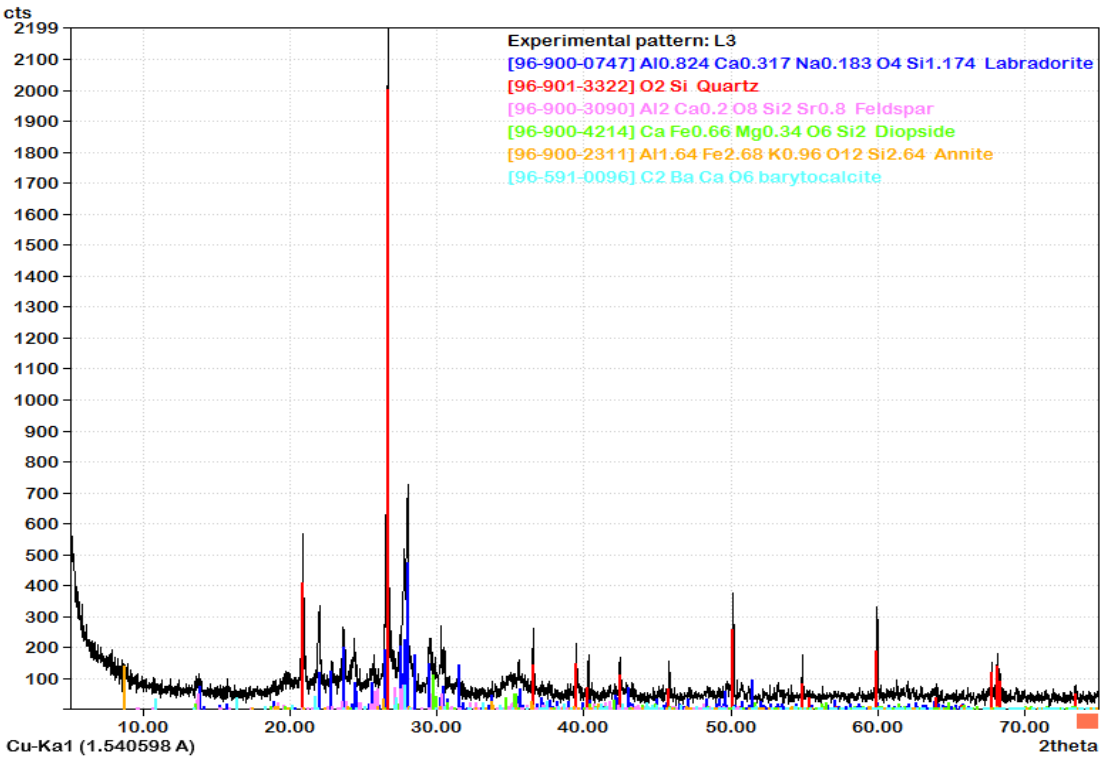

Appendix XI (cont.): X-Ray Diffraction spectra showing the qualitative mineralogical results for sediment samples M3 and P2.

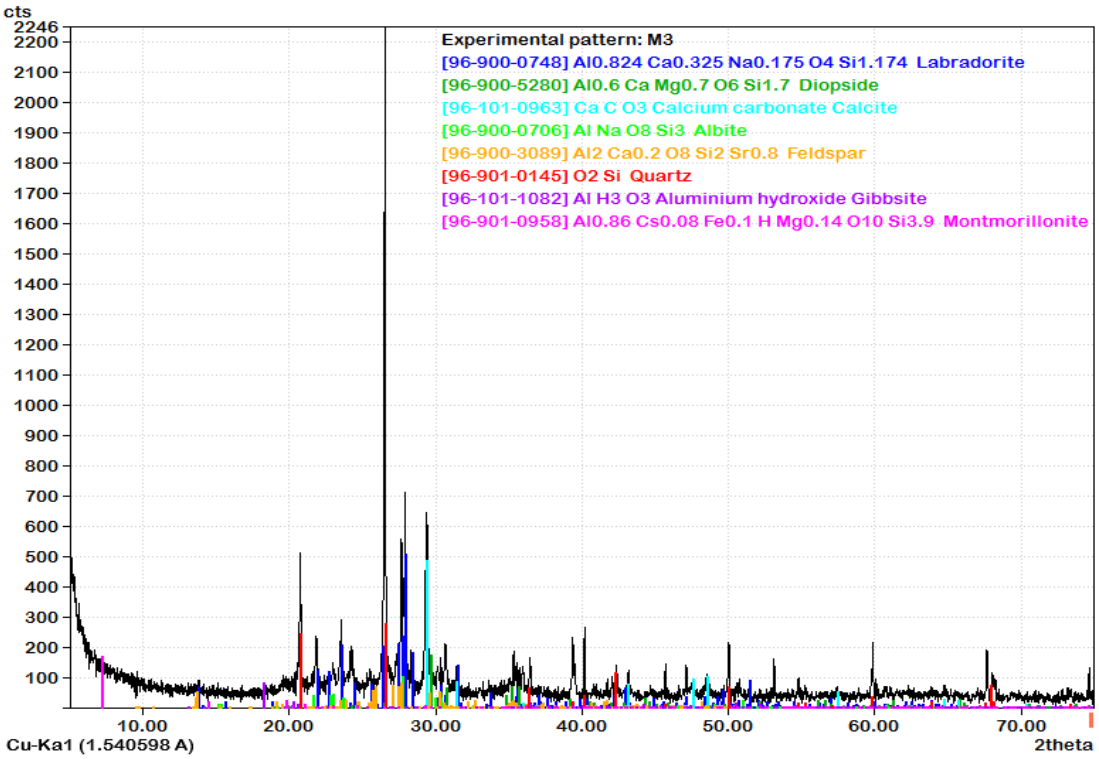

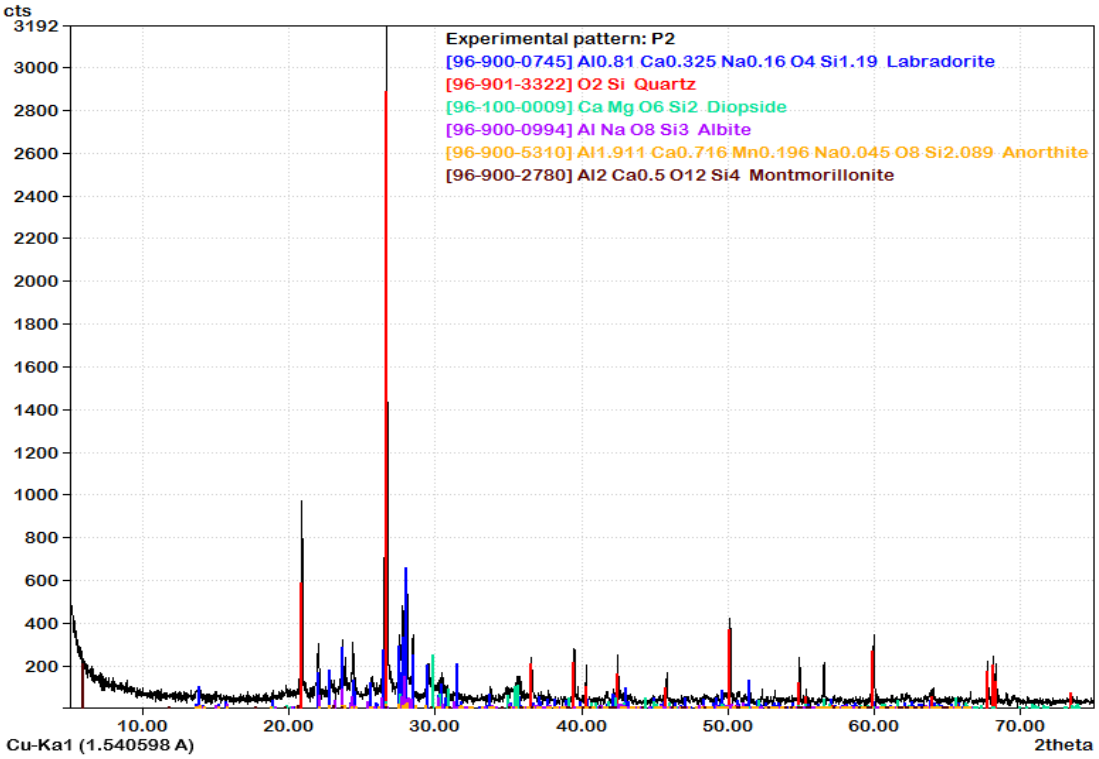

APPENDIX XII: Total aqueous speciation of selected groundwater samples modeled in PHREEQC.

		NE26		NE25		NE21		SE54		INO64	
Element	Species	Molality	%	Molality	%	Molality	%	Molality	%	Molality	%
Al		**3.14E-06**		**1.18E-06**		**7.80E-08**		**7.80E-08**		**1.12E-07**	
	$Al(OH)_4$-	3.07E-06	97.74	1.15E-06	97.80	7.63E-08	97.79	7.72E-08	98.97	9.80E-08	87.75
	$Al(OH)_3$	6.90E-08	2.20	2.49E-08	2.11	1.68E-09	2.15	7.94E-10	1.02	1.18E-08	10.57
	$Al(OH)^{2+}$	1.29E-09	0.04	7.84E-10	0.07	3.05E-11	0.04	5.69E-12	0.01	7.69E-10	0.69
	AlF_3	8.08E-10	0.03	6.11E-10	0.05	3.98E-12	0.01	2.66E-13	0.00	7.33E-10	0.66
	AlF4-	2.48E-10	0.01	2.77E-10	0.02	1.22E-12	0.00	6.16E-14	0.00	2.64E-10	0.24
	AlF2+	1.49E-10	0.00	1.38E-10	0.01	6.96E-13	0.00	6.04E-14	0.00	1.41E-10	0.13
As(3)		**3.09E-16**		**2.07E-16**		**1.73E-16**		**1.67E-16**		**1.71E-15**	
	H_3AsO_3	2.68E-16	86.61	1.82E-16	88.16	1.50E-16	86.84	1.22E-16	73.14	1.63E-15	95.50
	$H_2AsO_3^-$	4.14E-17	13.40	2.45E-17	11.83	2.27E-17	13.14	4.47E-17	26.80	7.74E-17	4.52
	$HAsO_3^{-2}$	1.14E-20	0.00	6.37E-21	0.00	5.79E-21	0.00	2.69E-20	0.02	7.02E-21	0.00
	$H_4AsO_3^+$	5.06E-25	0.00	4.57E-25	0.00	2.74E-25	0.00	1.15E-24	0.00	1.04E-23	0.00
	AsO_3^{-3}	2.38E-25	0.00	1.37E-25	0.00	1.06E-25	0.00	8.78E-26	0.00	5.48E-26	0.00
As(5)		**7.16E-06**		**4.35E-06**		**3.09E-06**		**6.48E-06**		**3.33E-06**	
	$HAsO_4^{-2}$	7.07E-06	98.74	4.29E-06	98.64	3.05E-06	98.71	6.43E-06	99.20	3.23E-06	96.96
	$H_2AsO_4^-$	7.87E-08	1.10	5.23E-08	1.20	3.68E-08	1.19	3.21E-08	0.49	9.86E-08	2.96
	AsO_4^{-3}	1.07E-08	0.15	6.61E-09	0.15	4.06E-09	0.13	2.00E-08	0.31	1.87E-09	0.06
	H_3AsO_4	3.28E-14	0.00	2.63E-14	0.00	1.58E-14	0.00	5.53E-15	0.00	1.20E-13	0.00
B		**4.75E-04**		**3.96E-04**		**1.71E-04**		**2.77E-04**		**3.22E-04**	
	H_3BO_3	3.96E-04	83.40	3.36E-04	84.83	1.43E-04	84.06	1.90E-04	68.55	3.01E-04	93.57
	$H_2BO_3^-$	7.47E-05	15.73	5.49E-05	13.87	2.62E-05	15.35	8.47E-05	30.63	1.86E-05	5.79
	NaH_2BO_3	3.03E-06	0.64	3.61E-06	0.91	7.67E-07	0.45	1.90E-06	0.69	1.32E-06	0.41
	MgH_2BO_3+	6.47E-07	0.14	9.32E-07	0.24	1.73E-07	0.10	1.98E-07	0.07	4.04E-07	0.13
	CaH_2BO_3+	3.38E-07	0.07	4.52E-07	0.11	8.71E-08	0.05	1.18E-07	0.04	2.46E-07	0.08
	$BF(OH)_3$-	8.95E-08	0.02	9.03E-08	0.02	1.84E-08	0.01	3.12E-08	0.01	4.05E-08	0.01
	$H_5(BO_3)_2$-	2.71E-08	0.01	1.69E-08	0.00	3.42E-09	0.00	1.47E-08	0.01	5.27E-09	0.00
C(4)		**1.76E-02**		**1.36E-02**		**1.71E-02**		**9.42E-03**		**1.03E-02**	
	HCO_3-	1.67E-02	94.60	1.26E-02	93.14	1.64E-02	95.50	8.80E-03	93.42	9.57E-03	93.38
	CO_3^{-2}	3.46E-04	1.97	3.11E-04	2.29	3.15E-04	1.84	4.05E-04	4.30	2.56E-04	2.49
	$NaHCO_3$	2.48E-04	1.41	2.44E-04	1.80	1.75E-04	1.02	9.03E-05	0.96	2.02E-04	1.97
	$NaCO_3$-	1.29E-04	0.74	1.36E-04	1.00	1.14E-04	0.67	7.19E-05	0.76	6.99E-05	0.68
	H_2CO_3	1.13E-04	0.64	1.02E-04	0.75	8.91E-05	0.52	2.49E-05	0.26	5.83E-05	0.57
	$MgHCO_3^+$	4.08E-05	0.23	6.13E-05	0.45	3.04E-05	0.18	1.10E-05	0.12	4.31E-05	0.42
	$MgCO_3$	3.01E-05	0.17	3.52E-05	0.26	2.32E-05	0.14	7.54E-06	0.08	3.09E-05	0.30
	$CaHCO_3$+	1.95E-05	0.11	2.73E-05	0.20	1.42E-05	0.08	5.78E-06	0.06	1.19E-05	0.12
	$CaCO_3$	1.80E-05	0.10	1.96E-05	0.14	1.35E-05	0.08	3.15E-06	0.03	8.32E-06	0.08
Ca		**2.88E-04**		**5.77E-04**		**1.75E-04**		**1.03E-04**		**9.50E-04**	
	Ca^{+2}	1.68E-04	58.23	3.65E-04	63.33	1.11E-04	63.54	4.46E-05	43.54	6.10E-04	64.18
	$CaHPO_4$	3.49E-05	12.14	1.14E-04	19.81	1.75E-05	10.02	3.00E-05	29.24	2.06E-04	21.64
	$CaPO_4$-	2.80E-05	9.72	2.90E-05	5.03	1.42E-05	8.09	1.56E-05	15.22	7.49E-05	7.88
	$CaHCO_3$+	1.98E-05	6.87	2.74E-05	4.75	1.38E-05	7.86	7.54E-06	7.36	3.09E-05	3.25
	$CaCO_3$	1.83E-05	6.35	1.97E-05	3.41	1.35E-05	7.69	3.15E-06	3.07	1.89E-05	1.99

	$CaSO_4$	1.78E-05	6.18	1.96E-05	3.40	4.62E-06	2.64	1.33E-06	1.30	8.32E-06	0.88
	$CaNO_3^+$	5.06E-07	0.18	9.65E-07	0.17	1.92E-07	0.11	1.18E-07	0.12	7.64E-07	0.08
	CaF^+	4.52E-07	0.16	4.52E-07	0.08	8.71E-08	0.05	1.03E-07	0.10	7.58E-07	0.08
	$CaH_2BO_3^+$	3.36E-07	0.12	1.14E-07	0.02	5.15E-08	0.03	1.81E-08	0.02	2.46E-07	0.03
	$CaH_2PO_4^+$	1.05E-07	0.04	1.08E-07	0.02	2.57E-09	0.00	1.86E-09	0.00	4.37E-08	0.00
	$CaOH^+$	2.56E-09	0.00	4.19E-09	0.00	1.88E-09	0.00	1.83E-09	0.00	2.04E-09	0.00
Cl		**5.58E-03**		**2.91E-02**		**1.12E-03**		**1.09E-03**		**3.30E-02**	
	Cl^-	5.58E-03	100.00	2.91E-02	100.00	1.12E-03	100.00	1.09E-03	100.00	3.30E-02	100.00
F		**6.34E-04**		**7.51E-04**		**3.59E-04**		**4.59E-04**		**3.92E-04**	
	F^-	6.12E-04	96.53	7.03E-04	93.61	3.49E-04	97.38	4.53E-04	98.71	3.63E-04	92.77
	MgF^+	1.43E-05	2.26	3.30E-05	4.39	6.25E-06	1.74	2.86E-06	0.62	2.05E-05	5.23
	NaF	7.12E-06	1.12	1.40E-05	1.86	2.95E-06	0.82	2.84E-06	0.62	6.95E-06	1.78
	CaF^+	4.52E-07	0.07	9.65E-07	0.13	1.92E-07	0.05	1.03E-07	0.02	7.64E-07	0.20
	$BF(OH)_3^-$	8.95E-08	0.01	9.03E-08	0.01	1.84E-08	0.01	3.12E-08	0.01	4.05E-08	0.01
	HF	2.00E-09	0.00	2.81E-09	0.00	1.18E-09	0.00	6.07E-10	0.00	3.41E-09	0.00
Fe(2)		**1.10E-08**		**1.05E-08**		**5.96E-09**		**8.22E-10**		**1.20E-08**	
	$FeHPO_4$	5.99E-09	54.35	6.01E-09	57.29	2.97E-09	49.79	5.67E-10	69.07	6.14E-09	50.99
	Fe^{+2}	4.19E-09	38.03	2.75E-09	26.25	2.58E-09	43.26	2.18E-10	26.51	4.16E-09	34.53
	$FeSO_4$	3.84E-10	3.49	1.37E-09	13.07	2.08E-10	3.49	1.84E-11	2.23	1.46E-09	12.09
	$FeHCO_3^+$	2.88E-10	2.62	2.24E-10	2.13	9.89E-11	1.66	1.00E-11	1.22	1.53E-10	1.27
	$FeOH^+$	1.18E-10	1.07	1.06E-10	1.01	8.55E-11	1.43	6.14E-12	0.75	1.03E-10	0.85
	$FeH_2PO_4^+$	4.45E-11	0.40	2.69E-11	0.26	2.15E-11	0.36	1.62E-12	0.20	3.18E-11	0.26
Fe(3)		**3.10E-07**		**2.27E-07**		**2.08E-07**		**1.03E-07**		**3.84E-08**	
	$Fe(OH)_4^-$	1.16E-07	37.37	1.01E-07	44.63	7.65E-08	36.86	7.25E-08	70.25	3.07E-08	80.08
	$Fe(OH)_2^+$	1.15E-07	36.95	6.45E-08	28.42	7.56E-08	36.41	1.94E-08	18.75	4.53E-09	11.82
	$Fe(OH)_3$	7.97E-08	25.69	6.12E-08	26.95	5.55E-08	26.76	1.14E-08	11.00	3.10E-09	8.09
K		**2.90E-04**		**5.40E-04**		**3.08E-04**		**2.38E-04**		**9.25E-04**	
	K^+	2.86E-04	98.65	5.25E-04	97.35	3.05E-04	99.32	2.36E-04	98.91	8.97E-04	96.92
	KSO_4^-	1.96E-06	0.68	1.27E-05	2.35	1.39E-06	0.45	2.27E-06	0.95	2.42E-05	2.62
	$KHPO_4^-$	1.92E-06	0.66	1.61E-06	0.30	7.39E-07	0.24	3.92E-07	0.16	4.28E-06	0.46
Mg		**7.84E-04**		**1.75E-03**		**4.95E-04**		**1.98E-04**		**2.34E-03**	
	Mg^{+2}	5.06E-04	64.57	1.19E-03	67.83	3.47E-04	70.04	1.17E-04	59.25	1.55E-03	66.44
	$MgHPO_4$	1.46E-04	18.67	3.00E-04	17.14	7.54E-05	15.25	5.66E-05	28.59	4.25E-04	18.20
	$MgSO_4$	4.34E-05	5.54	1.30E-04	7.43	3.04E-05	6.15	1.10E-05	5.56	2.63E-04	11.26
	$MgHCO_3^+$	4.08E-05	5.20	6.13E-05	3.50	2.32E-05	4.70	5.78E-06	2.92	5.83E-05	2.50
	$MgCO_3$	3.01E-05	3.84	3.52E-05	2.01	1.16E-05	2.35	2.84E-06	1.44	2.05E-05	0.88
	MgF^+	1.43E-05	1.83	3.30E-05	1.88	6.25E-06	1.26	2.83E-06	1.43	1.19E-05	0.51
	$MgPO_4^-$	1.33E-06	0.17	1.00E-06	0.06	6.70E-07	0.14	1.23E-06	0.62	4.06E-06	0.17
	$MgH_2PO_4^+$	6.76E-07	0.09	9.32E-07	0.05	3.40E-07	0.07	1.98E-07	0.10	7.51E-07	0.03
	$MgH_2BO_3^+$	6.47E-07	0.08	7.90E-07	0.05	1.73E-07	0.03	1.00E-07	0.05	4.04E-07	0.02
	$MgOH^+$	1.47E-07	0.02	2.59E-07	0.01	1.11E-07	0.02	9.24E-08	0.05	9.64E-08	0.00
Mn(2)		**9.49E-08**		**1.28E-08**		**1.82E-09**		**9.12E-09**		**7.68E-08**	
	Mn^{+2}	7.87E-08	82.92	1.02E-08	80.00	1.54E-09	84.43	8.14E-09	89.33	6.23E-08	81.10
	$MnHCO_3^+$	1.00E-08	10.54	1.68E-09	13.10	2.28E-10	12.52	6.95E-10	7.62	1.06E-08	13.77
	$MnSO_4$	5.18E-09	5.45	6.98E-10	5.45	4.24E-11	2.32	1.65E-10	1.81	3.00E-09	3.90
	MnF^+	6.61E-10	0.70	1.06E-10	0.83	8.80E-12	0.48	6.42E-11	0.70	6.92E-10	0.90

	MnCl+	2.22E-10	0.23	7.05E-11	0.55	3.22E-12	0.18	4.33E-11	0.47	2.00E-10	0.26
	MnOH+	1.40E-10	0.15	1.14E-11	0.09	1.03E-12	0.06	5.73E-12	0.06	2.05E-11	0.03
	$MnCl_2$	1.24E-12	0.00	2.79E-12	0.02	1.22E-15	0.00	6.74E-15	0.00	2.04E-11	0.03
N(5)		**1.71E-03**		**1.93E-04**		**1.37E-04**		**1.36E-04**		**9.99E-04**	
	NO_3-	1.71E-03	99.94	1.93E-04	99.95	1.37E-04	99.93	1.36E-04	100.00	9.98E-04	99.90
	$CaNO_3$+	5.06E-07	0.03	1.08E-07	0.06	2.95E-08	0.02	1.22E-08	0.01	9.38E-07	0.09
Na		**3.19E-02**		**5.88E-02**		**2.17E-02**		**1.61E-02**		**6.07E-02**	
	Na+	3.10E-02	97.24	5.70E-02	96.91	2.12E-02	97.88	1.57E-02	97.39	5.87E-02	96.69
	$NaHPO_4$-	3.22E-04	1.01	1.09E-03	1.85	1.75E-04	0.81	2.33E-04	1.45	1.27E-03	2.09
	$NaHCO_3$	2.48E-04	0.78	3.11E-04	0.53	1.50E-04	0.69	9.03E-05	0.56	4.33E-04	0.71
	$NaSO_4$-	1.69E-04	0.53	2.70E-04	0.46	8.91E-05	0.41	7.19E-05	0.45	2.56E-04	0.42
	$NaCO_3$-	1.29E-04	0.41	1.36E-04	0.23	4.06E-05	0.19	2.07E-05	0.13	4.31E-05	0.07
	NaF	7.13E-06	0.02	1.40E-05	0.02	2.95E-06	0.01	2.86E-06	0.02	6.95E-06	0.01
	NaH_2BO_3	3.03E-06	0.01	3.61E-06	0.01	7.67E-07	0.00	1.90E-06	0.01	1.32E-06	0.00
P		**2.78E-03**		**1.66E-03**		**1.63E-03**		**3.09E-03**		**2.98E-03**	
	HPO_4^{-2}	2.18E-03	78.26	1.17E-03	70.43	1.33E-03	81.35	2.71E-03	87.75	2.01E-03	67.44
	$NaHPO_4$-	3.22E-04	11.58	2.70E-04	16.21	1.50E-04	9.19	2.33E-04	7.55	4.33E-04	14.55
	$MgHPO_4$	1.46E-04	5.26	1.30E-04	7.83	7.54E-05	4.63	5.66E-05	1.83	2.63E-04	8.83
	H2PO_4-	6.74E-05	2.42	3.95E-05	2.37	4.43E-05	2.72	3.74E-05	1.21	1.69E-04	5.68
	$CaHPO_4$	3.52E-05	1.27	2.90E-05	1.74	1.75E-05	1.08	3.00E-05	0.97	7.49E-05	2.51
	$CaPO_4$-	2.82E-05	1.01	1.97E-05	1.18	1.38E-05	0.84	1.56E-05	0.51	1.89E-05	0.63
	$KHPO_4$-	1.92E-06	0.07	1.61E-06	0.10	1.39E-06	0.09	2.27E-06	0.07	4.28E-06	0.14
	$MgPO_4$-	1.33E-06	0.05	1.00E-06	0.06	6.70E-07	0.04	1.48E-06	0.05	4.06E-06	0.14
	MgH_2PO_4+	6.76E-07	0.02	7.90E-07	0.05	3.40E-07	0.02	1.23E-06	0.04	7.58E-07	0.03
	PO_4^{-3}	5.82E-07	0.02	3.18E-07	0.02	3.11E-07	0.02	1.00E-07	0.00	7.51E-07	0.03
S(6)		**2.34E-03**		**1.03E-02**		**7.21E-04**		**4.62E-04**		**1.22E-02**	
	SO_4^{-2}	2.10E-03	89.50	8.81E-03	85.27	6.63E-04	91.95	4.37E-04	94.50	1.03E-02	83.96
	$NaSO_4$-	1.69E-04	7.20	1.09E-03	10.51	4.06E-05	5.64	2.07E-05	4.47	1.27E-03	10.38
	$MgSO_4$	4.34E-05	1.85	3.00E-04	2.91	1.16E-05	1.61	2.83E-06	0.61	4.25E-04	3.48
	$CaSO_4$	1.78E-05	0.76	1.14E-04	1.11	4.62E-06	0.64	1.33E-06	0.29	2.06E-04	1.68
	NH_4SO_4-	1.41E-05	0.60	1.27E-05	0.12	7.39E-07	0.10	3.92E-07	0.08	3.69E-05	0.30
	KSO_4-	1.96E-06	0.08	5.76E-06	0.06	4.01E-07	0.06	1.97E-07	0.04	2.42E-05	0.20
Si		**3.04E-04**		**2.79E-04**		**2.87E-04**		**3.18E-04**		**2.88E-04**	
	H_4SiO_4	2.92E-04	95.96	2.69E-04	96.49	2.75E-04	96.06	2.89E-04	90.93	2.85E-04	98.68
	H_3SiO_4-	1.23E-05	4.03	9.79E-06	3.51	1.13E-05	3.93	2.88E-05	9.07	3.79E-06	1.31
V(3)		**4.86E-09**		**7.39E-10**		**7.66E-09**		**4.73E-09**		**3.10E-09**	
	$V(OH)_3$	4.86E-09	100.00	7.39E-10	100.00	7.66E-09	100.00	4.73E-09	100.00	3.10E-09	100.00
V(5)		**2.74E-05**		**4.26E-06**		**3.29E-05**		**3.88E-05**		**2.79E-20**	
	HVO_4-2	1.65E-05	60.38	2.63E-06	61.75	1.88E-05	57.20	2.94E-05	75.91	2.37E-06	59.58
	H_2VO_4-	1.05E-05	38.30	1.62E-06	37.97	1.36E-05	41.37	8.94E-06	23.05	1.41E-06	40.18
	$HV_2O_7^{-3}$	1.47E-07	0.54	5.10E-09	0.12	1.82E-07	0.55	1.74E-07	0.45	9.50E-07	0.07
	$H_3V_2O_7$-	1.78E-08	0.07	4.91E-10	0.01	3.15E-08	0.10	1.79E-08	0.05	1.70E-09	0.04
	$V_2O_7^{-4}$	9.08E-09	0.03	4.45E-10	0.01	8.21E-09	0.02	5.49E-09	0.01	9.24E-10	0.01
	$V_3O_9^{-3}$	4.76E-09	0.02			8.03E-09	0.02	2.04E-09	0.01		

APPENDIX XIII: Saturation Index of the mineral phases modeled in PHREEQC for selected groundwater samples.

Samples	NE26	NE25	NE21	NE54	INO64
Mineral Phases	**SI**	**SI**	**SI**	**SI**	**SI**
Anhydrite	-2.66	-1.94	-3.34	-3.88	-1.69
Aragonite	-0.56	0.41	0.25	0	0.05
Boehmite	0.15	-0.02	-1.25	-1.62	-0.59
$Ca_3(PO_4)_2$	3.19	3.01	2.4	2.74	3.34
$Ca_4H(PO_4)_3{:}3H_2O$	1.84	1.29	0.44	0.71	1.92
$CaHPO_4$	-0.06	-0.15	-0.35	-0.39	0.32
$CaHPO_4{:}2H_2O$	-0.36	-0.47	-0.68	-0.72	-0.02
Calcite	-0.37	0.61	0.46	0.21	0.26
Chalcedony	0.06	0.1	0.11	0.14	0.16
Cristobalite	-0.14	-0.1	-0.09	-0.06	-0.04
Diaspore	1.88	1.76	0.54	0.18	1.23
Dolomite(disordered)	-0.75	1.16	0.81	0.22	0.28
Dolomite(ordered)	-0.18	1.75	1.4	0.82	0.88
Ferrihydrite	2.6	2.32	2.29	1.84	1.25
Fluorite	-0.1	0.22	-0.71	-0.85	-0.13
Gibbsite	0.48	0.38	-0.83	-1.19	-0.13
Goethite	5.33	5.09	5.07	4.62	4.05
Gypsum	-2.39	-1.65	-3.04	-3.58	-1.38
Halite	-5.49	-4.56	-6.34	-6.47	-4.49
$FeAsO_4{:}2H_2O$	-7.9	-8.07	-8.29	-9.16	-8.33
Kaolinite	3.12	3.02	0.62	-0.04	2.12
Lepidocrocite	4.57	4.54	4.54	4.12	3.62
Quartz	0.51	0.56	0.57	0.6	0.63
SiO_2(am-gel)	-0.8	-0.78	-0.77	-0.74	-0.72
SiO_2(am-ppt)	-0.76	-0.74	-0.73	-0.7	-0.68
Strengite	-0.04	-0.31	-0.34	-1.24	-0.26